An Ethanol Conversion Study Over Titania Supported Catalysts

Yao-Kuan Chen

A Thesis Submitted to the Faculty of Science,
University of the Witwatersrand, Johannesburg,
for the Degree of Master of Science

Johannesburg, December 1992

ABSTRACT

The ethanol conversion to hydrocarbons over acidic catalysts proceeds with high activity and selectivity and has hence generated considerable interest. In this thesis an investigation of the use of a range of supports, loaded with metals as potential catalysts for the ethanol transformation reaction, is reported. In particular, TiO_2 was investigated as a support and the addition of a secondary component to the catalyst was examined with respect to product selectivities. Metal components loaded include Al, Co, Cu, Ni, Ru, Pd, Pt and Rh. The metal/TiO_2 catalyst was modified by varying the metal loadings and the reduction and calcination treatments.

Ethanol conversions were investigated between 100°C - 400°C. Of the metals Al, Co, Cu, Ni, Ru supported on the TiO_2, only Al and Ru on TiO_2 showed slightly increased catalytic activity but all catalysts gave a product spectrum with high selectivity towards longer chain hydrocarbon products (> C_6). Further, the incorporation of Ni into TiO_2 increased the catalyst lifetime and the yield of the liquid (C_5^+) products.

When Pt, Rh and Pd were loaded on TiO_2 the materials proved to be active catalysts for the conversion of ethanol to hydrocarbons with high selectivity towards C_6 - C_9^+ hydrocarbons. Further, at low temperatures (< 300°C) the Pd reacted with the ethanol to yield acetaldehyde and secondary products via a dehydrogenation route. However, at 300°C the dehydration reaction pathway, due to TiO_2, began to operate. The first route involved the favoured

production of odd numbered C-C bonded products and the second reaction pathway yielded even numbered C-C bonded products.

The 2% Pd loaded on TiO_2 catalyst, because it showed high activity and longer lifetime, was further investigated. Different Pd metal salts as well as different preparation procedures were found not to affect the catalyst activity or selectivity. Calcination temperatures were optimum below 400°C; reduction at 200°C.

This thesis also describes the theory and experimental methods necessary to perform a thermodynamic study of the ethanol reaction to yield hydrocarbons. In our studies over a 2% Pd/TiO_2 catalyst, the proposed ethanol dehydration reaction to ether or ethene was never achieved under equilibrium conditions. Only in the dehydrogenation reaction was some data measured which was consistent with theoretical equilibrium data.

DECLARATION

I declare that this Thesis is my own, unaided work. It is being submitted for the degree of Master of Science in the University of the Witwatersrand, Johannesburg. It has not been submitted before for any degree or examination in any other University.

Yao-kuan Chen

Yao-Kuan Chen

12 day of December 1992

Dedicated to my parents
and my dearest wife

Without whose love and attention this thesis would have been impossible.

ACKNOWLEDGEMENTS

I would like to express my sincerest appreciation to the following people for their help, encouragement, advice and support:

My supervisors, Professor N.J. Coville (Chem.) and Dr. D. Hildebrandt (Chem. Eng.), for their patience, guidance, encouragement, stimulating discussions and assistance during this project.

Professor D. Glasser (Chem. Eng.) for his assistance and invaluable discussions.

Dr. V.D. Sokolovskii (Chem.) for his ongoing enthusiasm, guidance and interest in my research.

Mr. M.V.B. Smith (Chem. Eng.) for permission to use the Process package and the invaluable assistance in the determination of equilibrium compositions.

Mr. J. Wollbrandt for his all friendship and the many helpful discussions.

Mr. B. Chassoulas for his technical help with instrumentation, and Mr. B. Fairbrother for the expert glass blowing.

My colleagues J.R. Mellor and other members of the Catalysis Group for their help concering the research. They certainly have made this period enjoyable and unforgettable.

Thanks are due to H.M. Chiu for her patience in typing this thesis and J.R. Sebola for his friendship and proof reading of the thesis.

Financial assistance from the FRD and the University of the Witwatersrand are acknowledged.

Finally I would like to thank my parents for their never-ending support, understanding and motivation.

LIST OF ABBREVIATIONS

Symbol	Definition
EtOH	: Ethanol
Et_2O (EtOEt)	: Diethyl-ether
MeCHO	: Acetaldehyde
$C_{2=}$	: Ethene
$C_{3=}$	: Propene
C_6^+ or C_9^+	: Complexes with carbon number greater than C_6 or C_9
H C's	: Hydrocarbons
A A	: Atomic Absorption
G C	: Gas Chromatography
O D	: Outer Diameter
I D	: Internal Diameter
v/v	: volume by volume
D S C	: Differential Scanning Calorimetry
T G A	: Thermal Gravimetric Analysis
F I D	: Flame Ionisation Detector

T C D	: Thermal Conductivity Detector
B E T	: Brunauer, Emmett, Teller
T P D	: Temperature Programmed Desorption
T O L	: Time On Line
H T R	: High Temperate Reduction
M T G	: Methanol to Gasoline
M T C	: Methanol to Chemicals
M T O	: Methanol to Olefins
B E T E	: Bioethanol to Ethene
W H S V	: Weight Hourly Space Velocity
W M S I	: Weak Metal Support Interactions
M M S I	: Medium Metal Support Interactions
S M S I	: Strong Metal Support Interactions
Z S M-5	: Zeolite Socony Mobil-5
S A P O	: Silicoaluminophosphates
Al-PILM	: Alumina Pillared Interlayered Montmorillonite
M O G D	: Mobil Olefins to Gasoline and Distillate

T C D	: Thermal Conductivity Detector
B E T	: Brunauer, Emmett, Teller
T P D	: Temperature Programmed Desorption
T O L	: Time On Line
H T R	: High Temperate Reduction
M T G	: Methanol to Gasoline
M T C	: Methanol to Chemicals
M T O	: Methanol to Olefins
B E T E	: Bioethanol to Ethene
W H S V	: Weight Hourly Space Velocity
W M S I	: Weak Metal Support Interactions
M M S I	: Medium Metal Support Interactions
S M S I	: Strong Metal Support Interactions
Z S M-5	: Zeolite Socony Mobil-5
S A P O	: Silicoaluminophosphates
Al-PILM	: Alumina Pillared Interlayered Montmorillonite
M O G D	: Mobil Olefins to Gasoline and Distillate

NOMENCLATURE AND UNITS

Symbol		Definition	SI units
$\Delta G°_f$	=	Standard Gibbs energy of formation (at 1 atm, 298°K)	J/mol
$\Delta H°_f$	=	Standard enthalpy of formation (at 1 atm, 298°K)	J/mol
C_p	=	Heat capacity	J/mol K
	=	$A + B * T + C * T^2 + D * T^3$	T = K
Ka(Keq)	=	Chemical-equilibium constant	variable
T	=	Temperature	K or °C
T^*	=	Temperature	298 K
$\acute{N}$	=	Total molar flow rate	mol/hr
X	=	Conversion	% by mass
R	=	Gas constant	J/mol K
k	=	Rate constant	$(mol/hr \cdot g \cdot cat \cdot atm)^{1/2}$

TABLE OF CONTENTS

LIST OF TABLES

LIST OF FIGURES

Things have their roots and their branches. Affairs have their end and their beginning. To know what is first and what is last w_ l lead near to the way.

Chinese classical text

CHAPTER ONE

INTRODUCTION

1.1 HETEROGENEOUS ACID CATALYSTS

Five steps are proposed as necessary for a reaction catalysed by a solid surface [1]. These are:

(1) Diffusion of reactant(s) "to" the surface.
(2) Adsorption of reactant(s) "onto" the surface.
(3) Reaction "on" the surface.
(4) Desorption of product(s) "off" the surface.
(5) Diffusion of product(s) "from" the surface.

Provided difussional (heat, mass transfer) effects are not important the reaction "on" the surface is regarded as the key step which can be understood by chemical principles. The reaction on the surface is thus regarded as a classical chemical reaction i.e. a reaction between the reagent molecules and the surface viewed from an atomic perspective. Solid acid catalysts provide a special type of surface for a reaction.

Solid acid catalysts used in industry include activated natural clays and synthetic binary oxides, such as bentonite, montmorillonite and silica-alumina, as well as supported acids such as phosphoric acid on alumina. These substances have the ability to promote a large number of acid-catalyzed reactions. For instance, reactions carried

out over zeolites, such as conversion of oxygenates into gasoline [2], isomerisation of aromatics [3], alkylaromatic disproportionation and hydroisomerisation [4] all require strongly Brönsted acidic sites centered on aluminum for their activity [5]. Most workers have considered that Brönsted acid surface acidity is solely responsible for the catalytic reaction in the methanol/ethanol conversion over H-ZSM-5 zeolite type catalysts [6, 7]. This reaction is not restricted to zeolites. Many materials that contain Brönsted or Lewis acid sites are able to accomplish this conversion, e.g. silica-alumina [8], WO_3/Al_2O_3 [9] etc.

The solid acid catalysts can provide several advantages over liquid acid catalysts [10]. These include high catalytic activity and selectivity, less corrosion of reactors, facile catalyst regeneration and repeated use, easy separation of a solid acid catalyst from a reaction mixture and less problems with the disposal of used solid acid catalysts. This disposal of supported acid catalysts is important since treatment of liquid acid catalysts, to make them environmentally safe, can be expensive.

Guisent [11] has reported that the acidity of catalyst surfaces can be estimated using appropriate test reactions. In certain cases, the activity in a test reaction can be related to the number and distribution of acidic sites on the catalyst surface. The initial apparent turnover frequency was suggested as a useful parameter for the comparison of the acidity of different solids. The turnover frequency measured for a catalyst with Brönsted acidic sites is generally believed to represent the average activity of the surface hydroxyls of the catalyst.

A number of more classical techniques have also been employed to examine the strength and the number of acid sites on acid forms of catalysts. These include acid-base

titrations using indicators, desorption of bases such as ammonia or pyridine at elevated temperatures, and infrared spectroscopy. The acid-base titration technique was first described by Benesi at 1956 [12]. The authors used Hammett indicators to measure the acid strength of metal oxides, supported acids, clays and cracking catalysts. This method involves equilibrating the solid with a base (usually n-butylamine) followed by addition of the indicators. Using a series of indicators an acidity distribution can be established. A modification of the method uses UV-spectrophotometric techniques [13]. This method improves the determination of the end point as well as the pH value. Another modification also allowed for the determination and differentiation of Brönsted and Lewis acid sites by introduction of a di-substituted pyridine before the titration [14]. Furthermore, the use of Temperature Programmed Desorption (TPD) is also an important technique for determining the strength of acid sites [15]. In this technique, all the chemisorption sites of a sample are initially occupied by the base (ammonia or pyridine) and the rate of desorption is measured during a controlled heating cycle. During desorption, starting with all sites covered, the base will first desorb from the most weakly acidic sites. The base adsorbed at stronger acid sites will desorb only at higher temperatures. This allows for the determination of the number as well as the relative strength of the acid sites on the catalysts. The acidic and/or basic properties of solid acids such as single oxides (Al_2O_3, SiO_2), clays (montmorillonite, kaolinite clay), mixed amorphous oxides (SiO_2-Al_2O_3) and zeolites etc. have been determined by this technique. Table 1.1 shows the acidity (pK_a) range of some common acid materials [16].

Table 1.1 Acidity of catalytic materials [16]

Solid	pK_a range
SiO_2-Al_2O_3	< -8.2
Montmorillonite clay	-5.6 to -8.2
Kaolinite clay	-5.6 to -8.2
γ-Al_2O_3	+3.3 to -5.6
SiO-MgO	+3.5 to -2.5
SiO_2	-2.0
TiO_2	+6.8 to +1.5
$MgAl_2O_4$	> 7.0
CaO	> 7.0
MgO	> 7.0

Two of the above acids (TiO_2, γ-Al_2O_3) have been used in this thesis study and their acidity will be described further.

The γ-Alumina, has been shown to be a defect lattice of the spinel type, which adsorbs water to reduce the surface energy [17]. This results in the formation of OH groups [18], which are extremely weak Brönsted acid centres [19]. Lewis acid sites are generated when these hydroxyl groups condense under heating to give exposed aluminium ions [18, 20]. The following scheme shows that γ-Al_2O_3 can be activated by calcination above 300°C [21 - 23]:

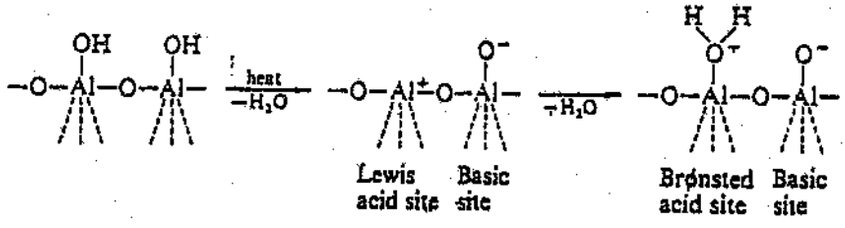

Dehydration of the hydrous oxide gives a surface containing both Lewis (electron acceptor) and basic sites. However, sufficient H_2O is always present to generate Brönsted sites.

Both Brönsted and Lewis acidity of titania has been investigated using diagnostic adsorbates combined with infrared spectrophotometry. Some hydroxyl groups on anatase have a sufficient acidic character to protonate trimethylamine [24]. The conversion of a surface oxide ion into a hydroxyl ion during dissociative water adsorption also amounts to Brönsted basicity. Further, a titania surface in contact with an aqueous environment can show both Brönsted acidity (adsorption of NaOH) and basicity (adsorption of H_3PO_4), and it has been suggested that these two functions are associated with the two types of hydroxyl groups thought to be present on the surface [24].

1.2 SUPPORTED METAL CATALYSTS

Over 70% of known catalytic reactions involve some form of metallic component [25]. The metal catalysts are used in catalytic reforming, hydrocracking, ammonia and methanol synthesis, indirect coal liquefaction, oxidation, and a vast number of organic hydrogenation and dehydrogenation processes [26, 27].

Successful catalytic applications are mainly found for d-electron transition metals. Alkali and alkaline s-metals revert too easily to ionic states under catalytic conditions and are used primarily as catalyst promoters. Rare earth f-metals likewise tend to be difficult to produce and too reactive to remain in the metallic state.

The d electron metals are most important for catalytic reactions because they provide a large concentration of degenerate low-energy electronic states within which charge fluctuations can occur involving electrons as well as electron vacancies [28]. The most active metallic catalysts are those of groups 8 - 10. An important function of transition metals in catalytic reactions is to atomize diatomic moleules and then to supply the atoms to other reactants and reaction intermediates [28].

Supported metals are used extensively as heterogeneous catalysts, the general role of the support being to disperse and stabilize the small metal particles. However, interaction between a metal and its support is a frequent occurrence [29]. About ten known types of metal-support interactions have been identified [30]. These include:

1. Genesis and preservation of high metal dispersion.
2. Metal particle shape.
3. Dual function - the reaction starts on the metal.
4. Dual function - the reaction starts on the support.
5. Spillover from metal to support.
6. Spillover from support to metal.
7. Contamination of the metal by the support.
8. Interfacial effects - adlineation.
9. Modification by the metal of the catalytic activity of the support.
10. Modification by the support of the catalytic activity of the metal.

A system of dispersed metal particles on a high surface area acidic oxide support will exhibit at least dual functionality [28]. For example when an acidic support containing a metal used for hydrocracking is used, the catalyst is bifunctional, combining a hydrogenating and an acidic function. The acidic function is provided by an

acidic carrier, like alumina, silica-alumina, silica-magnesia, etc. It gives the catalyst its cracking activity. The acidity level is determined by the feedstock and the required transformation [31].

However, according to the concept of bifunctionality the metal supported on the second compoent plays an important role in the overall reactions [25]. The bifunctional catalysts are of great use in the petroleum industry. Some examples are described below.

Csicsery [32, 33] has described the dehydrocyclodimerisation of lower alkanes over bifunctional catalysts to produce aromatics. The catalysts consisted of Pt and alumina, and converted propane, butane and pentane to aromatics. Likewise, Inui et al. [34] have shown that the conversion of propane to aromatics occurs over the bifunction catalyst Pt/ZSM-5. The main aromatic products were toluene, benzene and xylene. The authors [34] suggested that the first step in the reaction mechanism is the Pt-catalysed dehydrogenation of propane to give propene, which is then oligomerised to from aromatics on the ZSM-5 acid sites. Similar reactions were investigated on a Ga-containning catalyst [35]. Gnep and Doyemet [35], considered the conversion as occuring via a bifunctional process in which the dehydrogenation reactions were catalysed by the gallium species an igomerisation and oliglmer cyclisation by the acid sit. . Transition metal modified ZSM-5 also gave higher activity and higher selectivity for the light alkanes to aromatics conversion reaction, when compared to the metal free ZSM-5 [36 - 38]

Catalysts used in reforming reactions consist of small crystallites of metals (Pt or Pt alloys) supported on porous promoted alumina. Both the metal and oxide components play active roles. However, here the two

functions are present in separate phases. The metal provides the hydrogenation-dehydrogenation activity, and the promoted acidic alumina provides the isomerization activity. The hydrogenation-dehydrogenation activity of the supported metal and the isomerization activity of the alumina are much greater than the respective activities of the early-generation metal oxides [27].

Methanol and other light alcohols such as ethanol are selectively converted to gasoline range hydrocarbons (C_5 - C_{11}) and shorter hydrocarbons over ZSM-5 type zeolites [39, 40]. However, zeolite catalysts, when modified by metals (e.g. Zn, Mn, Mg etc.), are particularly selective for the production of monoaromatics [41], ethene [42] and light olefins [43]. Further, the stability, activity and selectivity of the zeolite (ZSM-5) under the combined effects of steam and high temperature was much lower than that of the metal modified zeolite [44].

1.3 STRONG METAL-SUPPORT INTERACTIONS (SMSI) CATALYSTS

A novel approach to metal-support interaction was hypothesized on the basis of findings in soli state chemistry. It was suggested that transition metal cations would interact strongly with adjacent metal atoms. Burch [30, 45] and Bond [46] proposed a classification of the diversity of metal-support support effects known, and distinguished between weak (WMSI), medium (MMSI), and strong (SMSI) metal-support interactions. The WMSI occurs predominantly with transition metals supported on "nonreducible" oxides such as SiO_2, Al_2O_3 and MgO. This involves Van Der Waals interactions, and produces only minor modifications in the metal (e.g. a change in particle

structure). The MMSI is ascribed to transition metal particle interactions in zeolite channels. The SMSI is found mainly with group 8 - 10 transition metals supported on reducible (transition-metal) oxides such as TiO_2, V_2O_3, Nb_2O_5, Ta_2O_5 etc. after reduction at moderately high temperatures. The SMSI effect is usually defined as the suppression of H_2 and CO chemisorption of a transition metal on a reducible metal oxidic support system after a high-temperature reduction (HTR) at about 700 K - 800 K in hydrogen. It was suggested that reducible metal oxide cations on a surface could interact with supported metal crystallites via d-orbital overlap. Thus, a support could alter the behavior of a metal in a variety of ways. The much larger effects produced at lower temperatures, is the so-called "strong metal-support interaction" (SMSI) [47 - 49].

The physical blockage of adsorption sites seems to play an essential role for the diminution of H_2 and CO chemisorption capacity on SMSI systems. Besides this, there are direct (activation barrier of dissociative chemisorption, change of strengths of adsorptive bonds at selected surface sites) as well as indirect (creation and filling, respectively, of "new" surface sites) support influences on the electronic properties of the active metallic phase in several systems. The electronic support effects can come about via either the underlying oxide or the partly reduced support species on the metal particle [50].

In principle, there are two completely different explanations of the SMSI effect; a geometric and an electronic one [50]. The first involves simple physical blockage of adsorption sites on the metal by migration of partially reduced oxidic particles from the support. The second involves modification of the electronic state of the

metal by the influence of the support, resulting in a change of heats of adsorption or in a change of activation barriers for dissociation.

The SMSI occurs as a physico-chemical interaction between the phases that lowers the free energy of the system, but is also defined in terms of catalytic effects [29]. It has been reported in the literature [51 - 57] that heating metal supported SMSI type catalysts in hydrogen can bring about changes in catalytic behaviour. The catalysts undergo sintering with loss of surface area and reconstruction of exposed faces. Hydrogen may also be transferred between the metal and the support. These changes may, and do, alter catalytic properties. The support can also modify the activity or selectivity of a metal catalyst by directly participating in the catalyic reaction.

General trends in catalytic activities for SMSI metals have been reviewed recently. The main features can be described as follows [30]:

(1) For structure-insensitive reactions, such as hydrogenation, the activity decreases by less than about an order of magnitude and the selectivity for partial hydrogenation increases.
(2) For structure-sensitive reactions, such as hydrogenolysis, the activity decreases by several orders of magnitude.
(3) For the CO/H_2 reaction the activity increases by about one order of magnitude and the selectivity toward higher hydrocarbons in enhanced.

When group 8 - 10 metals, were supported on titania and reduced in hydrogen at high temperatures, it was observed that the H_2 and CO uptake dropped sharply. There was, however, litte change in the average metal particle size

metal by the influence of the support, resulting in a change of heats of adsorption or in a change of activation barriers for dissociation.

The SMSI occurs as a physico-chemical interaction between the phases that lowers the free energy of the system, but is also defined in terms of catalytic effects [29]. It has been reported in the literature [51 - 57] that heating metal supported SMSI type catalysts in hydrogen can bring about changes in catalytic behaviour. The catalysts undergo sintering with loss of surface area and reconstruction of exposed faces. Hydrogen may also be transferred between the metal and the support. These changes may, and do, alter catalytic properties. The support can also modify the activity or selectivity of a metal catalyst by directly participating in the catalyic reaction.

General trends in catalytic activities for SMSI metals have been reviewed recently. The main features can be described as follows [30]:

(1) For structure-insensitive reactions, such as hydrogenation, the activity decreases by less than about an order of magnitude and the selectivity for partial hydrogenation increases.
(2) For structure-sensitive reactions, such as hydrogenolysis, the activity decreases by several orders of magnitude.
(3) For the CO/H_2 reaction the activity increases by about one order of magnitude and the selectivity toward higher hydrocarbons in enhanced.

When group 8 - 10 metals, were supported on titania and reduced in hydrogen at high temperatures, it was observed that the H_2 and CO uptake dropped sharply. There was, however, litte change in the average metal particle size

[47 - 49]. The effect of reduction temperatures and the effect of the the SMSI (TiO_2) state on the ethanol conversion reaction, will be disscussed later in the thesis (section 3.4.1 and 4.3.8).

1.4 ETHANOL TRANSFORMATION REACTIONS

The formation of hydrocarbons from methanol was reported in the literature as long ago as 1880 [58]. However, the discovery by Mobil workers of the selective catalytic conversion of methanol to gasoline range (C_5 - C_{11}) hydrocarbons over zeolite catalysts has provided a landmark event in the area of catalysis [2, 39]. This finding led to the development of a number of new processes such as Methanol to Olefins (MTO), to Gasoline (MTG), to Chemical (MTC) and the Mobil-Olefins to Gasoline and Distillate (MOGD) processes.

The processes for the conversion of methanol to olefins (alkenes) and gasoline or hydrocarbons and/or high value chemicals over ZSM-5 [59 - 62], clinoptilolite [63] and SAPO molecular sieve acidic catalysts [64] etc. are now well established. The first commercial plant, for the transformation of methanol into hydrocarbons came on stream in 1985 and is located in New Zealand.

The search for alternative raw materials to make fuels or petrochemicals has extended the studies of the transformation of methanol to other alcohols and oxygenated compounds [39]. Methanol is itself obtained from fossil fuels like petroleum, natural gas or coal.

The transformation of ethanol, which can be produced from a renewable source like biomass, into hydrocarbons is potentially of great importance to countries like Brazil and India which have a large agricultural base. In these countries, ethanol is generally produced by the fermentation of molasses, a by-product of their huge sugar industries.

A considerable amount of information on the conversion of ethyl alcohol to ethene and/or hydrocarbons over zeolite (H-ZSM-5), alumina (γ-Al_2O_3) or other strong acid catalysts is available in the literature.

Usually, feed ethanol leads to practically the same product spectrum as feed methanol [39, 44] over strong acid catalysts. Table 1.2 lists typical distributions of the major hydrocarbon products resulting from the full conversions of methanol and ethanol over H-ZSM-5. Although the sets of yields differ in detail, they have a broad degree of similarity [65].

Table 1.2 Representative distributions of major organic products from conversions of reactant vapours over H-ZSM-5 zeolite at temperatures close to 700 K[a] [65]

Products	Reactant	
	Methanol	Ethanol
Propane	16	22
Butanes	24	30
Pentanes	9	10
$C6^+$ aliphatics	4	4
Toluene	11	11
C8 aromatics	17	15
C9 aromatics	8	4

[a] yields expressed as weight percentages of the organic products.

Ethanol could in the future be used as a feed stock in the commercial production of hydrocarbons, particularly when its production from biomass becomes economically feasible. The conversion of ethanol to hydrocarbons and/or aromatics on H-ZSM-5 zeolite is expected to occur on protonic acid sites. A possible reaction pathway is shown below [66]:

$C_2H_5OH \longrightarrow C_2H_4 \longrightarrow C_nH_{2n} \longrightarrow$

$\longrightarrow$ Aromatics + Saturated Hydrocarbons
(Primary)

$\downarrow$ isomerization/dealkylation

$\downarrow$ disproportionation

Aromatics (final product)

The reaction path of acid catalyzed hydrocarbon formation from ethanol (or other light alcohol) over strong acids such as zeolite ZSM-5 or silica-alumina may be viewed essentially as composed of three key steps: (1) ether formation, (2) initial C-C bond formation, and (3) aromatization with H transfer [67 - 70]. Overall studies suggest that gasoline can also be produced from ethanol by catalytic conversion over ZSM-5 type zeolites [71 - 73].

Ethylene and propylene are two very important basic organic chemicals and are the feedstocks for more than 30% of all petrochemicals [6]. Today the world production of ethylene and propylene is mainly from naphtha cracking or from processing of natural gas. Ethylene derived from ethanol (which is a replenishable feedstock) has obvious potential for countries with abundance of grain or sugar crops, such as South Africa, Brazil, India and the U.S.A.

Ethene can be made with near 100% specificity from biomass and subsequently could be used for making polyethylene [74].

potatoes ——> ethanol ——> ethene ——> polythene
or molasses (biomass) (all kinds)

The ethanol transformation reaction is thus dependent on catalytic selectivity. In fact two different reaction pathways are possible: dehydrogenation and dehydration. For instance, ethanol when passed over copper yields CH_3CHO directly

$C_2H_5OH \rightarrow CH_3CHO + H_2$

When ethanol is passed over alumina it produces ethene

$2C_2H_5OH \rightarrow C_2H_5OC_2H_5 + H_2O$ or $C_2H_5OH \rightarrow C_2H_4 + H_2O$ [75].

The dehydrogenation reaction is well known. Some examples are listed below.

The reaction path of acid catalyzed hydrocarbon formation from ethanol (or other light alcohol) over strong acids such as zeolite ZSM-5 or silica-alumina may be viewed essentially as composed of three key steps: (1) ether formation, (2) initial C-C bond formation, and (3) aromatization with H transfer [67 - 70]. Overall studies suggest that gasoline can also be produced from ethanol by catalytic conversion over ZSM-5 type zeolites [71 - 73].

Ethylene and propylene are two very important basic organic chemicals and are the feedstocks for more than 30% of all petrochemicals [6]. Today the world production of ethylene and propylene is mainly from naphtha cracking or from processing of natural gas. Ethylene derived from ethanol (which is a replenishable feedstock) has obvious potential for countries with abundance of grain or sugar crops, such as South Africa, Brazil, India and the U.S.A.

Ethene can be made with near 100% specificity from biomass and subsequently could be used for making polyethylene [74].

potatoes ——> ethanol ——> ethene ——> polythene
or molasses (biomass) (all kinds)

The ethanol transformation reaction is thus dependent on catalytic selectivity. In fact two different reaction pathways are possible: dehydrogenation and dehydration. For instance, ethanol when passed over copper yields CH_3CHO directly

$C_2H_5OH \rightarrow CH_3CHO + H_2$

When ethanol is passed over alumina it produces ethene $2C_2H_5OH \rightarrow C_2H_5OC_2H_5 + H_2O$ or $C_2H_5OH \rightarrow C_2H_4 + H_2O$ [75].

The dehydrogenation reaction is well known. Some examples are listed below.

A SiO_2-supported niobium monomer catalyst dehydrogenates ethanol with high activity and selectivity to give acetaldehyde in the temperature range 473°K - 573°K [76]. Recently, Matsumura et al. [77, 78] have also shown that silicalite-1 catalyzes ethanol dehydrogenation to acetaldehyde. On the basis of the IR spectra of ethanol adsorbed on its surface, the active sites are believed to be the active oxygen bridges on which dissociative adsorption of ethanol can take place.

In some recent studies the combination of two alcohols in a feed stream for reaction over strong acids I ave also been reported.

Isobutyraldehyde and its derivatives (e.g. isobutanol, isobutyric acid, and neopentyl glycol) are also very useful chemical feedstocks in the plastics industry [31]. Currently, isobutyraldehyde is obtained by separation of the by-products in the OXO process i.e. hydroformylation of propylene with CO and H_2 [79 - 91]. However, this is an energy-consuming and uneconomical process. On the other hand, recently, Wang and Lee [82] have shown that isobutyraldehyde can be synthesized from methanol and ethanol in a single-step over a V/TiO_2 (V = 2.5 wt.%) catalyst. Similarly, Reddy et al. [83] reported an efficient $CuO-ZnO-Al_2O_3$ catalyst for the selective production of isobutyraldehyde from methanol and ethanol (2:1 mol ratio) in one step. Operating temperatures are typically about 260°C - 410°C. Greater than 90% selectivity towards the formation of isobutyraldehyde was obtained at high con. sion (close to 100%) even in the presence of water (50% v/v).

Finally it is to be noted that the ethanol does not have to be pure. Some significant reports are mentioned below.

As mentioned above, ethanol can be derived from grain or sugar crops etc.. The well-know fermentation to ethanol can yield mixtures containing about 95% ethanol and 5% water. However, concentration from aqueous (5% - 20% EtOH) to absolute ethanol is a particularly energy-consuming process. Oudejans et al. [84] hav published data on the conversion of ethanol over zeolite (H-ZSM-5) in the presence of water in order to be able to combine a continuous fermentation of carbohydrates to ethanol with a continuous catalytic conversion of ethanol to a range of hydrocarbons. Moser et al. [85] also demonstrated that silicon-rich H-ZSM-5 catalyzed conversion of aqueous ethanol to ethene.

The Bioethanol-to-Ethene (B.E.T.E.) process which allows the production of practically pure ethene from aqueous ethanol (concentration of ethanol in the aqueous solution ranging from 2 - 19 vol.%) has been developed [86]. This process is a novel route to convert biomass to ethene in a fermentation broth. However, the ethene can be produced directly from ethanol fermentation broth in a one-step process using zeolite type catalysts.

Nguyen and Van Mao [87] have reported the use of a steam-treated and asbestos-derived ZSM-5 zeolite at reaction temperatures below 260°C - 270°C, for the conversion of aqueous ethanol. A two-step pathway with diethyl-ether as the intermediate was shown to coexist with the direct conversion-to-ethene route. These catalysts have also been shown to be suitable for low concentration of aqueous ethanol in the B.E.T.E. process [87, 88].

Titania generally has fairly low catalytic activity. But it possesses activity for alcohol dehydration and dehydrogenation although, of the two, the former function is more important [89].

1.5 AIMS OF THIS THESIS

Acidic catalysts such as zeolites [59, 87], amorphous silica-alumina [90] etc. have been investigated for the transformation of ethanol into a range of high value commodity chemicals. Further, transition-metal elements have also been shown to be active for the ethanol transformation reaction (via. dehydration and/or dehydrogenation of ethanol to ether and/or acetaldehyde) [25, 91, 92]. The role of a bifunctional catalyst (metal, strong acid support) for the same reaction has however been little explored. In these systems catalytic reactions involving either the metal and/or the support are possible. This thesis is therefore aimed at investigating the effect of metals on supports for the ethanol transformation reaction.

Ethanol conversion reactions have thus been investigated on γ-Al_2O_3, ion-exchanged clay, and a pillared interlayered clay to establish the effect of the strong acid function on the reaction [90, 93, 94]. In this thesis TiO_2 was also used as a support to assess if it would enhance a chemistry different to that of conventional supports. Addition of a secondary component to a catalyst should influence the product spectrum. Different metals (Al, Co, Cu, Ni, Pd, Pt, Rh, Ru) were loaded onto the TiO_2 to study this effect. Three possibilities exist: (a) the metal could induce reactivity; (b) the product(s) produced from the reaction of ethanol over TiO_2 could react further over the metal; (c) a synergic effect between the metal and TiO_2 culd give rise to a new product slate. To assess the influence of the metal on the reaction, a thorough study of reaction variables was undertaken. This involved studies on the

effect of metal loading, different metallic salt counterions and different catalyst preparation methods on the reaction. Furthermore, calcination and reduction temperatures were varied to determine optimum catalytic performance.

This thesis also involved an equilibrium study to determine whether the reactions investigated above were under equilibrium control. In this study a glass, fixed-bed continuous flow reactor was loaded with 2% Pd/TiO_2 catalyst and the equilibrium conversion of ethanol to diethyl-ether, ethene and acetaldehyde via dehydration and dehydrogenation reaction pathways were investigated.

REFERENCES

[1] J.C.R. Turner, in "Catalysis: Science and Technology", J.R. Anderson and M. Boudart (Eds.), Springer-Verlag, Berlin, Heidelberg, New York, Vol.1 (1981) Ch.2 p.65.

[2] S.L. Meisel, J.P. McCullough, C.H. Lechthaler and P.B. Weisz, Chem. Technol., 6 (1976) 86.

[3] J.W. Ward, J. Catal., 17 (1970) 355.

[4] H.W. Kouwenhoven, Adv. Chem. Series, 121 (1973) 529.

[5] P.A. Jacobs, "Carboniogenic Activity of Zeolites", Elsevier, New York, Amsterdam, 1977, p.85.

[6] E.G. Derouane, J.B. Nagy, P. Dejaifve, J.H.C. Van Hooff, B.P. Spekman, J.C. Védrine and C. Naccache, J. Catal., 53 (1978) 40.

[7] J.R. Anderson, T. Mole and V. Christov, J. Catal., 61 (1980) 477.

[8] U.A. Sedran and N.S. Figoli, Appl. Catal., 19 (1985) 317.

[9] G.A. Olah, H. Doggweiler, J.D. Felberg, S. Frohlich, M.J. Grdina, R. Karpeles, T. Keumi, S. Inaba, W.I.K. Lammertma, G. Salem and D.C. Tabor, J Am. Chem. Soc., 106 (1984) 2143.

[10] K. Tanabe, in "Catalysis: Science and Technology", J.R. Anderson and M. Boudart (Eds.), Springer-Verlag, Berlin, Heidelberg, New York, Vol.2 (1981) Ch.5 p.232.

REFERENCES

[1] J.C.R. Turner, in "Catalysis: Science and Technology", J.R. Anderson and M. Boudart (Eds.), Springer-Verlag, Berlin, Heidelberg, New York, Vol.1 (1981) Ch.2 p.65.

[2] S.L. Meisel, J.P. McCullough, C.H. Lechthaler and P.B. Weisz, Chem. Technol., 6 (1976) 86.

[3] J.W. Ward, J. Catal., 17 (1970) 355.

[4] H.W. Kouwenhoven Chem. Series, 121 (1973) 529.

[5] P.A. Jacobs, "C ... Activity of Zeolites", Elsevier, New Yo ... m, 1977, p.85.

[6] E.G. Derouane, J.B. Nagy, ... Dejaifve, J.H.C. Van Hooff, B.P. Spekman, J.C. Védrine and C. Naccache, J. Catal., 53 (1978) 40.

[7] J.R. Anderson, T. Mole and V. Christov, J. Catal., 61 (1980) 477.

[8] U.A. Sedran and N.S. Figoli, Appl. Catal., 19 (1985) 317.

[9] G.A. Olah, H. Doggweiler, J.D. Felberg, S. Frohlich, M.J. Grdina, R. Karpeles, T. Keumi, S. Inaba, W.I.K. Lammertma, G. Salem and D.C. Tabor, J Am. Chem. Soc., 106 (1984) 2143.

[10] K. Tanabe, in "Catalysis: Science and Technology", J.R. Anderson and M. Boudart (Eds.), Springer-Verlag, Berlin, Heidelberg, New York, Vol.2 (1981) Ch.5 p.232.

[11] M. Guisnet, in "Catalysis by Acids and Bases", B. Imelik et al. (Eds.), Elsevier, Amsterdam, (1985) p.283.

[12] H.A. Benesi, J. Amer. Chem. Soc., 78 (1956) 5490.

[13] J. Take, T. Tsuruya, T. Sateo and Y. Yoneda, Bull. Chem. Soc., Japan, 57 (1984) 1693.

[14] L.L. Murrell and N.C. Dispenziere Jr., J. Catal., 117 (1989) 275.

[15] T. Themistocleous, Ph.D. Thesis, University of the Witwatersrand, Johannesburg, 1990.

[16] J.T. Richardson, "Principles of Catalyst Development", Plenum press, New York, (1989) Ch.4 pp.49-82.

[17] J.B. Peri, J. Phys. Chem., 69 (1965) 211.

[18] J.B. Peri, J. Phys. Chem., 69 (1965) 231.

[19] D.H.R. Barton and J.M. Beaton, J. Am. Chem. Soc., 83 (1961) 4083.

[20] S. Yoshida in "Theoretical Aspects of Heterogeneous Catalysis", J.B. Moffat (Ed.), Van Nostrand Reinhold, New York, (1990) Ch.12.

[21] K. Tanabe, "Solid Acids and Bases", Kodansha, Tokyo & Academic press, New York, (1970) Ch.4.

[22] K. Tanabe, in "Catalysis: Science and Technology", J.R. Anderson and M. Boudart (Eds.), Springer-Verlag, Berlin, Heidelberg, New York, Vol.2 (1981) Ch.5 p.250.

[23] A.T. Bell, in "Catalyst Design: Progress and Perspectives", L.L. Hegedus (Ed.), John Wiley & Sons, New York, (1987) Ch.4 p.106.

[24] J.R. Anderson, "Structure of Metallic Catalysts", Academic press, London, (1975) Ch.2 pp.56-61.

[25] G.C. Bond, "Catalysis by Metals", Academic press, London, New York, 1962.

[26] G.C. Bond, "Heterogeneous Catalysis: Principles and Applications", Oxford, Univ. Press, 2nd Edn., (1990) Ch.9.

[27] B.C. Gates, J.R. Katzer and G.C.A. Schuit, "Chemistry of Catalytic Processes", McGraw-Hill Inc., New York, (1979) Ch.3.

[28] G.A. Somorjai, in "Catalyst Design: Progress and Perspectives", L.L. Hegedus (Ed.), John Wiley & Sons, New York, (1987) Ch.2.

[29] G.C. Bond and R. Burch, in "Catalysis", G.C. Bond and G. Webb (Eds.), Royal Society of Chemistry, London, Vol.6 (1983) p.27.

[30] R. Burch, in "Hydrogen Effects in Catalysis", Z. Paál and P.G. Menon (Eds.), Marcel Dekker, Now York, (1988) Ch.13 pp.347-360.

[31] C. Marcilly and J.P. Franck, in "Catalysis by Zeolites", B. Imelik et al. (Eds.), Elsevier, Amsterdam, (1980) p.99.

[32] S.M. Csicsery, J. Catal., 17 (1970) 205.

[33] S.M. Csicsery, J. Catal., 18 (1970) 30.

[34] T. Inui and F. Okazumi, J. Catal., 90 (9184) 366.

[35] N.S. Gnep and J.Y. Doyemet, Appl. Catal., 43 (1988) 155.

[36] T. Mole and J.R. Anderson, Appl. Catal., 17 (1985) 141.

[37] M.S. Scurrel, International Coal and Gas Conversion Conference, Pretoria, S. Africa, 24-27 August, 1987.

[38] H. Kifagawa, Y. Sendoda and Y. Ono, J. Catal., 101 (1986) 12.

[39] C.D. Chang and A.J. Silvestri, J. Catal., 47 (1977) 249.

[40] W.W. Kaeding and S.A. Butter, J. Catal., 61 (1980) 155.

[41] R. Le Van Mao, P. Levesque, B. Sjiariel and T.M Nguyen, Can. J. Chem. Eng., 64 (1986) 462.

[42] R.M. Cursetji, A.N. Singh and A.V. Deo, Chem. age of India, 37 (6) (1986) 407.

[43] R. Le Van Mao, P. Levesque and B. Sjiariel, Can. J. Chem. Eng., 64 (1986) 514.

[44] R. Le Van Mao, P. Levesque, G, McLaughlin and L.H. Dao, Appl. Catal., 34 (1987) 163.

[45] R. Burch and A.R. Flambard, J. Catal., 78 (1982) 389.

[46] G.C. Bond, in "Metal-Support and Metal-Additive Effects in Catalysis", B. Imelik et al. (Eds.), Elsevier, Amsterdam, (1982) p.1.

[47] S.J. Tauster, S.C. Fung and R.L. Garten, J. Amer. Chem. Soc., 100 (1978) 170.

[48] S.J. Tauster and S.C. Fung, J. Catal., 55 (1978) 29.

[49] Metal-Support Interactions in Catalysis, Sintering, and Redispersion, S.A. Stevenson et al. (Eds.), Van Nostrand Reinhold, Now York, 1987.

[50] H. Haberlandt in,"Theoretical Aspects of Heterogeneous Catalysis", J.B. Moffat (Ed.), Van Nostrand Reinhold, New York, (1990) Ch.8.

[51] M.A. Vannice, J. Catal., 74 (1982) 199.

[52] M.A. Vannice and C.C. Twu, J. Catal., 82 (1983) 213.

[53] B.H. Chon and J.M. White, J. Phys. Chem., 86 (1982) 3534.

[54] X.Z. Jiang, T.F. Hayden and J.A. Dumesic, J. Catal., 83 (1983) 168.

[55] D.E. Resasco and G.L. Haller, J. Catal., 82 (1983) 279.

[56] C.C. Kao, S.C. Tsai and Y.W. Chung, J. Catal., 73 (1982) 136.

[57] S.C. Fung, J. Catal., 76 (1982) 225.

[58] J.A. LaBel and W.H. Greene, Amer. Chem. J., 2 (1880) 20.

[59] C.D. Chang, W.H. Lang and R.L. Smith, J. Catal., 56 (1979) 169.

[60] W.J.H. Dehertog and G.F. Froment, Appl. Catal., 71 (1991) 153.

[61] J.C. Vedrine, P. Dejaifve and E.D. Garbowski, in "Catalysis by zeolites", B. Imelik et al. (Eds.), Elsevier Scientific Publishing Co., Amsterdam, (1980) p.29.

[62] M.G. Palekar and R.A. Rajadhyaksha, Catal, Rev. Sic. Eng., 28 (4) (1986) 371.

[63] G.J. Hutchings, T. Themistocleous and R.G. Copperthwaite, S. Africa, J. Chem., 41 (4) (1988) 157.

[64] A.J. Marchi and G.F. Froment, Appl. Catal., 71 (1991) 139.

[65] I.M. Campbell, "Catalysis at Surfaces", Chapman and Hall, I ndon, (1988) p.231.

[66] V.R. Choudhary and S.D. Sansare, Appl. Catal., 10 (1984) 147.

[67] C.D. Chang, "Hydrocarbons from Methanol", Catal. Rev. Sci. Eng., 25(1) (1983) p.41.

[68] L. Kubelková, J. Nováková and K. Nedomová, J. Catal., 124 (1990) 441.

[69] V.B. Kazansky, React. Kinet. Catal. Lett., 35 (1987) 237.

[70] J. Nováková and L. Kubelková, Catal. Lett., 1 (1988) 223.

[71] E. Costa, A. Uguina, J. Aguado and P.J. Hernandez, Ind. Eng. Chem. Process Des. Dev., 24 (1985) 239.

[72] G.A. Aldridge, X.E. Veryklos and R. Mutharasan, Ind. Eng. Chem. Process Des. Dev., 23 (1984) 733.

[73] D.R. Whitcraft, X.E. Veryklos and R. Mutharasan, Ind. Eng. Chem. Process Des. Dev., 22 (1983) 452.

[74] D.S. Davies, Chemistry and Industry, 20 Sept., (1975) 771.

[75] C.N. Satterfield, "Heterogeneous Catalysis in Practice", McGraw-Hill, New York, (1980) Ch.1 p.9.

[76] M. Nishimura, K. Asakura and Y. Iwasawa, J. Chem. Soc., Chem. Commun., (1986) 1660.

[77] Y. Matsumura, K. Hashimoto and S. Yoshide, J. Catal., 117 (1989) 135.

[78] Y. Matsumura, K. Hashimoto and S. Yoshida, J. Catal., 122 (1990) 352.

[79] B. Cornils, R. Payer and K.C. Traenckner, Hydrocarbon Process, 54 (1975) 83.

[80] F.E. Paulic, Catal. Rev., 6 (1972) 49.

[81] M. Orchin and W. Rupilius, Catal. Rev., 6 (1972) 85.

[82] F.L. Wang and W.S. Lee, J. Chem. Soc. Chem. Commun., (1991) 1760.

[83] B.M. Reddy, E.P. Reddy and B. Manohar, J. Chem. Soc. Chem. Commun., (1992) 997.

[84] J.C. Oudejans, P.F. Van Den Oosterkamp and H. Van Bekkum, Appl. Catal., 3 (1982) 109.

[85] W.R. Moser, R.W. Thompson, C.C. Chiang and H. Tong, J. Catal., 11[illegible] 989) 19.

[86] R. Le Van Mao, T.M. Nguyen and G. McLaughlin, Appl. Catal., 48 (1989) 265.

[87] T.M. Nguyen and R. Le Van Mao, Appl. Catal., 58 (1990) 119.

[88] R. Le Van Mao, T.M. Nguyen and J. Yao, Appl. Catal., 61 (1990) 161.

[89] M.E. Winfield, in "Catalysis", P.H. Emmett (Ed.), Reinhold Publishing Co., New York, Vol.7 (1960) p.93.

[90] R.A. Comelli and N.S. Figoli, Appl. Catal., 36 (1988) 299.

[91] J. Hensel and H. Pines, J. Catal. 24 (1972) 197.

[92] S.K. Saha and S. Sivasanker, Catalysis Lett., 15 (1992) 413.

[93] M.P. Atkins and I.M. Wren, S. Afr. Pat. 873734.

[94] J.A. Ballantine, M. Davies, I. Patel, J.H. Purnell, M. Rayanakorn, K.J. Williams and J.M. Thomas, J. Mol. Catal., 26 (1984) 37.

CHAPTER TWO

EXPERIMENTAL

2.1 CATALYST PREPARATION

In this project TiO_2 was investigated as the support. It is known to induce a strong metal support interaction (SMSI) between itself and any metal supported on the TiO_2. Addition of a secondary component to a catalyst can influence the product distribution [1, 2]. Successful catalytic applications are usually found for the d-electron transition metals [3, 4]. Hence the metals used in this study were mainly choosen from the d-orbital metals in groups 8 - 10 (Co, Ni, Ru, Rh, Pd, Pt and Cu). Aluminum as a promoter was also studied.

Catalysts involving group 8 - 10 metals are usually prepared by dispersing the metal onto the support surface [5]. Various metal loadings were used in this study, typically results using impregnations giving nominally 1 to 5 wt.% metal loadings (weight percent defined as the ratio of the mass of the metal to sum of the masses of the metal plus support).

Two techniques were used to obtain the metal loaded support: Incipient wetness techniques and precipitation methods. The two methods of preparation of the catalysts are described in Appendix 1.

Incipient wetness impregnation was used to introduce a known amount of metal precursor onto the surface of the support [6, 7]. The samples were prepared by incipient wetness impregnation with aqueous metal salts (e.g. $Ni(NO_3)_2 \cdot 6H_2O$, $Co(NO_3)_2 \cdot 6H_2O$, $Pd(NO_3)_2 \cdot H_2O$ etc.), onto the support (TiO_2, Degussa, Titandioxid P 25). They were then dried at 110°C for 16 h and then ground to a fine powder with pestle and mortar. Certain catalysts were calcined at 400°C for 16 h in air. After calcination the samples were reground to a fine powder.

A second method of catalyst preparation was co-precipitation. This was used for the preparation of Pd and Pt supported on TiO_2. The sample preparations were based on procedures outlined in Appendix 1 [8, 9]. Typically, 10.0 g of TiO_2 (Degussa, Titandioxid P 25) was added to 150 ml of distilled water. The slurry was stirred and the solution temperature was maintained at 75°C to 80°C. This slurry was titrated very slowly with the metal salt in nitric acid solution and ammonia solution, and the pH of the sample solution was maintained at 8 - 9. Thereafter the suspension of supersaturated solution was filtered, extruded and dried. Determination of the metal content in the above samples was performed by Atomic Absorption (AA) Spectrophotometry using standards of titanium dioxide impregnated with known amounts of metal (1% to 5% by mass), using the incipient wetness technique. In this way, the catalyst could be accurately assayed for the metal content on supported TiO_2.

A blank TiO_2 support (5.0 g) was completely wetted with 7.5 ml of distilled water and stirred to make a white paste. The paste was dried at 110°C for 3 h and ground to a fine powder, after which it was calcined in air at 400°C for 16 h prior to use.

The catalysts were reduced in situ with hydrogen at different temperatures for 16 h at atmospheric pressure before being used in the reactor.

2.2 CATALYST TESTING APPARATUS

Stainless steel of 1/8" (OD) and glass tubing were used for interconnections in the reactor. A J-type thermocouple temperature controller was used to control temperature and to heat the heating tapes of the interconnections. A powered temperature controller (PN-4A1C-M, RKC instruments Inc.) was used to heat and control the temperature of the reactor. The heating tapes were lagged with glass fibre insulation. The flow-rate control was monitored by rotameter needle valves (union bonnet metering valve, micro-metering valve). This combination allowed for very fine control of the flow-rate.

The reactor used was a tublar downflow Pyrex microreactor which could reach a maximum temperature of 500°C. The reactor was heated by a nichrome wire wound round the inner glass tube of the unit. Two thermocouples (iron/copper-nickel type K) were used to monitor and control the temperature of the reactor. The thermocouple used for monitoring the temperature was inserted into the thermocouple well and extended into the centre of the catalyst bed. Another thermocouple was inserted from the bottom of the heating unit, so that its tip was level with the catalyst bed (see Figure 2.2). The catalyst bed temperature was established by electrical heating and thermostatically controlled to within 1°C. The temperatures were relayed to a multiselector and digital disply (RKC instruments Inc.). The experimental apparatus is shown in

Figure 2.1, and a detailed design of the Pyrex microreactor and heating unit is shown in Figure 2.2.

Two systems were used to feed hydrocarbon reagents to the reactor. For higher boiling point liquids e.g. ethanol, liquid was loaded into a Hamilton series 1010 Gastight syringe and pumped through the reactor by means of a syringe pump (Sage instruments, model 355). Volatile reagents (e.g. acetaldehyde) were vapourised at a regulated temperature in a Dreschel bottle using dry carrier gas (N_2, H_2) at a constant flow rate. Different feed rates were required for individual runs and were achieved by adjusting the temperature of the Dreschel bottle. The weight hourly space velocity (WHSV = mass of reactant(gram)/gram of catalyst/hour) of the reactants could be varied by control of the vapourization temperature.

The vapourized feed was used with nitrogen gas and to avoid condensation of the feed before it reached the reactor, the lines between the evaporation chamber and the reactor were heated with electric heating tape. A 3-way loop with on-off tapes between the evaporation chamber and the reactor allowed for reactor by-pass when needed.

The reactor normally contained 0.1 - 2.0 g of catalyst which was dried <u>in situ</u> under a stream of nitrogen at 100°C prior to reduction with hydrogen and before commencement of the reaction.

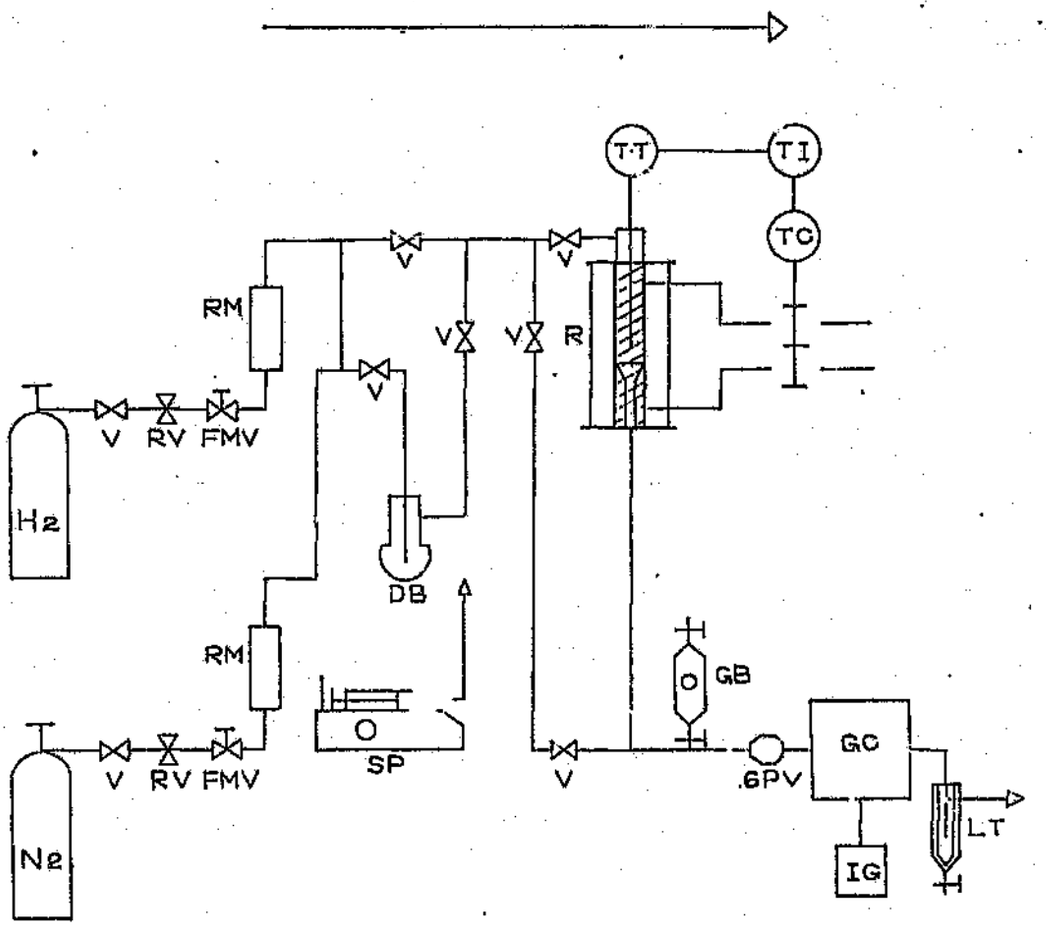

Legend

H_2 = Reduction gas supply	N_2 = Carrier gas supply
FMV = Fine metering value	V = On-Off value
6PV = 6 port value	TT = Thermocouple
DB = Dreschel bottle	RV = Regulating value
TI = Temperature indicator	RM = Rotometer
TC = Temperature Controller	SP = Syringe pump
LT = Liquid trap	IG = Integrator
R = Reactor	GB = Gas bomb
GC = Gas Chromatograph (FID detector)	

Figure 2.1 Schematic diagram of catalyst testing apparatus

The catalyst testing reactor was connected on-line to a gas chromatograph for product analysis. The GC was equipped with a flame ionization detector (FID). The FID was chosen because of its high sensitivity towards hydrocarbons [10, 11]; The column was placed in a temperature programmable oven. The GC set-up function and temperature programme used in the experiment are listed in Appendix 2.1

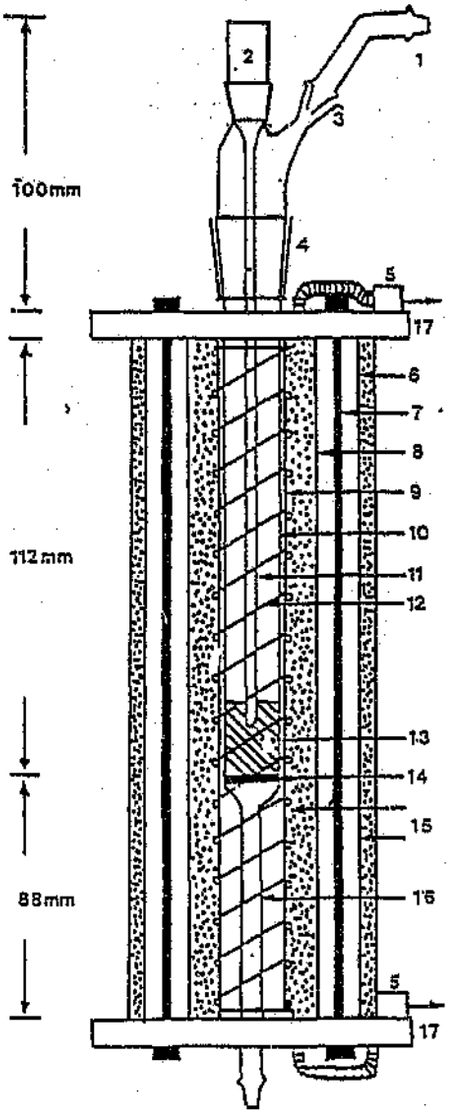

Key:

1. Ethanol - N_2 feed
2. Thermocouple well
3. B-10 ground glass joint
4. B-19 reactor head joint
5. Electrical connection block
6. Outer glass tube - 50 mm dia
7. Brass bolt
8. Insulating glass tube
9. Heating tube - 22 mm dia
10. Reactor tube - 18 mm dia
11. Thermocouple well - 4 mm dia
12. Nichrome heating wire
13. Catalyst
14. Sintered glass frit
15. Glass fibre
16. Reactor exit tube - 8 mm dia
17. Asbestos plate

Figure 2.2 Pyrex microreactor and heating unit

The reactor was connected via a 6 port valve, housing a 0.23 ml sample loop to a Packard model 428 GC. The 6 port valve was pneumatically operated and controlled from the Spectra-Physics (Chrom-Jet) integrator which had an external events cartridge to facilitate automation of gas sampling and analysis.

The vent passed through a gas sample bomb fitted with a subaseal septum so that off-line gas syringe (Precision sampling Corp., Pressure-Lock) analyses could be performed. A bubble flow meter situated after the gas sample vessel was used for measurement of flowrates. Exit gases were passed through a liquid trap to catch liquid products.

A two meter 1/8 inch stainless steel Porapack Q column (Water Associates Inc., mesh 80 - 100) was used for separating products. Appendix 2.2 lists the retention times of different components expected as products in this study.

2.3 DATA MANIPULATION

The gas chromatograph was connected to an intergrator (Spectra-Physics, model Chrom-Jet, double channel) for data capture.

The area counts of the various components were subsequently corrected to take into account the differing responses of the detector to each component.

Response factors [12, 13] were determined by injection of standard gas samples of C_1 - C_4 hydrocarbons, or their mixtures, as well as chemically pure reagents such as EtOH, Et_2O, and MeCHO. A sample GC trace and the definitions of conversion and selectivities are shown in Appendix 3.

2.4 OTHER APPARATUS AND TECHNIQUES USED FOR CATALYST CHARACTERIZATION

Off line G.C. Analysis

Catalysts were characterized using a variety of techniques as described below.

On occasion desired products were analyzed off-line using a Pye-Unicam series 204 GC (with temperature programmer and a two meter 1/8" stainless steel Porapack Q column) connected to a VG Quadrupoles Instruments Limited Mass Spectrometer. The apparatus was equipped with a computer network using a software package (Micromass PC from VG Quadrupoles Limited) permitting a residual gas analysis (RGA).

Differential Scanning Calorimetry (DSC)

The catalyst reduction temperatures were determined using a Du Pont instuments 910 DSC analyzer. Oxygen was removed from the metal by passing a stream of hydrogen gas over the sample; and a reference material was maintained at same temperature ($\Delta T = T_s - T_r = 0$) throughout the controlled temperature programme. Thermal events in the sample thus appear as deviations from the DSC baseline, in either an endothermic or exothermic direction, depending upon whether more or less energy has to be supplied to the sample relative to the reference material [14]. The signal-plots obtained can be correlated with the reduction temperature for the sample.

Thermo-Gravimetric Analyzer (TGA)

Water desorption from the catalysts, and changes in sample mass as a function of temperature were performed on a Du Pont 951 TGA linked to a Du Pont 9900 computer/thermal analyzer. The TGA was also used extensively in studying the reactivation of deactivated catalysts [14].

Atomic Absorption spectrophotometer (AA)

The TiO_2 support was impregnated with a metal (metal = Ni, Cu, Co, Ru, Rh, Pd etc.) and metal loading was ascertained by means of an emission AA spectrophotometer (Varian, AA-1275 series spectrophotometer).

BET Surface Area Measurements

Determination of the total surface area of a catalyst sample by physical adsorption was obtained from BET adsorption isotherm measurements [15, 16]. The measurements were performed on an apparatus constructed in our laboratory by group members. Typical operating conditions, as established previously for measurements using nitrogen as an adsorbate, were used.

A 30% nitrogen in helium stream was used as the carrier gas. This gas was passed over the catalyst while liquid nitrogen in a Dewar flask was raised over the U-tube

containing the catalyst. This caused the gaseous nitrogen to adsorb onto the surface of the catalyst, and an imbalance in the TCD detector in the GC to occur. Thereafter the Dewar flask was lowered and the U-tube heated. This caused the adsorbed nitrogen to be desorbed and a corresponding imbalance in the TCD detecter was found. This was monitored on a model SP 4290 Spectra-Physics integrator. The area count of the detected peak was then related to a volume of nitrogen adsorbed onto the surface by calibration of known volumes of nitrogen passed through the GC.

REFERENCES

[1] S.J. Tauster, S.C. Fung and R.L. Garten, J. Am. Chem. Soc., 100 (1978) 170.

[2] G.C. Bond and R. Burch, in "Catalysis", G.C. Bond and G. Webb (Eds.), Royal Society of Chemistry, London, 6 (1983) 27.

[3] J.T. Richardson, "Principles of Catalyst Development", Plenum press, New York, (1989) Ch.4 p.51.

[4] G.A. Somorjai, in "Catalyst Design: Progress and Perspectives", L.L. Hegedus (Ed.), John Wiley & Sons, New York, (1987) Ch.2 p.20.

[5] A.T. Bell, in "Catalyst Design: Progress and Perspectives", L.L. Hegedus (Ed.), John Wiley & Sons, New York, (1987) Ch.4 pp.103-136.

[6] C.N. Satterfield, "Heterogeneous Catalysis in Practice", McGraw-Hill, New York, (1980) Ch.4.

[7] R.B. Anderson, in "Catalysis", P.H. Emmett (Ed.), Reinhold Publishing Co., New York, Vol.4, 1956.

[8] V.A. Dzisko, in "The Bases of Methods of the Catalysts Preparation", Nauka (Ed.), Novosibirsk, 1983 (USSR).

[9] J.T. Richardson, "Principles of Catalyst Development", Plenum press, New York, (1989) Ch.6 pp.95-133.

[10] A.B. Littlewood, "Gas chromatograph, Principles, Techniques, and Applications", 2nd Edn., Academic press, London, (1970) p.280.

[11] C.J. Cowper and A.J. DeRose, "The Analysis Gases by Chromatography", Pergamon press, Oxford, Vol.7 (1983) Ch.5 and 6.

[12] W.A. Dietz, J. Gas Chromatog., 5 (1967) 68.

[13] J.T. Scanion and D.E Wllls, J. of Chromatographic Science, 23 (1985) 333.

[14] M.E. Brown, "Introduction to Thermal Analysis: Techniques and Applications", Chapman and Hall, New York, 1988.

[15] P.H. Emmett, "Catalysis", Reinhold Publishing Co., New Yorl., Vol.I (1954) Ch.1 and 2.

[16] J.M. Thomas and W.J. thomas, "Introduction to the Principles of Heterogeneous Catalyst", Academic press, London, (1967) p.45.

CHAPTER THREE

INVESTIGATION OF THE ETHANOL TRANSFORMATION REACTION USING METAL SUPPORTED TITANIUM DIOXIDE CATALYSTS AND ALUMINA SUPPORTS

3.1 INTRODUCTION

The acidic nature of TiO_2 can be used to induce chemical reactions which require the presence of strong acids. An example of a reaction that requires an acid catalyst is the conversion of alcohols into alkenes, ethers and longer chain products.

To further investigate the above reaction, modification of the catalyst can be induced by adding metals or other chemicals to the TiO_2 support. The changes that can be induced by the use of modified TiO_2 include:

(1) The acidity of the TiO_2 can be changed.
(2) The added material can react with the EtOH prior to the TiO_2; the TiO_2 will then act on the secondary products.
(3) The TiO_2 could induce the normal alcohol conversion reactions and the products could react with the added material.

To explore these possibilities a study has been undertaken of the reaction of a variety of modified TiO_2 catalysts and

the alcohol chosen for investigation was ethanol. The reason for the choice of ethanol as a reagent alcohol has been described in Chapter one. An investigation of the effect of Al, Co, Cu and Ni supported on TiO_2 on the ethanol transformation reaction is described in this Chapter.

Comparative studies using Al pillared montmorillonite and γ-Al_2O_3 were also performed to assess the effect of Al and different counterions on the above reaction.

3 ? EXPERIMENTAL

Al, Co, Cu and Ni were supported on TiO_2 (1% - 2% by mass). The catalysts were prepared from metal nitrates using the incipient wetness technique described in Appendix 1. These catalysts were individually used in the ethanol conversion reaction.

The study was carried out in a glass Pyrex reactor in the temperature range 100°C - 400°C under atmospheric pressure as described previously (see Chapter two, section 2.2). The catalyst (1.0 g, fine powder form, < 200 μm) was placed in the reactor and dried at 110°C for 3 hours in a flow of nitrogen gas. Reduction gas (hydrogen) was then fed (flow rate: 21 ml min^{-1}) over the catalyst at 200°C (or 400°C) for 16 hours. Ethanol (aqueous ethanol 96%, water 4%, v/v) was then fed over the catalyst in a stream of nitrogen gas (flow rate, 1.26 liter h^{-1}; ethanol feed, 1.0 ml h^{-1})

3.3 RESULTS

3.3.1 Reaction of ethanol over metal free TiO_2

The metal free TiO_2 support was calcined at 400°C/16 h and tested as a catalyst in the ethanol conversion reaction and results are listed in Table 3.1. The table shows the selectivity and conversion data obtained at various reaction temperatures. Ethanol conversion started at approximately 225°C and increased with increasing temperature. Diethyl-ether was the major initial product (maximum yield 17.70 wt.%; 348°C). At 398°C maximum ethanol conversion was reached (54.28 wt.%) with conversion to a wide range of hydrocarbons (C_1 to C_6^+) and a small amount of acetaldehyde (1.13 wt.%). Analysis of products at high temperature (398°C) indicates that even numbered hydrocarbons are favoured. However, at these temperatures the main products were C_2 hydrocarbons (ethene: 16.62 wt.%, ethane: 14.71 wt.%).

3.3.2 Reaction of ethanol over Al/TiO_2

The effect of alumina loading on TiO_2 was monitored using 0.36%, 0.72% and 2% alumina levels and compared to 0% loading i.e. metal free TiO_2. The influence of reduction temperatures on the reaction was also investigated. The catalysts were each reduced at 200°C and 400°C and individually tested for ethanol conversion. The results, shown in Tables 3.2 to 3.5 and Figures 3.1 and 3.2,

indicate that 0.36% Al/TiO_2 reduced at 400°C gave high ethanol conversions, and about twice the yield of diethyl-ether, when compared to metal free TiO_2. However, at higher reaction temperature (*ca.* 400°C) the metal free TiO_2 and the 0.36% Al/TiO_2 reduced at 400°C seem to have similar catalytic activity.

In all cases, for the various Al/TiO_2 catalysts, conversion increased with increasing temperature between *ca.* 200°C - 350°C, after which the conversion appeared constant (see Figure 3.1). The product spectra obtained when using these catalysts were similar to the product spectrum obtained using metal free TiO_2. However the addition of Al to TiO_2 enhances the conversion to longer chain liquid hydrocarbon (C_6^+) products. As in the case of metal loaded catalysts (see below), there is a good correlation between metal concentration and C_6^+ selectivity; the higher the Al concentration the higher the C_6^+ hydrocarbon content (see Table 3.15).

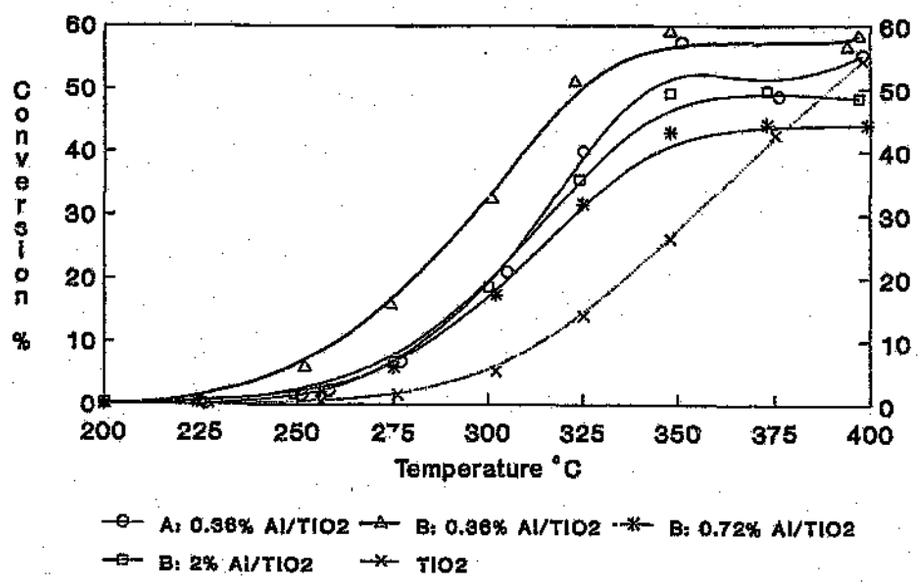

Figure 3.1 Effect of varying the Al concentration and reduction temperature for Al/TiO_2 catalysts in the ethanol transformation reaction (A: reduced at 200°C; B: reduced at 400°C)

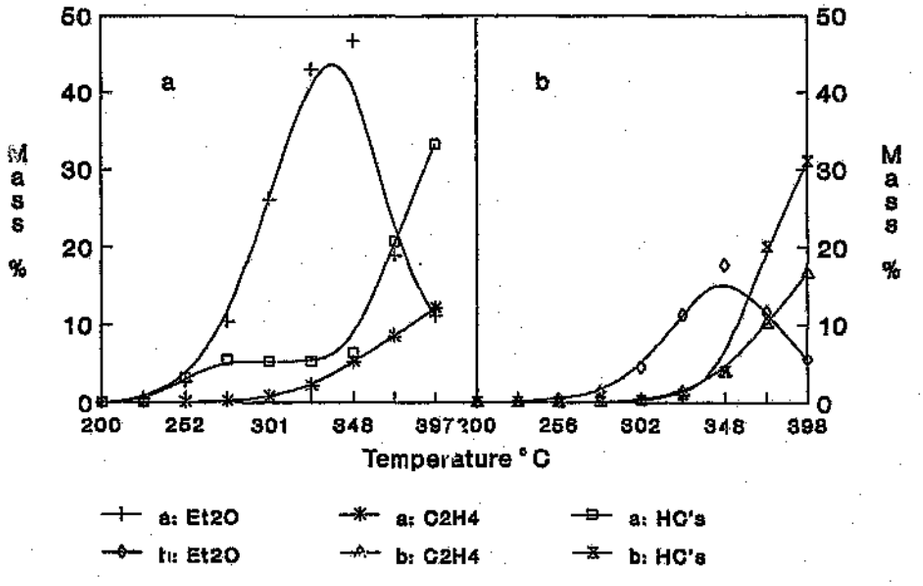

Figure 3.2 Comparison of the catalytic selectivity of the 0.36% Al/TiO_2 and metal free TiO_2 catalysts (a: Al/TiO_2 reduced at 400°C; b: metal free TiO_2 reduced at 400°C)

3.3.3 Reaction of ethanol over Co/TiO_2 and Cu/TiO_2

The 1%, and 2% Co/TiO_2 and 1.3% Cu/TiO_2 (% by mass) catalysts were reduced at 200°C and 400°C. These catalysts were examined in the ethanol transformation to hydrocarbon reaction at various temperatures between 100°C and 400°C. The results are shown in Tables 3.6 to 3.10 and Figures 3.3 and 3.4. Results from the use of the metal free TiO_2 support are included for comparison. Generally, the metal containing catalysts showed catalytic activity and a product spectrum similar to that of metal free TiO_2. Only at temperatures approaching 400°C was appreciable selectivity towards C_6^+ products observed (see Table 3.15).

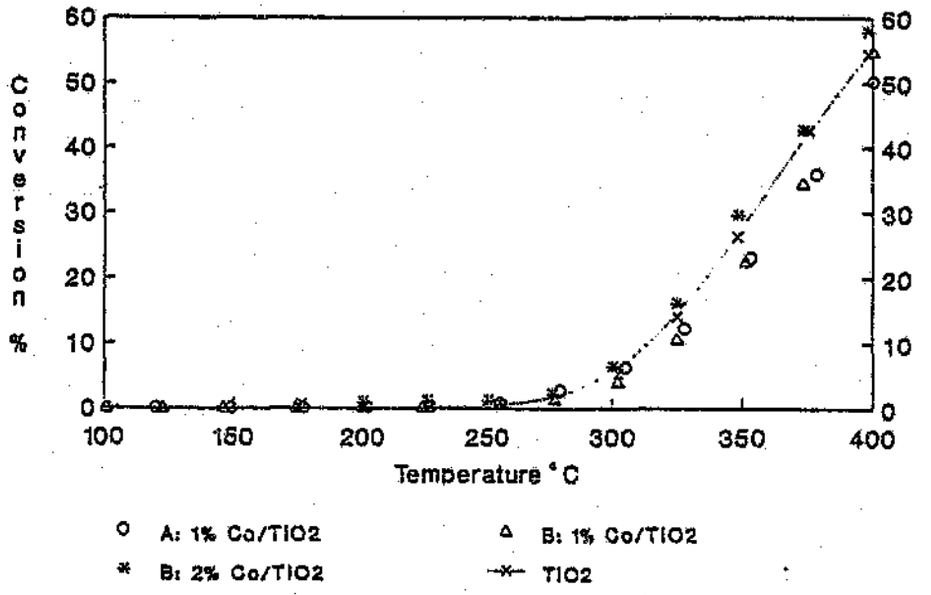

Figure 3.3 Effect of Co concentration and reduction temperature on Co/TiO_2 catalysts in the ethanol transformation reaction (A: reduced at 200°C; B: reduced at 400°C)

Table 3.15 Influence of metal loaded TiO_2 catalysts on C_6^+ hydrocarbon yield[a]

Catalyst (1.0 g)	Reduction[b] (°C)	Conversion (%)	C_6^+ (%)
TiO_2	400	54.28	6.72
0.36% Al/TiO_2	200	55.24	10.00
0.36% Al/TiO_2	400	58.29	10.87
0.72% Al/TiO_2	400	44.10	11.98
2% Al/TiO_2	400	48.43	14.35
1% Co/TiO_2	200	50.14	10.42
1% Co/TiO_2	400	54.77	9.29
2% Co/TiO_2	400	57.79	32.31
1.3% Cu/TiO_2	200	63.95	16.15
1.3% Cu/TiO_2	400	48.47	10.20
1% Ni/TiO_2	200	52.06	19.62[c]
1% Ni/TiO_2	400	70.38	27.10[c]
2% Ni/TiO_2	200	66.57	22.51[c]
2% Ni/TiO_2	400	71.30	17.93[c]

[a] Reaction temperature *ca.* 400°C; Metal loaded TiO_2 by mass percentage

[b] Catalyst reduced at 400°C or 200°C for 16 h in H_2

[c] C_5^+ liquid hydrocarbons

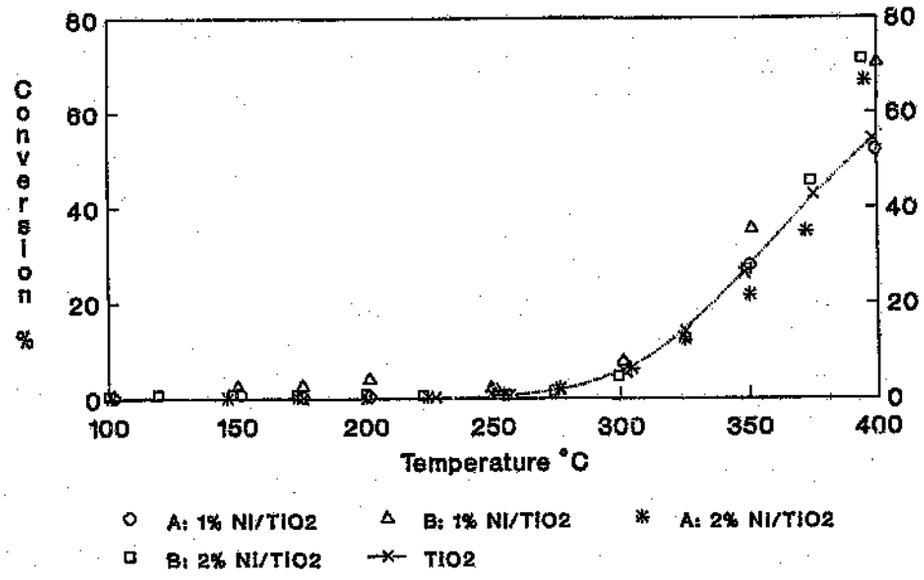

Figure 3.5 Effect of Ni concentration and reduction temperature on the Ni/TiO_2 catalysts used in the ethanol transformation reaction (A: reduced at 200°C; B: reduced at 400°C)

Lifetime experiments were carried out for 80 h on a 1% Ni/TiO_2 (reduced at 200°C and 400°C) and metal free TiO_2 catalyst (at 400°C). From figure 3.6, it is clear that the reduced catalyst (400°C) exhibited longer catalytic lifetime than metal free TiO_2. Furthermore, the rate of loss in acti ity is much slower for the 1% Ni/TiO_2 reduced at 400°C than at 200°C.

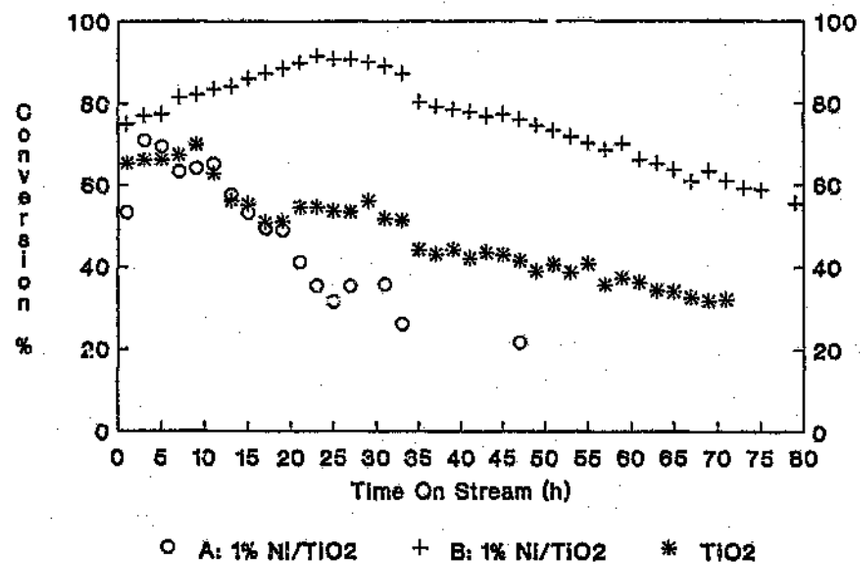

Figure 3.6 Comparison of the effect of reduction temperature of 1% Ni/TiO_2 and metal free TiO_2 on catalyst lifetime (T = 400°C; A: reduced at 200°C; B: reduced at 400°C)

For the 1% Ni/TiO_2 catalyst reduced at 400°C, the ethanol conversion after one hour was 75%. This increased with time on line and reached *ca.* 90% (*ca.* 30 h), then slowly decreased to *ca.* 55% (*ca.* 80 h). Analysis of the liquid products showed that C_5^+ hydrocarbon production remained constant for much longer time periods than the 1% Ni/TiO_2 (reduced at 400°C). A rapid decrease in the yield of diethyl-ether was found to occur within 30 hours (*ca.* from 14% to 3%). On the contrary, metal free TiO_2 showed a rapid increase in the yield of diethyl-ether (see Figure 3.7). However, the decrease in concentration of the primary product, viz. diethyl-ether, in the product mixture can be related to the favourable formation of C_1 - C_4 gaseous hydrocarbon products (within 30 h, mainly C_2). On the other hand, the metal free TiO_2 was found to show a rapid decrease in gaseous (mainly C_2) hydrocarbon products (see Figure 3.8).

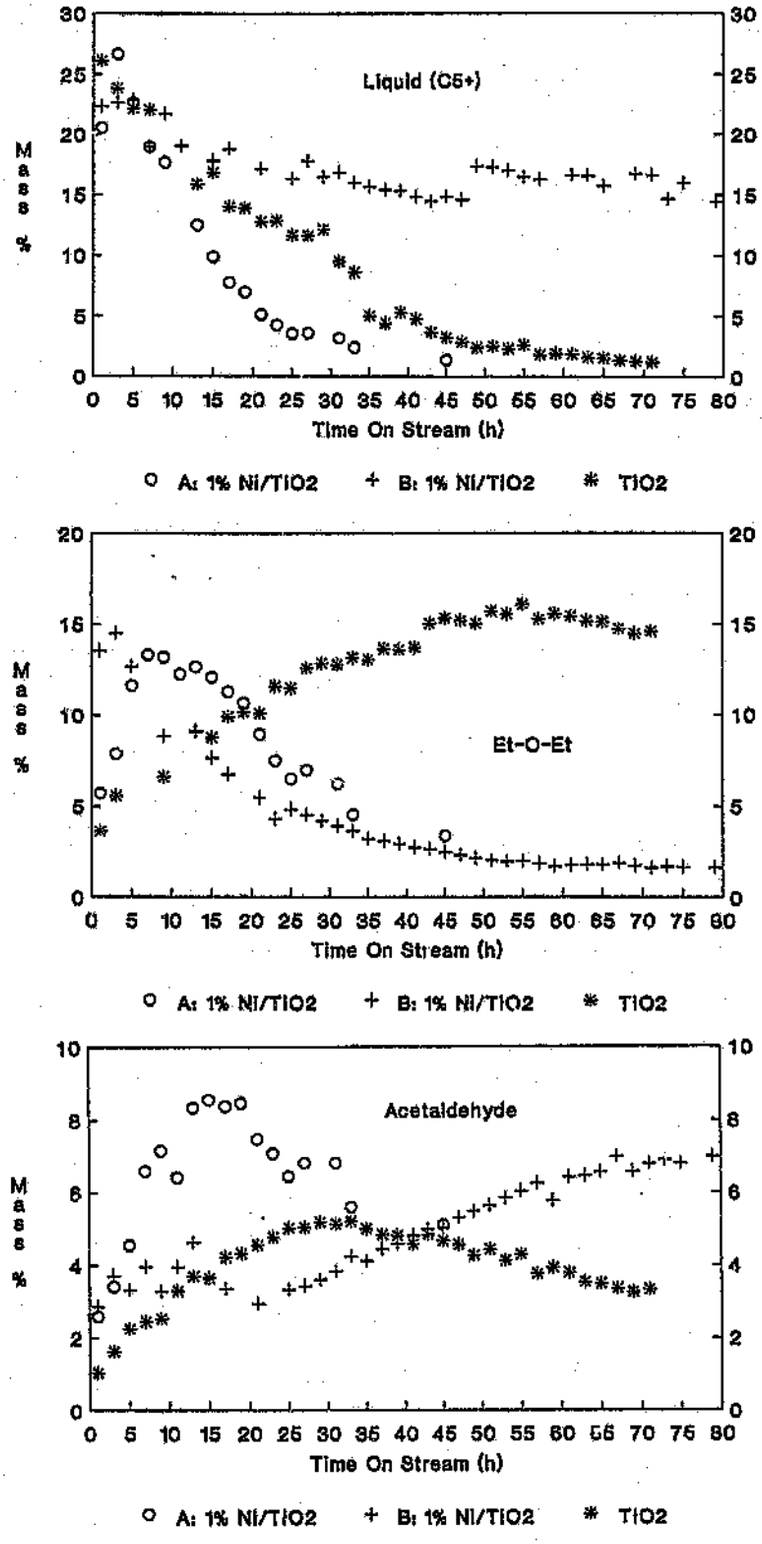

Figure 3.7 Liquid product distribution obtained from 1% Ni/TiO_2 and metal free TiO_2 catalysts (T = 400°C; A: reduced at 200°C; B: reduced at 400°C)

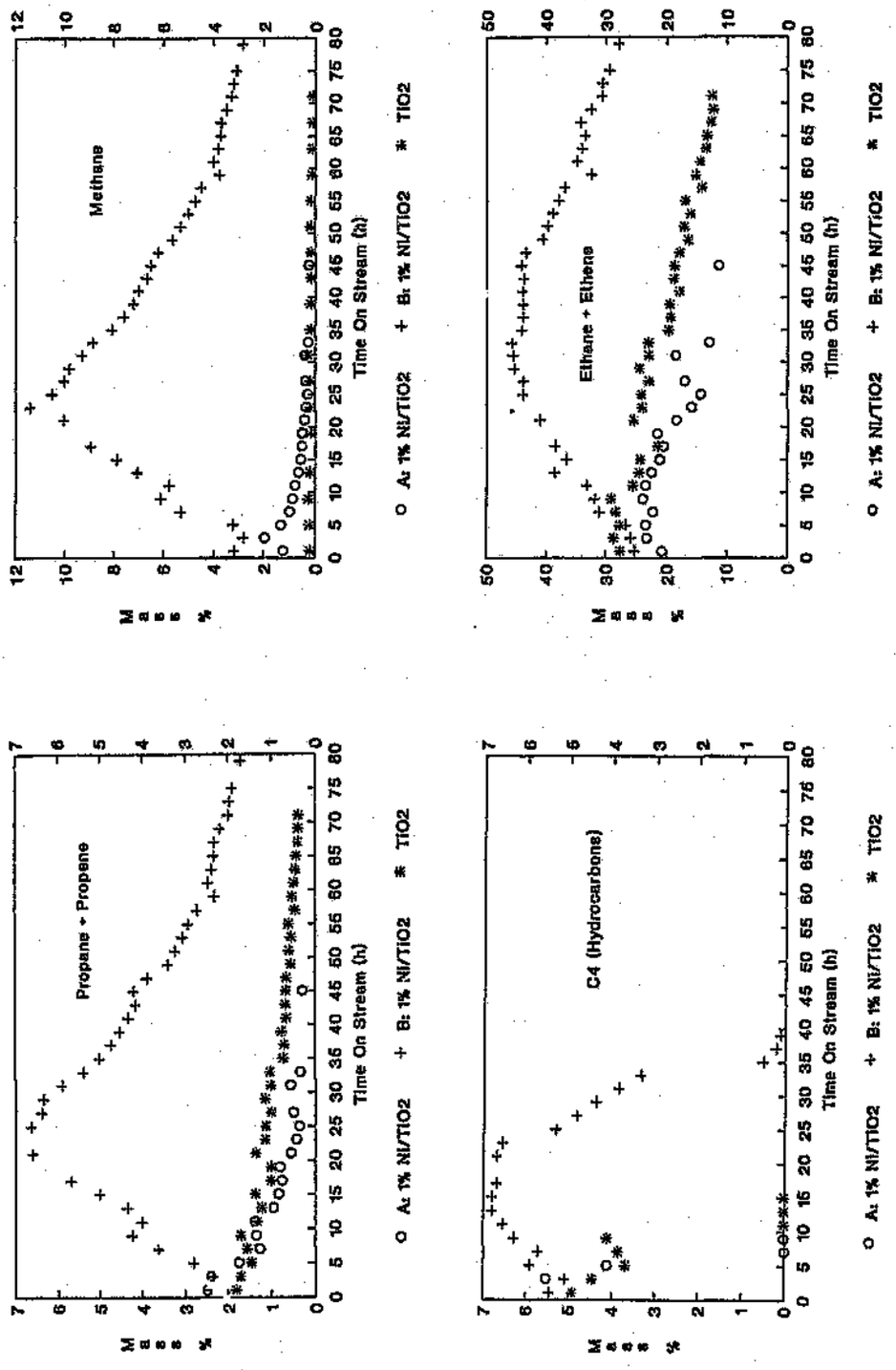

Figure 3.8 Gaseous product distribution obtained from 1% Ni/TiO_2 and metal free TiO_2 catalysts (T = 400°C; A: reduced at 200°C; B: reduced at 400°C)

Table 3.1 Reaction of ethanol over metal free TiO_2; Catalyst reduced at 400°C

Temp. (°C)	Conv. %	Product distribution (% by mass) Et_2O	C_2H_4	CH_3CHO	HC's[a]
175	0	0	0	0	0
200	0	0	0	0	0
2.	0.07	0.07	0	0	0
256	0.47	0.45	0.02	0	0
276	1.47	1.34	0.07	0.04	0.02
302	5.16	4.49	0.35	0.12	0.20
325	13.95	11.20	1.43	0.27	1.05
348	26.13	17.70	3.95	0.52	3.96
375	42.58	11.61	10.10	0.87	20.00
398	54.28	5.53	16.62	1.13	31.00

[a] Other hydrocarbons

Temp. (°C)	Other hydrocarbons distribution (% by mass) CH_4	C_2H_6	C3	C3=	C4	C5	C6+
348	0.01	2.12	0	0.08	0	0	1.76
375	0.05	8.63	0	0.63	0	1.64	9.05
398	0.16	14.71	0.13	1.58	3.53	4.17	6.72

Table 3.2 Reaction of ethanol over 0.36% Al/TiO_2; Catalyst reduced at 200°C

Temp. (°C)	Conv. %	Product distribution (% by mass) Et_2O	C_2H_4	CH_3CHO	HC's[a]
251	1.40	1.40	0	0	0
258	2.12	2.12	0	0	0
277	6.61	6.30	0.21	0	0.10
305	20.87	19.62	0.63	0.23	0.39
325	39.84	35.88	1.91	0.49	1.56
351	57.29	42.56	4.83	0.69	9.21
376	48.75	23.34	7.69	0.93	16.79
398	55.24	9.79	12.96	1.36	31.13

[a] Other hydrocarbons

Temp. (°C)	Other hydrocarbons distribution (% by mass) CH_4	C_2H_6	C3	C3=	C4	C5	C6+
351	0	2.81	0	0.12	0	0.43	0.57
376	0.06	7.75	0	0.51	1.23	0.18	7.06
398	0.17	13.01	0	1.29	3.66	3.00	10.00

Table 3.3 Reaction of ethanol over 0.36% Al/TiO_2; Catalyst reduced at 400°C

Temp. (°C)	Conv. %	Product distribution (% by mass) Et_2O	C_2H_4	CH_3CHO	HC's[a]
225	0.45	0.45	0	0	0
252	5.85	2.68	0	0	3.17
274	15.81	10.33	0.12	0	5.36
301	32.53	26.16	0.79	0.31	5.27
323	50.97	43.01	2.16	0.49	5.31
348	59.04	46.76	5.21	0.68	6.39
378	49.30	18.94	8.52	1.13	20.71
397	58.29	11.15	12.19	1.72	33.23

[a] Other hydrocarbons

Temp. (°C)	Other hydrocarbons distribution (% by mass) CH_4	C_2H_6	C3	C3=	C4	C5	C6+
348	0	2.86	0	0.13	0	0.49	2.91
378	0.06	9.36	0	0.70	0	1.83	8.76
397	0.19	13.44	0	1.39	3.99	3.35	10.87

Table 3.4 Reaction of ethanol over 0.72% Al/TiO_2; Catalyst reduced at 400°C

Temp. (°C)	Conv. %	Product distribution (% by mass) Et_2O	C_2H_4	CH_3CHO	HC's[a]
224	0.21	0.21	0	0	0
256	1.99	1.98	0.01	0	0
275	5.76	5.66	0.03	0.05	0.02
302	17.27	16.74	0.18	0.12	0.23
325	31.63	30.10	0.61	0.23	0.69
348	43.03	37.83	1.86	0.44	2.90
373	44.23	27.92	5.07	0.78	10.46
399	44.10	7.79	9.05	1.08	26.18

[a] Other hydrocarbons

Temp. (°C)	Other hydrocarbons distribution (% by mass) CH_4	C_2H_6	C3	C3=	C4	C5	C6+
348	0	1.10	0	0.06	0	0.05	1.69
373	0.02	4.75	0	0.30	0	1.08	4.31
399	0.11	10.28	0.10	0.86	0	2.85	11.98

Table 3.5 Reaction of ethanol over 2% Al/TiO_2; Catalyst reduced at 400°C

Temp. (°C)	Conv. %	Product distribution (% by mass) Et_2O	C_2H_4	CH_3CHO	HC's[a]
104	1.36	0	0	0	1.36
152	0.62	0	0	0	0.62
176	0.04	0	0	0	0.04
199	0.35	0.35	0	0	0
225	0.33	0.31	0	0.02	0
249	1.54	1.51	0	0.03	0
275	6.76	6.65	0.02	0.06	0.03
300	18.61	18.27	0.11	0.11	0.12
324	35.50	34.30	0.39	0.21	0.60
348	49.32	44.49	1.12	0.34	3.37
373	49.67	37.04	2.90	0.59	9.14
397	48.43	23.56	4.84	1.30	18.73

[a] Other hydrocarbons

Temp. (°C)	Other hydrocarbons distribution (% by mass) CH_4	C_2H_6	C3	C3=	C4	C5	C6+
348	0	0.38	0	0.03	0	0.03	2.93
373	0.01	1.34	0	0.14	0	0.10	7.55
397	0.05	3.54	0	0.42	0	0.37	14.35

Table 3.6 Reaction of ethanol over 1% Co/TiO_2; Catalyst reduced at 200°C

Temp. (°C)	Conv. %	Product distribution (% by mass) Et_2O	C_2H_4	CH_3CHO	HC's[a]
202	0.03	0	0.01	0.02	0.02
227	0.17	0.06	0.04	0.07	0.07
255	0.77	0.40	0.14	0.21	0.23
279	2.68	1.41	0.32	0.41	0.95
305	6.16	4.11	0.85	0.75	1.20
328	12.14	8.18	1.88	1.14	2.08
353	22.92	14.59	4.27	1.69	4.06
378	35.80	16.66	9.01	2.46	10.13
401	50.14	11.23	14.53	3.35	24.38

[a] Other hydrocarbons

Temp. (°C)	Other hydrocarbons distribution (% by mass) CH_4	C_2H_6	C3	C3=	C4	C5	C6+
353	0.01	0.62	0	0.07	0	0.15	3.21
378	0.04	2.77	0	0.29	0	1.69	5.34
401	0.16	9.39	0.06	1.03	0	3.32	10.42

Table 3.7 Reaction of ethanol over 1% Co/TiO_2; Catalyst reduced at 400°C

Temp. (°C)	Conv. %	Product distribution (% by mass) Et_2O	C_2H_4	CH_3CHO	HC's[a]
200	0.03	0	0	0.03	0
224	0.10	0	0.01	0.09	0
256	0.52	0.30	0.07	0.15	0
277	1.25	0.82	0.14	0.2	0.06
302	3.86	2.80	0.47	0.38	0.21
325	10.55	7.67	1.51	0.56	0.81
351	22.34	14.78	4.15	0.80	2.61
373	34.33	16.59	8.48	1.11	8.15
401	54.77	10.98	16.44	1.53	25.82

[a] Other hydrocarbons

Temp. (°C)	Other hydrocarbons distribution (% by mass) CH_4	C_2H_6	C3	C3=	C4	C5	C6+
351	0.02	0.79	0	0.03	0	0.64	1.13
373	0.04	2.79	0	0.13	0	1.10	4.09
401	0.13	10.69	0	0.70	2.72	2.38	9.29

Table 3.8 Reaction of ethanol over 2% Co/TiO_2; Catalyst reduced at 400°C

Temp. (°C)	Conv. %	Product distribution (% by mass) Et_2O	C_2H_4	CH_3CHO	HC's[a]
176	0.56	0	0	0.25	0.31
200	0.90	0	0	0.20	0.70
226	1.11	0.01	0	0.20	0.90
250	1.24	0.28	0.01	0.20	0.75
276	2.16	1.13	0.07	0.28	0.68
300	6.34	3.39	0.22	0.39	2.34
325	16.06	8.57	0.76	0.59	6.14
348	29.56	15.78	2.17	0.88	10.73
373	42.63	17.17	4.35	1.59	19.52
398	57.79	11.72	6.73	2.57	36.87

[a] Other hydrocarbons

Temp.	Other hydrocarbons distribution (% by mass)						
(°C)	CH_4	C_2H_6	C3	C3=	C4	C5	C6+
348	0.06	0.93	0	0.04	0	0.09	9.61
373	0.09	2.03	0	0.12	0	0.26	17.02
393	0.13	3.61	0	0.44	0	0.38	32.31

Table 3.9 Reaction of ethanol over 1.3% Cu/TiO_2; Catalyst reduced at 200°C

Temp. (°C)	Conv. %	Product distribution (% by mass) Et_2O	C_2H_4	CH_3CHO	HC's[a]
201	0.41	0	0	0.41	0
229	1.30	0.11	0.01	0.83	0.35
255	3.08	0.31	0.05	0.87	0.85
279	11.46	0.46	0.12	5.10	5.78
306	12.50	2.68	0.45	3.01	6.36
330	16.89	10.89	1.61	0.79	3.60
348	28.49	11.35	3.15	1.93	12.06
376	38.95	10.34	7.03	3.86	17.72
401	63.95	12.99	14.23	5.78	30.95

[a] Other hydrocarbons

Temp. (°C)	Other hydrocarbons distribution (% by mass) CH_4	C_2H_6	C3	C3=	C4	C5	C6+
348	0.03	1.57	0	0.19	0	1.20	9.07
376	0.09	3.75	0.06	0.74	0	2.42	10.66
401	0.22	6.91	0.17	1.19	0	6.31	16.15

Table 3.10 Reaction of ethanol over 1.3% Cu/TiO_2; Catalyst reduced at 400°C

Temp. (°C)	Conv. %	Product distribution (% by mass) Et_2O	C_2H_4	CH_3CHO	HC's[a]
200	0.05	0	0	0.05	0
229	0.20	0	0	0.16	0.04
256	1.24	0.23	0.02	0.44	0.55
276	3.35	0.52	0.07	0.89	1.87
300	4.54	2.72	0.26	0.47	1.09
329	16.77	12.32	1.91	0.37	2.17
350	28.49	18.29	4.34	0.52	5.34
374	35.17	11.46	8.86	1.08	13.77
396	48.47	7.57	12.82	2.89	25.69

[a] Other hydrocarbons

Temp. (°C)	Other hydrocarbons distribution (% by mass) CH_4	C_2H_6	C3	C3=	C4	C5	C6+
350	0.01	2.59	0	0.08	0	0.42	2.24
374	0.04	6.40	0	0.48	0	1.57	5.28
396	0.11	9.33	0.06	1.14	0	2.69	10.20

Table 3.11 Reaction of ethanol over 1% Ni/TiO_2; Catalyst reduced at 200°C

Temp. (°C)	Conv. %	Product distribution (% by mass) Et_2O	C_2H_4	CH_3CHO	HC's[a]
102	0.04	0	0	0.04	0
151	0.76	0	0	0.37	0.39
175	0.19	0	0	0.19	0
201	0.15	0	0	0.15	0
250	1.58	0.43	0.05	0.36	0.74
301	7.20	3.30	0.47	0.78	2.65
350	27.80	9.95	3.86	1.23	12.76
399	52.06	7.05	13.04	3.32	28.65

[a] Other hydrocarbons

Temp. (°C)	Other hydrocarbons distribution (% by mass) CH_4	C_2H_6	C3	C3=	C4	C5	C6+
301	0.01	0.03	0	0.01	0	0.34	2.26
350	0.05	1.03	0	0.19	0	0.58	10.89
399	0.83	5.68	0	2.52	0	5.70	13.92

Table 3.12 Reaction of ethanol over 1% Ni/TiO_2; Catalyst reduced at 400°C

Temp. (°C)	Conv. %	Product distribution (% by mass) Et_2O	C_2H_4	CH_3CHO	HC's[a]
102	0.64	0		0.63	0.01
150	2.43	0		1.06	1.37
175	2.56	0.08	0	0.85	1.63
201	4.01	0.29	0.01	1.04	2.67
249	2.12	0.24	0.01	0.78	1.09
301	7.66	4.25	0.38	0.54	2.49
351	35.45	17.19	4.47	1.00	12.79
400	70.38	10.36	12.20	2.99	44.83

[a] Other hydrocarbons

Temp. (°C)	Other hydrocarbons distribution (% by mass) CH_4	C_2H_6	C3	C3=	C4	C5	C6+
301	0.07	0.12	0	0.01	0.01	0	1.98
351	0.25	2.10	0	0.19	0	0.37	9.87
400	2.35	8.29	0	1.98	5.12	4.44	22.66

Table 3.13 Reaction of ethanol over 2% Ni/TiO_2; Catalyst reduced at 200°C

Temp. (°C)	Conv. %	Product distribution (% by mass) Et_2O	C_2H_4	CH_3CHO	HC's[a]
173	0.04	0	0	0.04	0
200	0.14	0	0	0.14	0
224	0.16	0	0	0.16	0
254	0.77	0.25	0.03	0.35	0.17
276	2.02	0.82	0.11	0.57	0.52
304	6.21	2.79	0.50	0.92	2.00
325	12.19	5.14	1.30	1.10	4.65
350	21.56	9.25	4.13	1.41	6.77
372	34.89	10.42	8.76	2.12	13.59
395	66.57	9.17	15.54	2.57	39.29

[a] Other hydrocarbons

Temp. (°C)	Other hydrocarbons distribution (% by mass) CH_4	C_2H_6	C3	C3=	C4	C5	C6+
350	0.08	0.83	0	0.15	0	0.71	4.99
372	0.23	2.42	0	0.57	0	3.01	7.36
395	1.53	6.72	0	2.21	6.32	6.07	16.44

Table 3.14 Reaction of ethanol over 2% Ni/TiO_2; Catalyst reduced at 400°C

Temp. (°C)	Conv. %	Product distribution (% by mass) Et_2O	C_2H_4	CH_3CHO	HC's[a]
100	0.42	0	0	0.42	0
119	0.75	0	0	0.69	0.06
148	0.88	0	0	0.55	0.33
173	0.59	0	0	0.40	0.19
200	0.78	0.04	0	0.44	0.30
222	0.54	0	0	0.42	0.12
255	0.63	0.28	0.01	0.26	0.08
274	1.54	0.91	0.05	0.37	0.20
299	4.65	3.22	0.27	0.35	0.77
325	12.47	8.50	1.20	0.53	2.24
349	27.02	14.63	4.06	0.85	7.48
374	45.48	11.44	8.09	2.01	23.94
394	71.30	13.07	12.16	2.12	43.95

[a] Other hydrocarbons

Temp. (°C)	Other hydrocarbons distribution (% by mass) CH_4	C_2H_6	C3	C3=	C4	C5	C6+
349	0.30	1.96	0	0.17	0	0.94	4.10
374	1.05	4.73	0	0.80	0	2.39	14.97
394	4.76	13.65	0.23	1.84	5.54	3.51	14.42

Table 3.15 Influence of metal loaded TiO_2 catalysts on C_6^+ hydrocarbon yield[a]

Catalyst (1.0 g)	Reduction[b] (°C)	Conversion (%)	C_6^+ (%)
TiO_2	400	54.28	6.72
0.36% Al/TiO_2	200	55.24	10.00
0.36% Al/TIO_2	400	58.29	10.87
0.72% Al/TiO_2	400	44.10	11.98
2% Al/TiO_2	400	48.43	14.35
1% Co/TiO_2	200	50.14	10.42
1% Co/TiO_2	400	54.77	9.29
2% Co/TiO_2	400	57.79	32.31
1.3% Cu/TiO_2	200	63.95	16.15
1.3% Cu/TiO_2	400	48.47	10.20
1% Ni/TiO_2	200	52.06	19.62[c]
1% Ni/TiO_2	400	70.38	27.10[c]
2% Ni/TiO_2	200	66.57	22.51[c]
2% Ni/TiO_2	400	71.30	17.93[c]

[a] Reaction temperature *ca.* 400°C; Metal loaded TiO_2 by mass percentage

[b] Catalyst reduced at 400°C or 200°C for 16 h in H_2

[c] C_5^+ liquid hydrocarbons

3.3.5 Ethanol conversion over alumina pillared interlayered montmorillonite (Al-PILM)

The pillared interlayered clays were synthesized using commercial montmorillonite K-10 clay. The Al-PILM catalyst was prepared according to the method described in Appendix 4. After the acid treatment procedure, the clay was investigated for the ethanol conversion reaction. The reaction of ethanol over the clays was carried out at constant WHSV (0.806 h^{-1}) and constant nitrogen carrier gas flow rate (21ml min^{-1}) in the 100°C to 500°C temperature range. The results obtained from all samples studied are summarized below.

Na^{+}-montmorillonite

The ethanol conversion reaction increased with increasing reaction temperature. At 474°C the conversion was 98.79 wt.%. At lower temperatures diethyl-ether and ethene were the two major products formed, with maximum yields of diethyl-ether being 34.45 wt.% at 302°C and ethene 96.27 wt.% at 474°C. Small yields of acetaldehyde and other hydrocarbons were also obtained (see Figure 3.9 and Table 3.16).

Al-PILM; no ammonia exchange procedure

Using this catalyst, ethanol conversion to diethyl-ether and ethene commenced at approximately 227°C. At 478°C total conversion had occured. Maximum production of diethyl-ether was observed at 304°C (45.17 wt.%) and maximum ethene formation (> 98 wt.%) was observed in the temperature range 441°C - 478°C (see Figure 3.10 and Table 3.17).

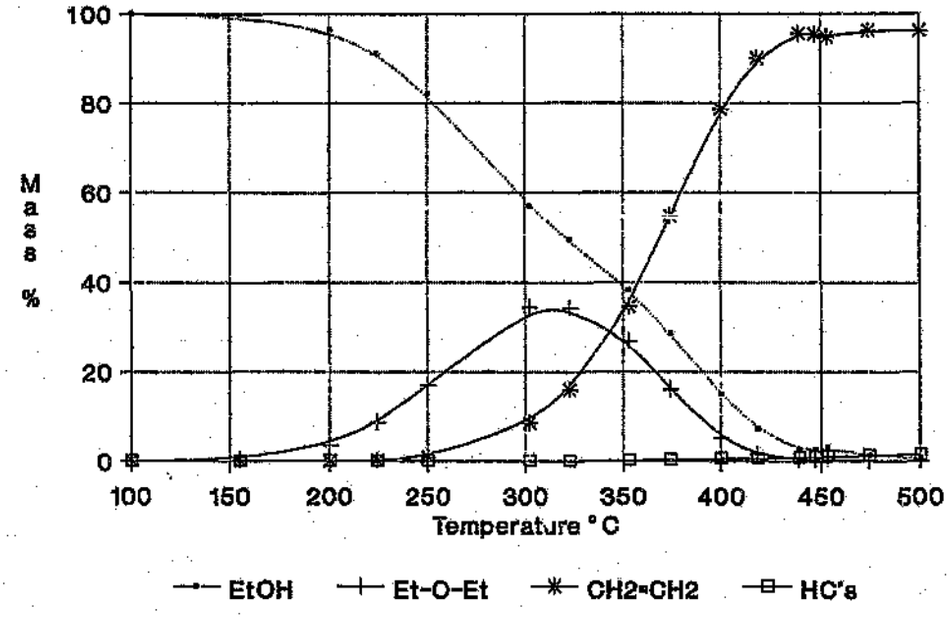

Figure 3.9 Reaction of ethanol over Na^+-montmorillonite (sodium ion exchanged montmorillonite)

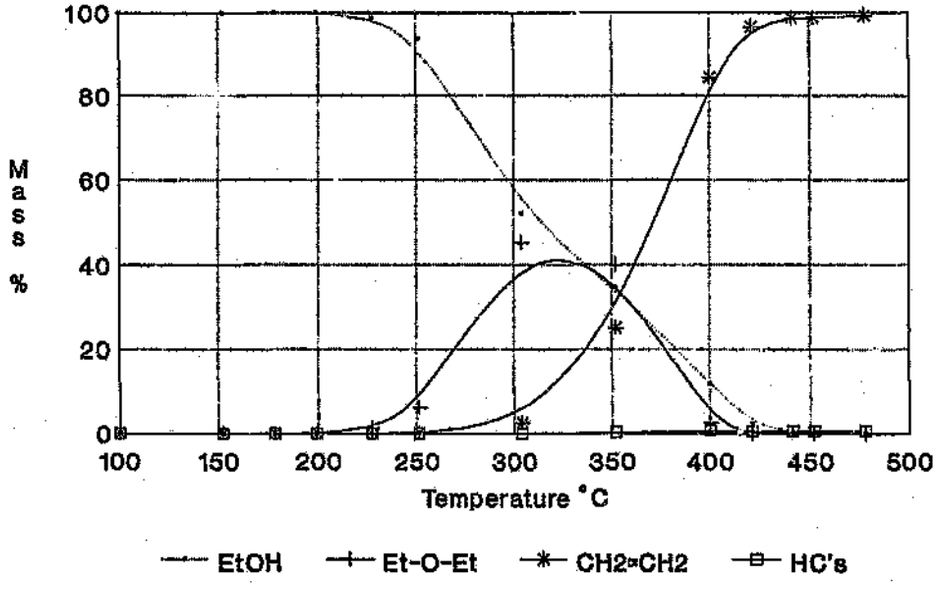

Figure 3.10 Reaction of ethanol over Al-PILM (unactivated Al-PILM)

Al PILM; ammonia exchange treatment

The activity of this catalyst was far superior to the catalyst in which no ammonium ion exchange had taken place. The beginning of ethanol to diethyl-ether conversion commenced at 126°C and formation of ethene started at 175°C. The maximum conversion to diethyl-ether occured at 255°C (51.66 wt.%) and maximum ethene formation between 327°C and 403°C (> 98 wt.%), (see Figure 3.11 and Table 3.18). No deactivation of the Al-PILM (activated) catalyst occured over a 43 hour time period (T = 400°C). Ethene was the major product formed (> 98 wt.%) during the time on line study.

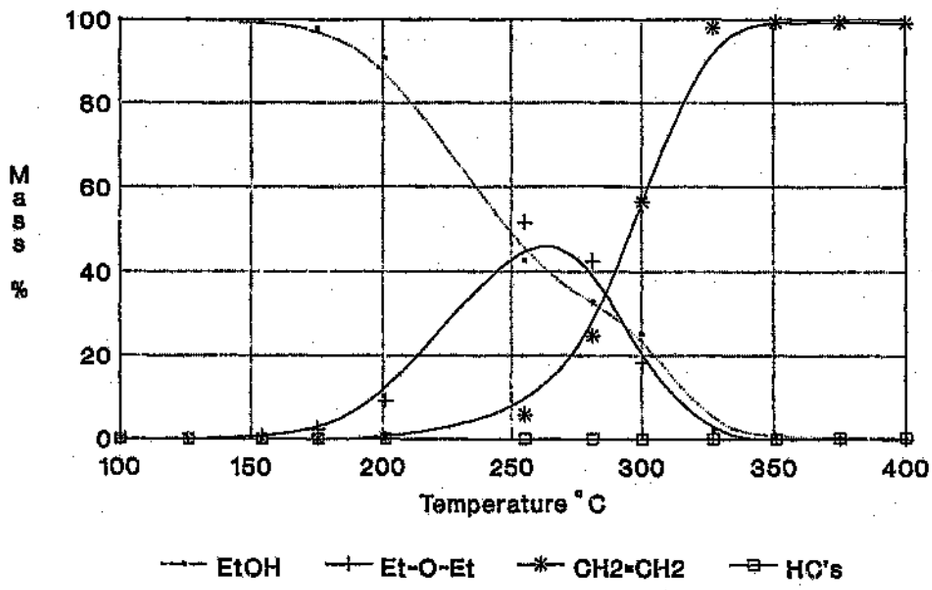

Figure 3.11 Reaction of ethanol over Al-PILM (activated Al-PILM)

Table 3.16 Catalytic performance of Na^+-montmorillonite (sodium ion exchanged montmorillonite)

Temp. (°C)	Conv. %	Product distribution (% by mass) Et_2O	C_2H_4	CH_3CHO	HC's[a]
155	0.30	0.30	0	0	0
200	3.53	3.49	0.04	0	0
224	8.91	8.70	0.21	0	0
250	17.86	17.01	0.83	0.02	0
302	43.09	34.45	8.57	0.06	0.01
323	50.47	34.39	15.90	0.09	0.09
353	61.81	26.84	34.62	0.17	0.18
374	71.49	16.10	54.76	0.33	0.30
400	85.00	5.16	78.70	0.62	0.52
418	92.81	1.49	90.04	0.68	0.60
439	97.43	0.33	95.55	0.81	0.74
447	97.38	0.30	95.41	0.85	0.82
453	97.05	0.39	94.76	0.92	0.98
474	98.79	0.10	96.27	1.17	1.25
501	99.28	0	96.09	1.56	1.52

[a] Other hydrocarbons

Table 3.17 Catalytic performance of sample Al-PILM (unactivated Al-PILM)

Temp. (°C)	Conv. %	Product distribution (% by mass) Et_2O	C_2H_4	CH_3CHO	HC's[a]
99	0	0	0	0	0
152	0	0	0	0	0
178	0	0	0	0	0
199	0	0	0	0	0
227	1.36	1.34	0.01	0	0.01
251	6.23	6.14	0.08	0	0.01
304	47.75	45.17	2.51	0.05	0.02
352	65.34	39.84	25.06	0.22	0.22
400	88.12	2.54	84.33	0.61	0.64
421	97.65	0	96.50	0.52	0.63
441	99.67	0	98.68	0.41	0.58
452	99.77	0	98.85	0.37	0.55
478	100.0	0	99.17	0.34	0.49

[a] Other hydrocarbons

Table 3.18 Catalytic performance of sample Al-PILM (activated Al-PILM)

Temp. (°C)	Conv. %	Product distribution (% by mass) Et_2O	C_2H_4	CH_3CHO	HC's[a]
101	0	0	0	0	0
126	0.05	0.05	0	0	0
154	0.50	0.50	0	0	0
175	2.24	2.23	0.01	0	0
201	9.21	9.07	0.14	0	0
255	57.34	51.66	5.68	0	0
281	67.32	42.48	24.77	0.06	0.01
300	74.81	18.26	56.45	0.09	0.01
327	98.19	0.13	97.92	0.14	0
351	99.38	0	99.26	0.12	0
375	99.70	0	99.23	0.14	0.33
403	99.65	0	99.10	0.15	0.40

[a] Other hydrocarbons

In summary, all samples showed the reaction of ethanol to be dependent on reaction temperature. The conversion to diethyl-ether reached a maximum yield (~50 wt.%) and then decreased once the ethene yield increased. At high temperatures a maximum yield of ethene (> 98 wt.%) was achieved for all reactions. Only small amounts of other products were formed e.g. acetaldehyde and other hydrocarbons (< 1 wt.%). No coke formation was observed on the catalyst surface during the reaction. Hence the clays make an efficient catalyst for the conversion of ethanol to diethyl-ether and/or ethene.

3.3.6 Reaction of ethanol over γ-alumina

Two commercial γ-Al_2O_3 catalysts (powder form, 300 μm) were obtained from Harshaw and Merck Both γ-Al_2O_3 catalysts were utilized for the reaction of ethanol conversion (100°C to 400°C) using a feed rate of 1.0 ml h^{-1} and a nitrogen carrier gas flow rate of 21 ml min^{-1}. Table 3.19 show the selectivities and conversions obtained at various reaction temperatures between 100°C and 400°C. Figure 3.12 shows the conversion and selectivities as a function of reaction temperatures. When compared, the two catalysts showed that Harshaw γ-Al_2O_3 had a much higher activity and selectivity than the Merck γ-Al_2O_3. However in the higher temperature range (Tables 3.19), Merck γ-Al_2O_3 gave slightly higher yields of saturated and unsaturated hydrocarbons than the Harshaw γ-Al_2O_3. The maximum diethyl-ether formation was at 62.33 wt.% at 253°C (Harshaw) and 53.61 wt.% at 323°C

(Merck). In the higher temperature range both catalysts favoured ethene formation. For example, the Harshaw γ-Al_2O_3 catalyst gave a 100% conversion (99.82% ethene, 374°C) while the Merck γ-Al_2O_3 catalyst showed 88.92% conversion (83.47% to ethene; 394°C).

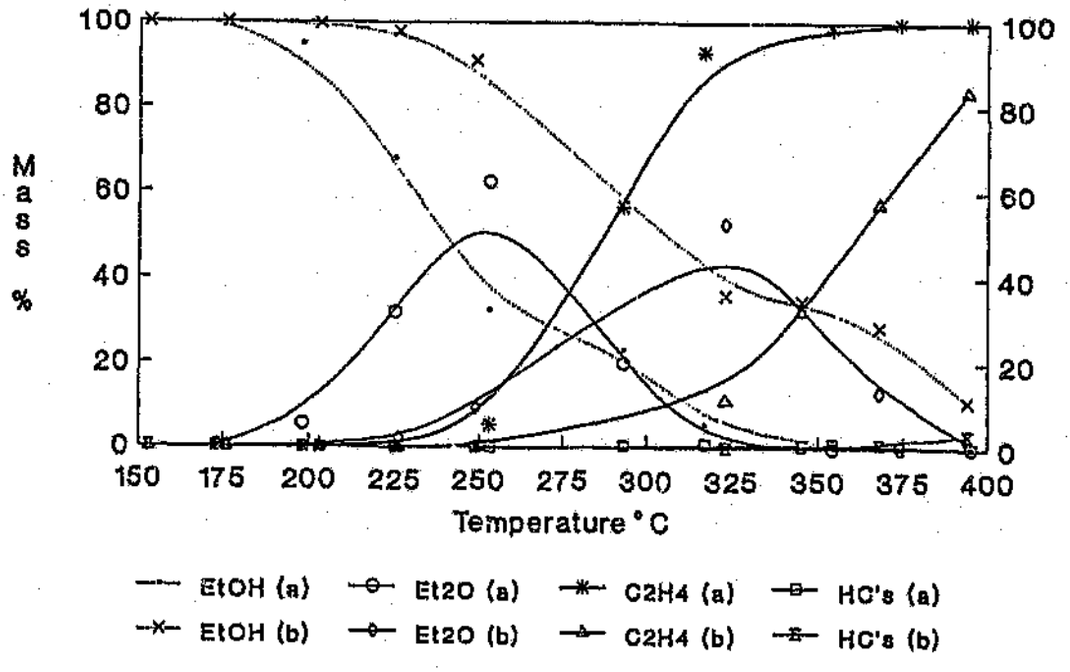

Figure 3.12 Ethanol conversion over γ-Al_2O_3 catalyst; conversion and selectivities as a function of reaction temperature (a: Harshaw γ-Al_2O_3 b: Merck γ-Al_2O_3)

Table 3.19 Ethanol conversion over γ-Al_2O_3 catalyst (Harshaw and Merck)

Temp. (°C)	Conv. %	Product distribution (% by mass) Et_2O	C_2H_4	CH_3CHO	HC's[a]
		Harshaw γ-Al_2O_3			
173	0.29	0.29	0	0	0
198	5.33	5.32	0.01	0	0
225	32.22	31.93	0.29	0	0
253	67.69	62.33	5.34	0	0.02
293	77.04	20.03	56.63	0.11	0.27
317	94.52	0.73	92.96	0.12	0.71
354	99.57	0	98.54	0.10	0.93
374	100.0	0	99.61	0	0.39
395	100.0	0	99.82	0	0.18
		Merck γ-Al_2O_3			
105	0	0	0	0	0
153	0	0	0	0	0
176	0	0	0	0	0
203	0.42	0.40	0	0.02	0
226	2.18	2.15	0.01	0.02	0
249	9.30	9.19	0.08	0.03	0
323	64.03	52.61	11.11	0.15	0.16
345	65.43	32.57	32.06	0.33	0.47
368	71.56	13.06	57.19	0.58	0.73
394	88.92	1.58	83.47	0.78	3.09

[a] Other hydrocarbons

3.4 DISCUSSION

3.4.1 Ethanol transformation over metal loaded TiO_2 catalysts

The use of metal supported acid catalysts for conversions of alcohols to a range of products have been reported in the literature. Two routes are possible - a dehydration route and a dehydrogenation route - and both have been observed under appropriate conditions. For instance, copper on Al_2O_3 has been reported to act only as a dehydrogenation catalyst [1]. Similary, copper-chromium oxides have been shown to be very active for the alcohol dehydrogenation reaction [2]. In this investigation the ethanol transformation over transition metals such as Co, Cu, Ni and group 3 elements such as Al, all loaded on TiO_2, were studied. The catalysts did not favour dehydrogenation of ethanol to acetaldehyde but rather dehydration to form diethyl-ether (favoured at low temperatures), ethene, ethane and other liquid hydrocarbons (favoured at high temperatures) occured. It is to be noted that Pd, Pt, Rh and Ru loaded on TiO_2 did show this reaction (see chapter four). Hence, addition of the above metals to TiO_2 did not increase the acetaldehyde formation by dehydrogenation of ethanol.

Ono and Kanae [3] have observed the transformation of butanes over Zn-ZSM-5 and Ga-ZSM-5. The metal cations were found to be very efficient catalyst centres for dehydrogenating the intermediate alkenes into aromatic hydrocarbons. The absolute rate of cracking was enhanced by the introduction of zinc or gallium cations. Recently, Saha

and Sivasanker [4] have also revealed that ethanol conversion over H-ZSM-5 and ZSM-5 loaded with Zn and Ga ions also increased the yield of the gasoline - kerosene range hydrocarbons (heavier products) and aromatics. The cations also increased the life of the catalyst. The authors [4] concluded that metal containing catalysts have a larger H-transfer ability than metal free acid catalysts. The greater H-transfer ability of these catalyst assisted in the desorption of the strongly adsorbed olefins as saturated and aromatic complexes.

For the TiO_2 containing metal catalysts described above the ethanol conversion reaction gave diethyl-ether as a major product in the low temperature range with a maximum yield at approximatly 350°C. Increasing the reaction temperature to 400°C resulted in higher yields of C_2 (ethene and ethane) and other heavier hydrocarbon products (C_6^+). It thus appears that initially the primary product is converted to light hydrocarbons with C_2 being the major product. It is proposed that the polymerization to the higher hydrocarbons (C_6^+) takes place from these light gaseous products. The sequence of reactions taking place on the catalyst surface is thus as follows:

$$EtOH \xrightarrow{\text{step 1}} EtOEt \xrightarrow{\text{step 2}} C_2H_4 \xrightarrow[\text{H-transfer}]{\text{step 3}} \text{oligomers}$$

$$\longrightarrow \text{longer chain liquid hydrocarbons } (C_6^+)$$

Table 3.15 summarises the relative yield of C_6^+ liquid hydrocarbons as a function of metal concentration and reduction temperature for the ethanol conversion over the metal loaded TiO_2 catalysts (metal = Al, Co, Cu, Ni). In all the studies, the metal containing catalyst favours the

production of the longer chain C_6^+ hydrocarbons. Furthermore, incorporation of Ni not only increases the yield of the longer chain liquid hydrocarbon products, but also increases the life of the catalyst.

Tauster et al. [5 - 8] have reported that strong metal-support interactions (SMSI) occur between group 8 - 10 noble metals and transition metal oxide supports such as TiO_2, V_2O_3, Nb_2O_5, and Ta_2O_5 when the catalysts are reduced at high temperatures (700 K - 800 K). The main feature of the SMSI effect is the almost complete suppression of H_2 and CO adsorption on the supported metal after a high-temperature reduction. The more noble metals are more strongly affected, and the more reducible the oxide support, the more extensive is the metal-support interaction. Furthermore, the effects associated with the strong metal-support interaction can be recovered after oxidation followed by low-temperature reduction at 473 K. By contrast, adsorption of H_2 and CO on titania-supported nickel, ruthenium, and osmium is considerable even after reduction at 773 K [8]. The extent of adsorption on rhodium and palladium, while measurable, is low after high temperature reduction. However, Tauster et al. [5 - 8] concluded that iron, cobalt, and nickel require a higher reduction temperature for the induction of the SMSI effect.

In our studies the Ni/TiO_2 catalyst reduced at 473 K showed poor stability, while reduction at 673 K gave superior stability. This suggests that SMSI effects are not necessarily important in this study.

3.4.2 Ethanol conversion over alumina pillared interlayered montmorillonite (Al-PILM)

Calcination of a clay mineral, usually results in a collapse of the layer structure and, as a consequence, the interlayer space is virtually eliminated [9 - 11]. Therefore, spent clay catalysts cannot be regenerated by calcination in air to burn-off carbonaceous deposits. Interlamellar reactions involving metal ion exchange of smectite clays at high temperatures (> 200°C) are precluded due to the dehydration and collapse of the interlayer region [9]. The limitations imposed by interlayer collapse can however be circumvented by the intercalation of thermally stable, robust cations which act as molecular props or pillars, and keep the silicate layers separated in the absence of a swelling solvent [9 - 11]. The pillared clays are synthesized by ion exchange of the Na^+ or Ca^{2+} ions in a clay with the cationic pillaring agents [9 - 13].

Recently interest in pillared clays has been renewed, as a result of the finding that clay pore sizes can be made larger than those of faujasitic zeolites [9, 12, 13]. For instance Pesquera et al. [14] have reported that the montmorillonite specific surface area (61 m^2/g) was increased by pillaring (366 m^2/g). The structure of the aluminium oxide pillared montmorillonite also proved to be stable up to 500°C.

In the studies the pillared montmorillonite was synthesized by the direct cation exchange method. Consequently we undertook a study of an Al pillared clay to assess its behavior in the ethanol transformation reaction.

It has been established [15, 16] that aliphatic primary alcohols, when passed over intercalated Al^{3+}-exchanged montmorillonites, react perferentially via intermolecular nucleophilic displacement of water to give high yields of ethers, rather than via competitive intramolecular dehydration to alkenes. A reaction scheme showing both the above possibilities is shown below [15].

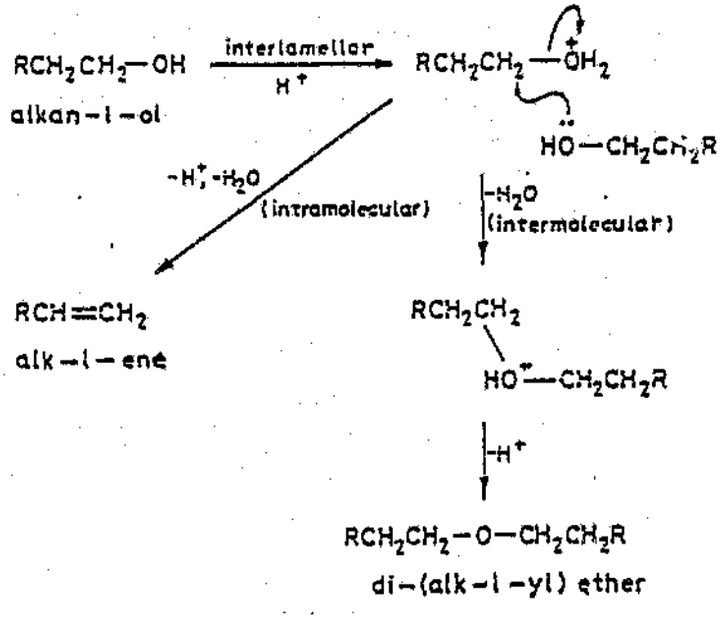

Calcination of NH_4^+ exchanged solid acids has been reported. For instance, Papp et al. [17] found that NH_4^+-exchange of clinoptilolite followed by calcination yielded the acid from the zeolite. Detreköy et al. [18] reported that when clinoptilolite was reacted with 2.0 M NH_4NO_3 a 70% NH_4^+-exchanged sample could be obtained. Calcination of this catalyst at temperatures higher than 400°C resulted in complete dealumination and also increased catalytic activity. Likewise, calcination of the NH_4^+-exchanged zeolite at 500°C for 4 h also resulted in a significantly enhanced activity in the methanol conversion [19].

In the studies described above, the three samples, Na^+-montmorillonite, and ammonium exchanged and non-exchanged Al-PILM showed similar product selectivities towards diethyl-ether (at low temperatures) and ethene (at high temperatures) formation. Further the NH_4^+-exchanged Al-PILM sample calcined at 500°C for 3 h resulted in a superior catalyst which completely converted ethanol to ethene (100%) at ca. 350°C, without deactivation over a 43 hour period.

The increased activity of the Al-PILM-NH_4^+ catalyst is due to an increase in the Brönsted acidity of these samples. This increase was brought about by the replacement of metal cations by NH_4^+, which were later converted to H^+ during calcination [19]. The higher acidity was induced by isolated Al_{13} pillars, which contain a tetrahedral aluminum cation. This change in acidity is similar to that observed in zeolites where dealumination increases the acid strength by reducing the number of neighbour Al atoms [20]. This treatment procedure also increased the catalyst activity and thermal stability of the Al-PILM catalyst [21].

From the above studies, an order of catalytic activity could be deduced: Na^+-montmorillonite < Al-PILM < Al-PILM-NH_4^+. It can be concluded that increased catalytic surface area due to the ammonia exchange procedure influenced the catalytic activity in the ethanol conversion reaction.

3.4.3 Reaction of ethanol over γ-alumina.

Ethanol conversion over γ-alumina in the low temperature range gave a maximum diethyl-ether (62.33%, 253°C, Harshaw) and (53.61%, 323°C, Merck) yield. The Lewis acid sites [22] as well as residual surface hydroxyls [23] provide the alumina with weak Brönsted acid centres. The dominant pathway for ethanol interaction with the catalyst surface is hence via nucleophilic attack at the Lewis acid centres. This generates surface ethoxy species, which, via recombination with neighbouring ethoxy species, gives rise to the observed diethyl-ether formation.

In the higher temperature range, ethene is the dominant product (99.82%, 374°C, Harshaw; 83.47%, 394°C, Merck). Figure 3.12 illustrates the product selectivities in the conversion of ethanol over both Harshaw and Merck γ-Al_2O_3 catalysts at different reaction temperatures. The selectivities are similar. The reaction pathway could involve diethyl-ether as a reaction intermediate [24, 25], which is subsequently converted to ethene by dehydration (E1 mechanism) or to ethanol by dehydration. However, an E2-type mechanism that leads directly to ethene is possible if there are coexisting basic and acidic sites on the catalysts' surface [26 - 28].

Swecker and Datye [29], using model nonporous alumina powder, have shown that ethanol dehydration produced diethyl-ether, ethene, water, and a small amount of acetaldehyde at T > 300°C. They concluded that formation of ether occurs via a bimolecular reaction and is therefore favored when the surface coverage of reactants is high. Diethyl-ether was proposed to be the major product from

ethanol. The ethene formation could also occur via the same reaction intermediate as for diethyl-ether, namely a surface ethoxy species [30].

Various proposals have been made regarding the manner in which the exthoxide participates in the surface reaction. A detailed sequence of reactions have been described which rationalize the selectivities towards diethyl-ether (favored at low temperatures) and ethene (favored at high temperatures) [31].

(1) Weak adsorption of ethanol.

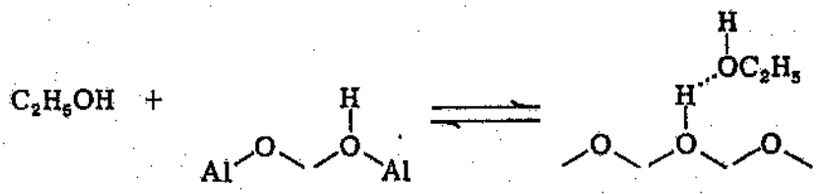

(2) Chemisorption of the weakly-adsorbed ethanol.

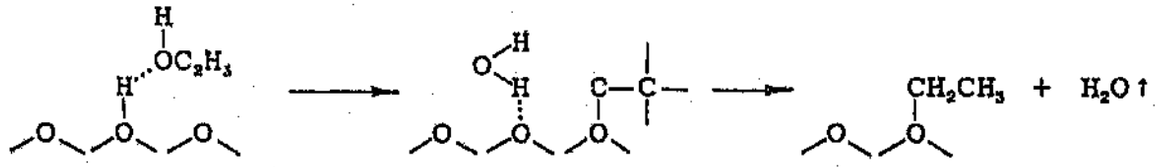

(3) (a) Ether formation.

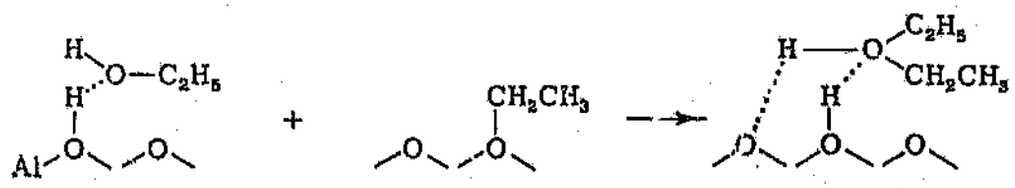

(b) Ethene formation.

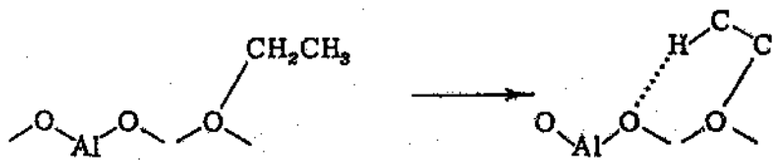

(4) (a) Desorption of ether.

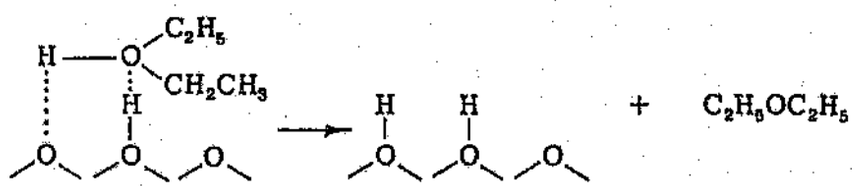

(b) Desorption of ethene.

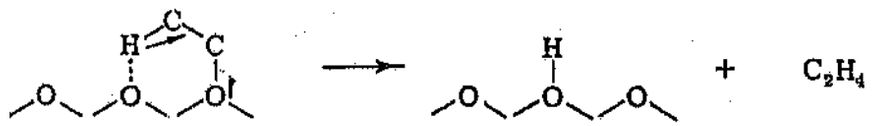

3.5 CONCLUSIONS

In the transformation of ethanol to hydrocarbons, use of a metal free TiO_2 catalyst was studied. This catalyst exhibited acidic properties at low reaction temperatures for the dehydration of ethanol to the first major product diethyl-ether. At higher reaction temperatures, C_2 (ethene and ethane) was the dominant product and only a small quantity of higher hydrocarbons were formed. Incorporation of metal (Co, Cu and Ni) onto the TiO_2, gave no significant difference in catalytic activity compared to the metal free TiO_2. Ni showed a slightly increased activity and yield to diethyl-ether. However, addition of these metals gave rise to a change in catalytic selectivity to yield heavier liquid products (C_6^+). Further, Ni/TiO_2 reduced at 400°C not only increased the higher hydrocarbon products, but also increased the lifetime of the catalyst.

The γ-Al_2O_3 and modified AL-PILM, acted as dehydration catalysts. These catalysts converted ethanol with high selectivity to ethene (T > 350°C).

REFERENCES

[1] C. Sivaraj and P.K. Rao, Appl. Catal., 45 (1988) 103.

[2] I. Yasumor and E. Miyazaki, Nippon Kagaku Zasshi, 92 (1971) 669.

[3] Y. Ono and K. Kanae, J. Chem. Soc. Faraday Trans., 4 87 (1991) 669.

[4] S.K. Saha and S. Sivasanker, Catalysis Letter, 15 (1992) 413.

[5] S.J. Tauster, S.C. Fung, R.L. Garten, J. Am. Chem. Soc., 100 (1978) 170.

[6] S.J. Tauster, S.C. Fung, J. Catal., 55 (1978) 29.

[7] S.J. Tauster, S.C. Fung, R.T.K. Baker and Horsley, J. A. Science, 211 (1981) 1121.

[8] S.A. Stevenson, G.B. Paupp, J.A. Lumesic, S.J. Tauster and R.T.K. Baker, in "Metal-support Interaction in Catalysis Sintering, and Redispersion", S.A. Stevenson et al. (Eds.), Van Nostrand Reinhold Co., New York, (1987) Ch.2.

[9] T.J. Pinnavaia, Science, 220 (1983) 365.

[10] J.J. Fripiat, Clays Clay Miner., 34 (1986) 501.

[11] D. Tilak, B. Tennakoon, W. Jones and J.M. Thomas, J. Chem. Soc., Faraday Trans., 1 82 (1986) 3081.

[12] D.E.W. Vaughan, Catal. Today, 2 (1988) 187.

[13] R. Burch, Catal. Today, 2 (1988) 185.

[14] C. Pesquera, F. Gonzalez, I. Benito, S. Mendioroz and J,A. Pajares, Appl. Catal., 69 (1991) 97.

[15] J.A. Ballantine, M. Davies, H. Purnell, M. Rayanakorn, J.M. Thomas and K.J. Williams, J.C.S. Chem. Comm., (1981) 427.

[16] J.A. Ballantine, M. Davies, I. Patel, J.H. Purnell, M. Rayanakorn, K.J. Williams and J.M. Thomas, J. Mol. Catal., 26 (9184) 37.

[17] J. Papp and D. Kalló, Magyar Kémiai Fólyoiral, 69 (1973) 373.

[18] E.J. Detreköy, P.A. Jocobs, D. Kalló and B. Uytterhoeven, J. Catal., 32 (1974) 442.

[19] T. Themistocleous, Ph.D. Thesis, University of the Witwatersrand, Johannesburg, 1990.

[20] D. Tichit, Z. Mountassir, F. Figueras and A. Auroux, in "Preparation of Catalysts: Scientific Bases for the Preparation of Heterogeneous Catalysts", B. Delmon et al. (Eds.) Vol.V, Elsevier, Amsterdam, (1991) P.345.

[21] F. Figueras, Z. Klapyta, P. Massiani, Z. Mountassir, D. Tichit, F. Fajula, C. Gueguen, J. Bousquet and A. Auroux, Clays clay Miner, 38 (1990) 257.

[22] R.G. Greenler, J. Phys. Chem., 37 (1962) 2094.

[23] W.S. Brey and K.A. Krieger, J. Am. Chem. Soc., 71 (1949) 3637.

[24] M.T. Aronson. R J. Gorte and W.E. Farneth. J. Catal., 98 (1985) 434.

[25] M.T. Aronson. R.J. Gorte and W.E. Farneth. J. Catal., 105 (1987) 455.

[26] C.D. Chang, Hydrocarbons from Methanol, Marcel Dekker. Inc., New. York. p.198.

[27] J. Fuhse and F. Bandermann, Chem. Eng. Technol., 10 (1987) 323.

[28] H. Knözinger, H. Bühl and K. Kochloefl, J. Catal., 24 (1972) 57.

[29] J.L. Swecker and A.K. Datye, J. Catal., 121 (1990) 196.

[30] K.H. Schnabel, E. Schreier and C. Peuker, Catal. Today, 3 (1988) 513.

[31] L.E. Dabrowski, J.B. Butt and H. Bliss, J. Catal., 18 (1970) 297.

CHAPTER FOUR

ETHANOL CONVERSION REACTIONS OVER PALLADIUM/TITANIUM DIOXIDE CATALYSTS

4.1 INTRODUCTION

The ethanol conversion reaction to hydrocarbons is of industrial importance as ethanol is readily available for conversion to high value chemicals. It has already been described in Chapter three that when Al, Co, Cu and Ni are loaded onto TiO_2, ethanol dehydration was observed. The major products were diethyl-ether, ethene and small amounts of acetaldehyde. Although the addition of these metals did not significantly increase catalytic activity, they did favour higher liquid hydrocarbons at high temperatures (*ca.* 400°C).

Sabatier [1], in 1910, showed that ethyl alcohol could undergo two important types of decomposition reaction; one to diethyl-ether/ethene and water, a reaction promoted chiefly by oxide catalysts, and the other to hydrogen and acetaldehyde promoted by metals. Though many catalysts promote both reactions, we wished to explore the influence of Pd on the two-pathways (dehydration/dehydrogenation) starting from ethanol. Both reaction pathways are expected to depend on reaction temperature.

This Chapter describes a detailed investigation of the activity of Pd/TiO_2 for the ethanol conversion reaction. Variables investigated include different preparation procedures, effect of Pd metal salts, optimum calcination

and reduction temperatures, and also an investigation of the effect of different carrier gases (N_2 and H_2) on the ethanol transformation reaction.

The reaction of acetaldehyde and diethyl-ether over Pd/TiO_2 using H_2 and N_2 as a carrier gas were also carried out in order to determine whether the first step in ethanol conversion leads to either Et_2O or CH_3CHO formation. This study was also extended to allow for a comparison of the routes for the ethanol conversion reaction over Pd loaded on other acid supports (γ-Al_2O_3 and Al-PILM).

The more noble metals are known to show an increased selectivity towards C_2^+ hydrocarbons when supported on reducible oxides in the CO hydrogenation reaction [2]. In the present chapter an investigation of other transition metal (Pt, Ru and Rh) effects on TiO_2 were also investigated.

4.2 EXPERIMENTAL

The conversion of ethanol into longer chain carbon containing molecules over Pd supported TiO_2 catalysts (1%, 2% and 5% Pd by mass) was studied at atmospheric pressure and the experimental details are described in Chapter 2, section 2.2. In addition Ru, Pt and Rh supported on TiO_2, were also examined for activity and selectivity in the ethanol conversion reaction and the results compared to the Pd/TiO_2 catalyst. Pd on other supports (γ-Al_2O_3 and Al-PILM) were also studied for their transformation capabilities and the results compared with the TiO_2 supported catalyst. These latter catalysts were prepared by co-precipitation and/or

incipient wetness methods, as described in Appendix 1.

Catalysts (1.0 g) were tested using a standard laboratory microreactor (see Chapter 2, section 2.2). The liquid ethanol feed (aqueous: 96% v/v, alcohol/water; absolute: 99.8% - 100%, Labchem Ltd.) was injected into the evaporation chamber using a syringe pump (pumping rate: 1.0 ml h^{-1}). The ethanol vapour was carried into the reactor by a nitrogen (or hydrogen) stream (flow rate: 21 ml min^{-1}).

Acetaldehyde, diethyl-ether, ethene and water were also fed into the reactor in separate reactions. The volatile liquids were vapourised at a regulated temperature in a stream of dry N_2 (or H_2) at a constant flow-rate. The WHSV of the reactant was varied by controlling the vapourisation temperature.

The ethanol conversion activity and selectivities were calculated as described in Appendix 3, in a range of temperatures (100°C - 400°C).

4.3 RESULTS AND DISCUSSION

As mentioned in the introduction of this thesis only a limited amount of research has been reported on the use of Pd/TiO_2 as a catalyst in the ethanol to hydrocarbons conversion reaction. Below is described a detailed study of the reaction using this system. The catalytic activities and selectivities were studied as a function of catalyst calcination temperature, reduction temperature and Pd concentrations in the temperature range 100°C - 400°C.

4.3.1 Palladium loading

The effect of palladium loading (1%, 2% and 5% by mass) on TiO_2 on the reaction was monitored and the data compared to the reaction over pure TiO_2. The Pd loaded TiO_2 catalysts (< 200 μm) were prepared by a co-precipitation method and used in the extrudate form (extrudate size 2 x 3 mm). The Pd content was determined by Atomic Absorption (AA) spectroscopy. The results are shown in Table 4.1.

Table 4.1 Correlation between surface area and content of metal

Sample	Actual Pd content[a]	Surface area m^2/g[b]
1% Pd/TiO_2	1.1	70.5
2% Pd/TiO_2	1.94	77.5
5% Pd/TiO_2	5.18	65.9
TiO_2	0	55.5

[a] % by mass; error ± 0.03%

[b] Surface area: measured by BET method described in Chapter 2, section 2.4; error ± 0.5 $m^2\ g^{-1}$

Also shown are the BET determined surface areas. The observed Pd loaded values are close to the predicted values expected from the synthetic procedure. The BET values are variable with the loaded supports showing larger surface areas then the metal free TiO_2 support. No clear trend is observed relating the BET surface area to the % Pd on the support.

Ethanol was passed over the catalysts and catalytic performances were examined between 100°C and 400°C. The results are listed in Tables 4.2 to 4.4. As expected, ethanol conversion increased with increasing temperature, but an optimum conversion occured between 100°C and 275°C, after which the conversion of ethanol was found to decrease with increasing temperature. At T > 325°C the conversion again increased with increasing temperature. In the low temperature range (100°C - 275°C) the maximum conversion of ethanol was: 1% Pd/TiO_2, 85.3% (264°C); 2% Pd/TiO_2, 92.1% (264°C); and 5% Pd/TiO_2, 88.3% (275°C).

Comparison of TiO_2 and Pd/TiO_2 (Figure 4.1) indicates a dramatic change in the ethanol conversion rate in the low temperatures region (< 300°C); see Figure 4.1. Little to no product is found over TiO_2. A comparison of the product spectra in the range 200°C - 250°C is shown in Figure 4.2.

The spectra reveal the following:

1. The 1%, 2% and 5% loaded Pd gives the same product spectrum at all temperatures. (Figure 4.2 and 4.3)
2. The product spectra in the 200°C - 280°C range show that odd numbered products are synthesized in preference to even numbered products. (Figure 4.2)
3. Small amounts of acetaldehyde are observed (Table 4.2 to 4.4).
4. No diethyl-ether is detected in the temperature range 100°C and 265°C (see Table 4.2 to 4.4).

At T > 290°C the TiO_2 becomes active (Figure 4.1 and Table 4.5). In the temperature range 270°C - 320°C the Pd/TiO_2 catalysts shows a decrease in activity. Above 320°C the activity once again increases but the product spectrum now resembles that of the TiO_2 support (see Figure 4.1). This product spectrum is quite different to that observed in the lower temperature range with even numbered products being preferred to odd numbered products (Figure 4.3).

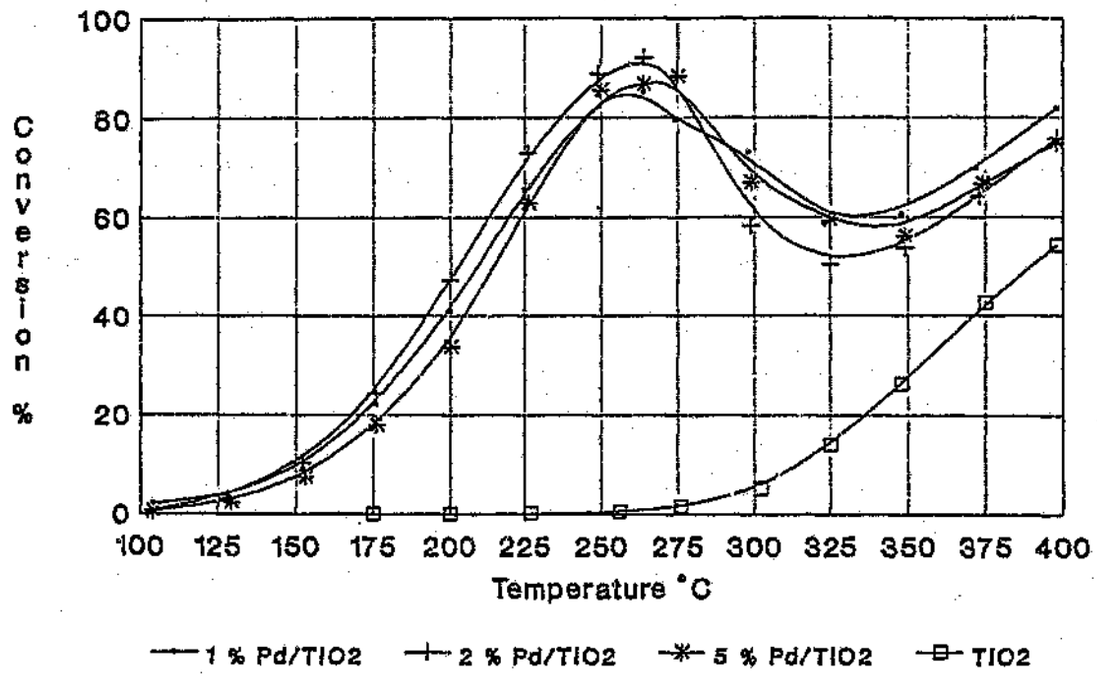

Figure 4.1 Comparison of ethanol conversion over Pd/TiO_2 (1%, 2% and 5% Pd by mass) and TiO_2 catalyst (Catalysts: uncalcined, reduced at 400°C/16 h in H_2)

Table 4.2 Catalytic performance of 1% Pd/TiO_2 in the ethanol conversion reaction: effect of temperature on product selectivity (catalyst: uncalcined, reduced at 400°C/16 h)

Temp. (°C)	Conv. %	Product distribution (% by mass)												
		Et_2O	MeCHO	C1	C2	C2=	C3	C3=	C4	C5	C6	C7	C8	C9+
104	2.25	0	0.65	0	0	0	0	0	0	0.13	0.34	0.13	1.00	0
128	3.30	0	1.24	0.02	0	~	0.02	0.01	0	0.31	0.39	0.17	0.96	0.18
152	9.12	0	1.47	0.04	0	0	0.07	0.05	0	1.47	1.15	0.86	2.57	1.44
176	22.15	0	1.69	0.13	0	0	0.27	0.12	0	3.44	1.89	2.78	5.48	6.35
200	41.00	0	2.12	0.42	0.02	0	0.91	0.27	0	7.10	2.81	.04	6.72	13.59
225	65.49	0	2.54	1.18	0.05	0	2.44	0.55	0	12.57	3.16	7.47	7.86	27.67
249	84.72	0	3.23	1.79	0.11	0.01	1.24	1.41	0	10.53	3.94	14.73	17.25	30.48
264	85.30	0	3.67	1.77	0.16	0.02	0.74	1.93	0	9.48	4.49	12.12	25.34	25.58
274	79.61	1.96	3.81	1.10	0.14	0.04	0	2.18	0	9.09	6.72	11.06	26.85	16.66
298	73.03	3.37	4.19	1.44	0.30	0.14	0	2.82	0	7.04	8.61	6.80	25.34	12.98
323	58.91	3.81	1.91	0.89	0.63	0.36	0	0.67	0	1.79	14.98	1.20	22.14	10.53
348	60.58	7.58	1.30	1.08	1.66	1.02	0	0.59	0	1.12	15.09	1.95	21.51	7.68
372	69.85	11.33	2.00	1.80	3.52	2.61	0	1.01	5.28	1.36	16.45	2.33	19.62	2.54
398	81.89	9.16	3.25	2.52	6.44	6.29	0	1.71	6.43	4.99	17.19	2.51	17.27	4.13

Table 4.3 Catalytic performance of 2% Pd/TiO_2 in the ethanol conversion reaction: effect of temperature on product selectivity (catalyst: uncalcined, reduced at 400°C/16 h)

Temp.	Conv.	Product distribution (% by mass)												
(°C)	%	Et_2O	MeCHO	C1	C2	C2=	C3	C3=	C4	C5	C6	C7	C8	C9+
104	0.88	0	0.81	0.01	0	0	0	0	0	0.02	0.04	0	0	0
128	3.25	0	1.49	0.03	0	0	0.03	0.02	0	0.52	0.57	0.11	0.48	0
152	10.25	0	1.79	0.07	0	0	0.13	0.05	0	1.83	1.54	0.88	2.71	1.25
176	24.24	0	2.22	0.01	0	0	0.46	0.14	0	4.80	2.48	3.26	5.10	5.77
200	47.27	0	2.98	0.62	0.02	0	1.37	0.26	0	9.49	3.25	7.66	6.81	14.81
226	73.01	0	3.44	2.34	0.07	0	5.26	0	0	17.45	2.83	10.01	6.20	25.41
249	88.87	0	2.88	5.77	0.19	0	10.20	0	0	21.50	1.33	18.77	3.57	24.66
264	92.10	0	2.77	5.77	0.29	0	6.96	1.23	0	17.98	2.80	18.67	4.73	30.90
275	88.47	0	3.87	4.09	0.44	0.03	2.18	2.98	0	13.14	4.32	15.63	15.59	26.20
299	58.28	2.54	4.72	1.83	0.51	0.24	0	2.85	0	4.91	8.14	3.35	18.37	10.82
325	50.49	3.20	1.81	0.90	0.62	0.34	0	0.53	0	1.44	12.07	0.88	18.68	10.02
349	53.82	7.95	1.27	1.04	1.49	0.81	0	0.50	0	1.16	14.74	1.86	17.29	5.71
373	64.13	12.01	2.04	1.59	2.90	1.59	0	0.94	3.66	1.59	18.77	3.45	14.20	1.39
398	75.85	9.50	2.32	1.98	4.92	2.44	0	1.58	5.59	2.21	18.39	4.08	17.56	5.28

Table 4.4 Catalytic performance of 5% Pd/TiO_2 in the ethanol conversion reaction: effect of temperature on product selectivity (catalyst: uncalcined, reduced at 400°C/16 h)

Temp. (°C)	Conv. %	Product distribution (% by mass)												
		Et_2O	MeCHO	C1	C2	C2=	C3	C3=	C4	C5	C6	C7	C8	C9+
104	0.52	0	0.52	0	0	0	0	0	0	0	0	0	0	0
129	2.33	0	1.07	0.02	0	0	0.02	0.02	0	0.33	0.23	0.10	0.54	0
153	7.45	0	1.39	0.05	0	0	0.09	0.07	0	1.61	0.90	0.93	1.59	0.82
176	17.95	0	1.79	0.17	0.01	0	0.34	0.18	0	3.76	1.57	2.34	3.17	4.62
200	33.75	0	2.29	0.55	0.03	0	1.26	0.37	0	7.77	2.23	5.78	4.06	9.41
226	62.88	0	2.75	1.96	0.12	0	4.39	0.64	0	15.05	2.45	12.45	4.06	19.01
250	85.62	0	2.49	3.47	0.29	0	6.20	1.27	0	19.44	2.63	17.01	4.14	28.68
264	86.84	0	3.09	2.86	0.40	0.02	2.74	2.66	0	15.36	3.60	16.78	8.72	30.61
275	88.29	0	2.87	2.08	0.37	0.05	1.30	2.71	0	12.25	4.55	19.21	14.42	28.48
299	66.97	1.05	2.80	0.77	0.26	0.24	0	1.39	0	3.54	7.56	2.67	16.85	29.84
325	59.43	4.00	2.69	1.54	0.87	0.73	0	1.46	0	1.67	11.99	1.92	19.38	13.18
349	56.17	6.57	1.69	1.54	1.99	1.39	0	0.92	0	1.08	13.05	1.83	16.16	9.95
374	56.78	10.20	2.19	2.75	4.22	2.95	0	1.56	4.69	1.21	12.90	2.59	14.30	7.22
397	74.79	9.08	3.11	3.07	5.85	5.27	0	2.02	5.37	1.84	13.38	3.01	15.60	7.19

Table 4.5 Catalytic performance of metal free TiO_2 in the ethanol conversion reaction: effect of temperature on product selectivity (catalyst: reduced at 400°C/16 h)

Temp. (°C)	Conv. %	Product distribution (% by mass)												
		Et_2O	MeCHO	C1	C2	C2=	C3	C3=	C4	C5	C6	C7	C8	C9+
227	0.07	0.07	0	0	0	0	0	0	0	0	0	0	0	0
256	0.47	0.45	0	0	0	0.02	0	0	0	0	0	0	0	0
276	1.47	1.34	0.04	0	0.02	0.07	0	0	0	0	0	0	0	0
302	5.16	4.49	0.12	0	0.15	0.35	0	0	0	0	0.05	0	0	0
325	13.95	11.20	0.27	0	0.55	1.43	0	0.01	0	0	0.43	0.06	0	0
348	26.13	17.70	0.52	0.01	2.12	3.94	0	0.08	0	0	1.15	0.51	0.10	0
375	42.58	21.61	0.87	0.05	8.63	10.10	0	0.63	0	1.64	6.06	0.89	1.85	0.25
398	54.28	5.53	1.13	0.16	14.71	16.62	0.13	1.58	3.53	2.40	4.17	0.96	3.02	0.34

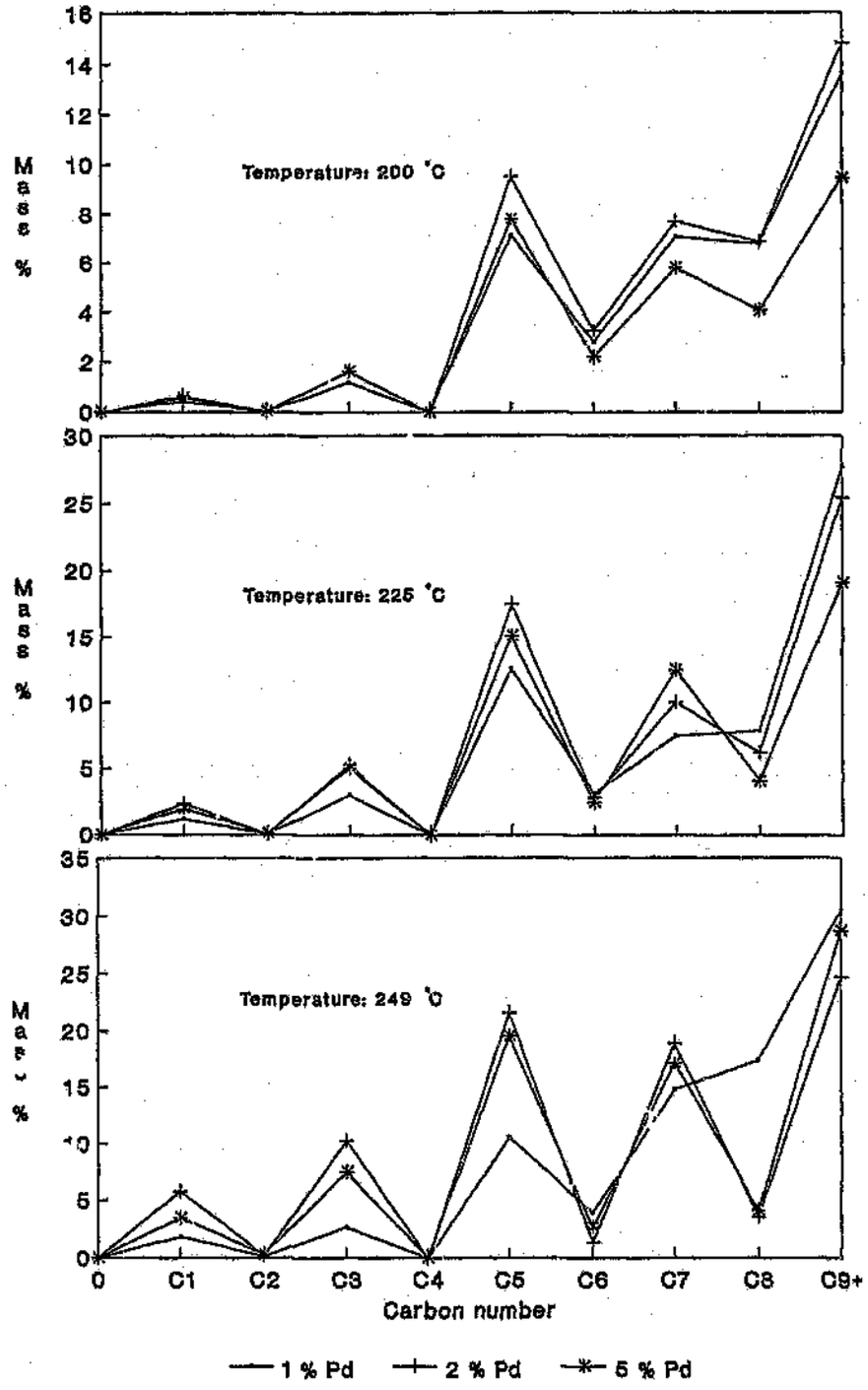

Figure 4.2 Product distribution from the ethanol transformation to hydrocarbons over Pd/TiO_2 (1%, 2% and 5% Pd by mass) catalysts at low temperature (Catalysts: uncalcined, reduced at 400°C/16 h in H_2)

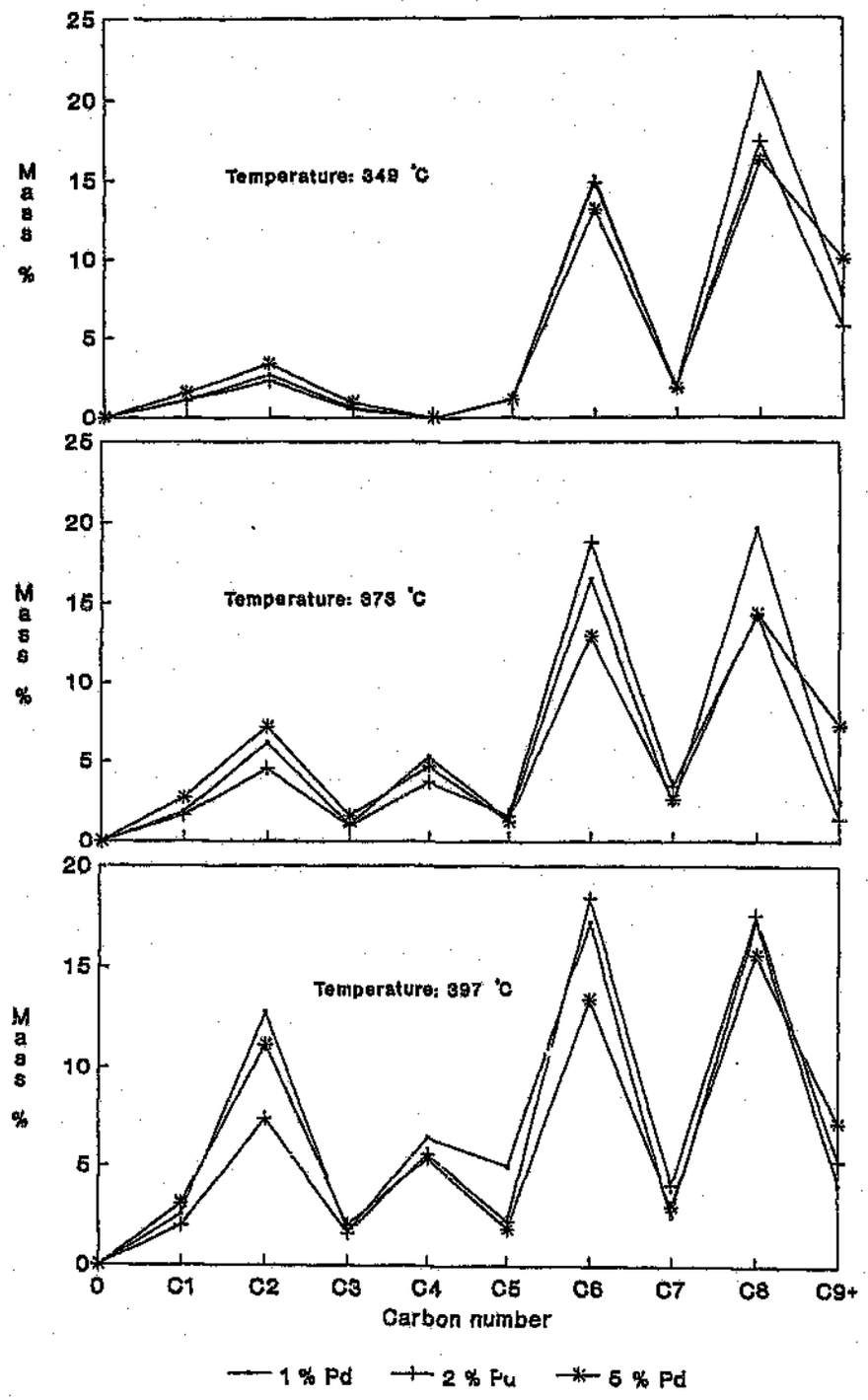

Figure 4.3 Product distribution in the ethanol transformation to hydrocarbons over Pd/TiO_2 (1%, 2% and 5% Pd by mass) catalysts at high temperature (Catalysts: uncalcined, reduced at 400°C/16 h in H_2)

Figure 4.4 below shows the ratio of heavy products (> C_7^+) to acetaldehyde as a function of the increasing ethanol conversion rate. This ratio is expressed as a selectivity, S. The figure also shows the selectivity at different Pd loadings.

The data reveals:

(1) An increase of heavy product (> C_7^+) formation with increasing ethanol conversion.

(2) Similar selectivity data was observed for all three of the loaded materials. However the 1% Pd loaded material does appear to give the highest selectivity. A comparison of the ratio of acetaldehyde plus heavy products (> C_7^+) to all the products obtained, expressed as a selectivity, S' is shown in Figure 4.5. From this figure it can be seen that the initial conversion data (< 10%) show predominantly acetaldehyde (and heavy product) formation, but when conversion is > 10%, the selectivity to acetaldehyde plus heavy products remains constant at about 60%. This would suggest that heavy product cracking may be occuring under the reaction conditions.

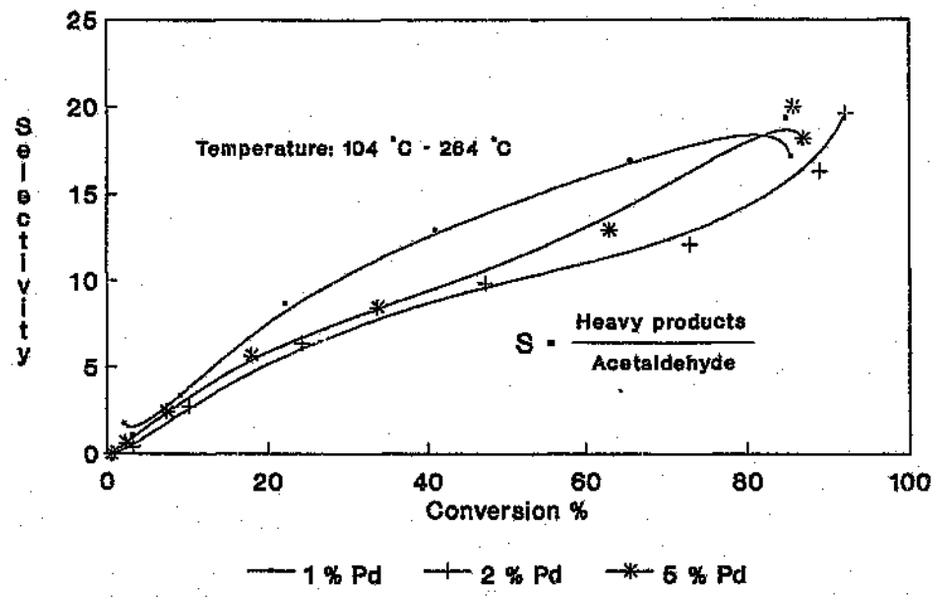

Figure 4.4 Ethanol conversions and selectivities for Pd/TiO_2 as a function of variation in Pd loading; (selectivity (S) = heavy products/ acetaldehyde)

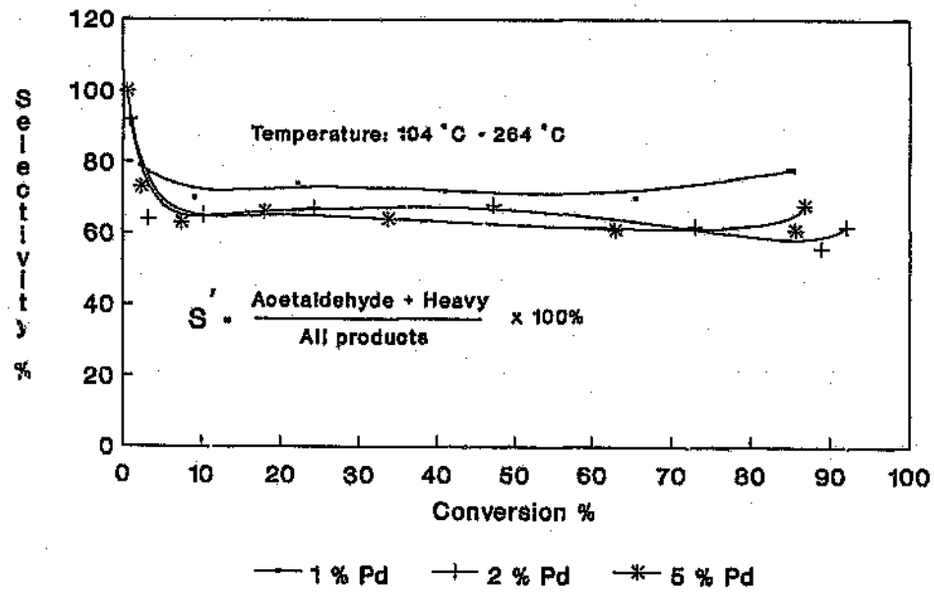

Figure 4.5 Ethanol conversions and selectivities for Pd/TiO_2 as a function of variation in Pd loading; (selectivity (S') = acetaldehyde + heavy products/ all products)

The following preliminary commemt can be made about the reaction mechanism. At low temperatures the Pd reacts with the ethanol to yield acetaldehyde and seconday products via the dehydrogenation route; this has a maximum rate at ca. 265°C. It thus appears that the primary product is acetaldehyde. Further, in the low temperature range (100°C - 275°C) no diethyl-ether or C_4 hydrocarbons were oberved suggesting little dehydration had occurred. However, at 300°C a second reaction pathway begins to operate - a dehydration reaction. This is shown schematically below:

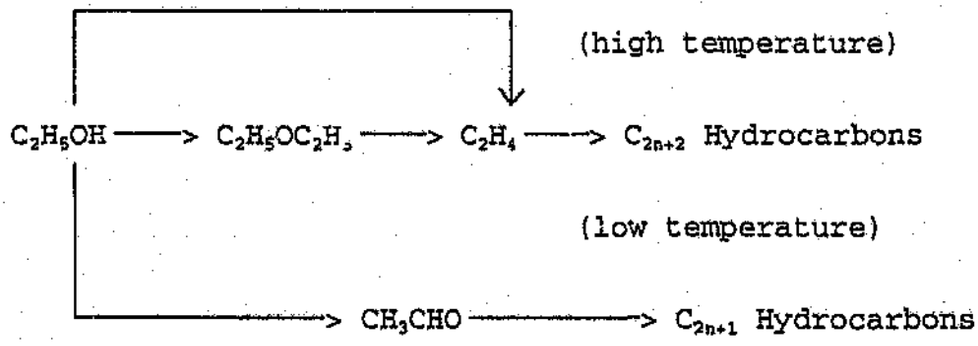

The first mechanism (at low temperature) involves the favoured production of odd numbered hydrocarbons; see Figure 4.2, whereas the second reaction pathway yielded even numbered hydrocarbons, as illustrated in Figure 4.3.

4.3.2 Lifetime study

The ethanol to hydrocarbons reaction, is known to require acid sites and/or a metal interaction to proceed [3]. However, a catalyst may lose its activity or its selectivity change with time and temperature during the process for a wide variety of reasons [4 - 6]:

(a) The particular active species may be converted to an inactive form (e.g. metal).

(b) Loss of active surface area due to crystalline growth (sintering).
(c) Loss of active area due to the deposition of carbonaceous material (coke).
(d) Chemical poisoning of the surface.

The results of a lifetime study of the 1%, 2% and 5% Pd/TiO_2 catalysts at 264°C are summarized in Figure 4.6 and Table 4.6. This temperature (264°C) was chosen as it is near the temperature at which maximum product yield in the low temperature region is observed. As can be seen the fall-off in activity increases: 2% Pd/TiO_2 < 1% Pd/TiC_2 < 5% Pd/TiO_2 (Figure 4.6). A linear decay is observed for all three samples.

Hydrocarbon product selectivities for the 2% Pd/TiO_2 catalyst varied with reaction time; the C_6 and C_8 hydrocarbon yields steadily increased with increasing reaction time (see Figure 4.7). It was also noticed that the catalyst was dark in colour after use. These findings suggest that coke has deposited on the catalyst during use, a well known phenomena in alcohol dehydration reactions. Further this coke was deposited on the palladium atoms. This results in the generation of a modified "Pd-coke" catalyst with different characteristics to that of the original catalyst. Normally this results in an increase in CH_3CHO formation and a decrease in CH_4 formation. The spectrum suggests that the catalyst is acting more like an "acid" catalyst as coke is formed (see Figure 4.7 and Table 4.6).

From these studies on the effect of palladium concentration on activity, selectivity and lifetime it is clear that the 2% Pd by mass loaded TiO_2 support gave a superior performance compared with the 1% and 5% Pd/TiO_2 catalysts

under the conditions examined. This catalyst was therefore used in later experiments.

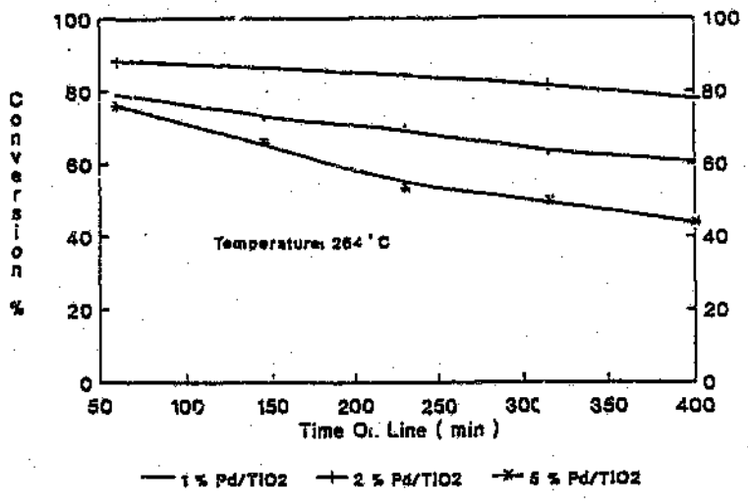

Figure 4.6 Comparison of the lifetime of Pd/TiO_2 (1%, 2% and 5% Pd by mass) in the ethanol conversion reaction (Catalysts: uncalcined, reduced at 400°C/16 h in H_2; T = 264°C)

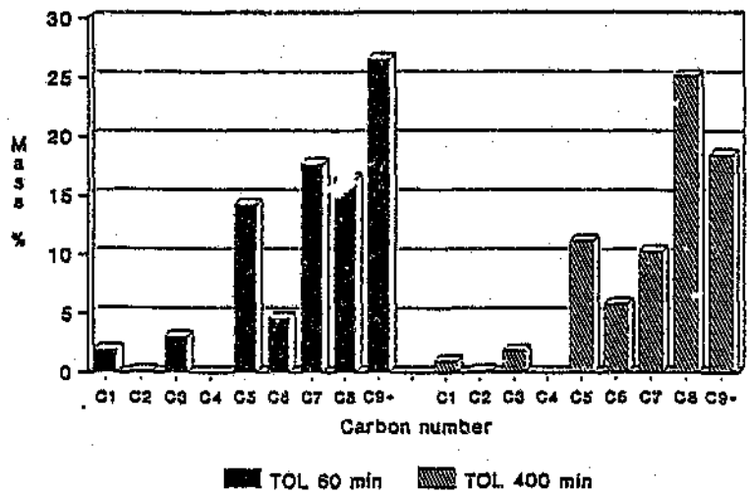

Figure 4.7 Changes in product selectivity with time on line; ethanol conversion over 2% Pd/TiO_2 catalyst (Catalysts: uncalcined, reduced at 400°C/16 h in H_2; T = 264°C)

Table 4.6 Comparison of the catalytic lifetime of 1% Pd/TiO_2, 2% Pd/TiO_2 and 5% Pd/TiO_2 catalyst in the ethanol conversion reaction

Catalyst	1% Pd/TiO_2[a]			2% Pd/TiO_2[a]			5% Pd/TiO_2[a]		
Time on line (min)	60	230	400	60	230	400	60	230	400
Conversion (%)	79.05	70.17	60.71	88.25	84.52	77.99	75.91	53.37	43.75
Product distribution[b]									
EtOEt	0	1.49	1.51	0	0	0	0	1.04	1.02
MeCHO	4.25	4.60	4.76	3.42	3.83	4.07	3.18	3.62	3.92
Methane	1.76	1.00	0.63	1.99	1.58	0.99	1.08	0 45	0.38
Ethene	0.04	0.05	0.04	0.01	0.02	0.02	0.05	0.06	0.06
Ethane	0.17	0.12	0.08	0.18	0.19	0.15	0.18	0.10	0.08
Propene	2.16	1.89	1.43	1.37	1.54	1.04	2.22	1.29	1.10
Propane	0.60	0	0	1.71	0.91	0.53	0	0	0
C4	0	0	0	0	0	0	0	0	0
C5	8.91	6.69	6.70	14.24	11.41	11.18	8.64	6.78	5.62
C6	4.52	5.57	5.62	4.62	5.14	5.84	5.08	6.48	5.76
C7	10.34	6.11	5.30	17.69	12.75	10.28	17.47	11.03	7.57
C8	23.21	26.39	21.51	16.43	24.57	25.12	15.98	14.64	13.19
C9+	23.09	16.26	13.13	26.59	22.58	18.47	22.03	7.88	5.05

[a] Uncalcined, reduced at 400°C/16 h; [b] % by mass; EtOH flow rate, 1.0 ml h^{-1}; T = 264°C

4.3.3 Comparison of different palladium metal salt preparations

The catalysts (Pd/TiO_2) discussed above were prepared by co-precipitating the palladium from an aqueous palladium nitrate solution with an ammonia solution, in the presence of dispersed TiO_2 support. Palladium chloride ($PdCl_2$) supported catalysts were prepared according to the same method (co-precipitation) to assess the effect of the Cl^- ion on the reaction. The results obtained were compared with those obtained earlier (2% $Pd(NO_3)_2$ on TiO_2 catalyst) using the same conditions (see footnote to Figure 4.8 for experimental details). These results are summarized in Figure 4.8 and 4.9.

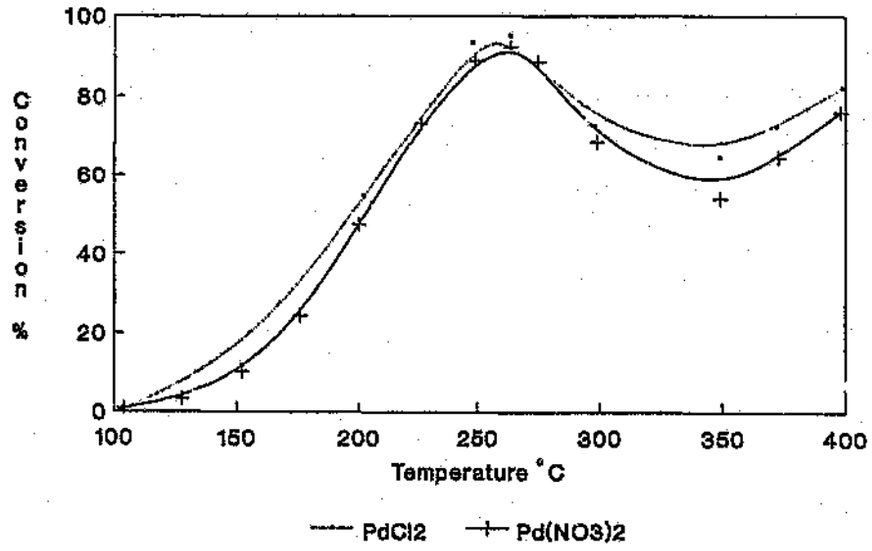

Figure 4.8 Comparison of $PdCl_2$ and $Pd(NO_3)_2$ supported salts[a]

[a] Aqueous ethanol (96.0%) feed, WHSV = $0.833h^{-1}$, reaction temperature between 100°C and 400°C, catalyst: uncalcined, and reduced at 400°C for 16 h with hydrogen.

Both $PdCl_2$ and $Pd(NO_3)_2$ give similar results in terms of activity and selectivity. In the low temperature range (100°C - 275°C) both Pd salts give similar conversions with maximum yields of 95.02% (Pd from palladium chloride) and 92.10% (Pd from palladium nitrate) at 264°C. In the high temperature range (350°C - 400°C) conversions of 80.93% (Pd from palladium chloride) and 75.85% (Pd from palladium nitrate) were obtained at 400°C, see Figure 4.8.

The interactions taking place between the metal precursor species and the support during the impregnation process, may play a decisive role in determining the resulting properties of the catalysts. Possible types of interactions are [7 - 9]:

(a) adsorption of metal precursor species on the oxide support.
$Ti\text{-}OH + H^+ + ML_x^- \text{-------} > Ti\text{-}OH_2^+ \; ML_x^-$

(b) adsorbed species may undergo a subsequent surface reaction with support.
$Ti\text{-}OH_2^+ \; ML_x^- + Ti\text{-}OH \text{-----} > Ti\text{-}OH_2^+ \; ML_{x-1} \text{-}O\text{-}Ti + HL$
where L is the ligand and M the central metal atom.

(c) acidic attack of the support. For instance, Fenoglio et al. [10] have reported that impregnation of TiO_2 with aqueous solutions of rhodium chloride at low pH (about 3), results in acid attack of TiO_2 support causing a partial dissolution of Rh in the TiO_2.

From Figure 4.8 it is clearly illustrated that the different sources of palladium metal do not have a significant effect on the ethanol conversion reactions. This also suggests that the different acids used in the impregnation reaction (nitric acid for $Pd(NO_3)_2$, and HCl for $PdCl_2$) do not affect the support.

This could be due to the preparation procedure (co-precipitation) used which required an ammonia solution to control the solution pH value between 8 - 9. The washing procedure to remove Cl^- and NO_3^- must also have been effective.

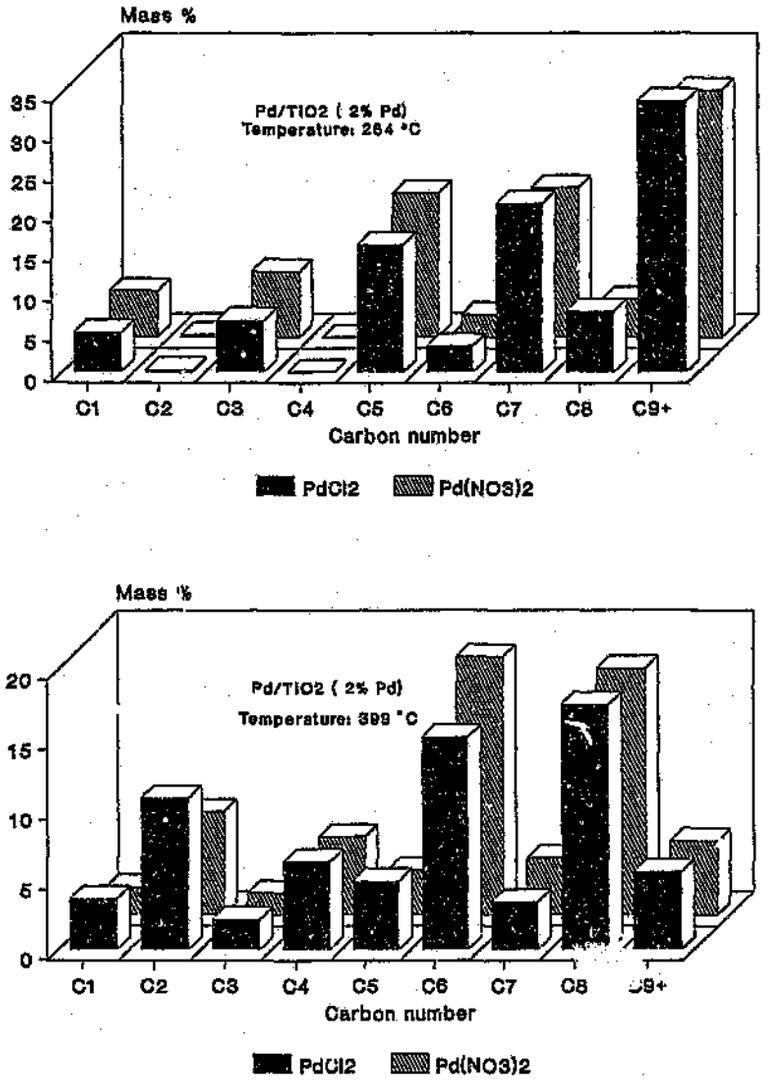

Figure 4.9 Comparison of product selectivities for ethanol conversion over 2% Pd/TiO_2; metal derived from palladium chloride and palladium nitrate (Catalysts: uncalcined, reduced at 400°C/16 h in H_2)

4.3.4 Effect of catalyst preparation procedure

For industrial catalysts high activity, selectivity and long life are essential. To accomplish these requirements, catalysts should possess a large and thermostable active surface area. In supported mixed oxide catalysts, activity, stability and physical characteristics are likely to be dependent on the concentration of the active component, its state of sub-division and phase composition as well as on the physico-chemical properties of the supporting medium [11, 12]. Their physico-chemical properties are very much dependent on the method of preparation [13, 14]. It is, therefore, important to select materials that have the requisite catalytic properties and also to choose an appropriate method to prepare a catalyst with the desired structure and stability.

Generally, dispersion of a metal on a support is carried out by: (1) precipitation (co-precipitation), (2) adsorption, (3) ion exchange, and (4) impregnation (incipient wetness). Each technique has advantages and disadvantage [5, 15]. As mentioned in Chapter two, the "incipient wetness" impregnation is the simplest and most direct method of deposition. The impregnation technique requires less equipment since the filtering steps are eliminated and washing is not needed. It is the preferred process in preparing supported noble metal catalysts where economic considerations are important [5]. However, it is not a suitable method of preparing high metal loadings and the procedure also requires a high calcination (*ca.* 400°C - 500°C) procedure for the removal of reagent anions. On the other hand, the "precipitation" technique is the preferred deposition route when higher metal loadings are required [4]. The procedure also generally provides more uniform

mixing on a molecular scale of the various catalyst ingredients, good distribution of active species throughout the catalyst and the ultimate particle sizes and shapes are not limited by the carriers commercially available. Also, more control of pore size and pore-size distribution may be possible.

An investigation on the effects of the actual catalyst preparation methods (incipient wetness and co-precipitation methods) on the ethanol conversion reaction was thus undertaken. Since, there was no significant difference in the activity/selectivity data for either $PdCl_2$ or $Pd(NO_3)_2$, either of the Pd salts could have been employed. $Pd(NO_3)_2$ was thus used and Figure 4.10 illustrates the results obtained from the different preparation methods. These results indicate that the preparation method does not significantly affect the catalyst character or properties of the catalyst (see Figures 4.10 and 4.11).

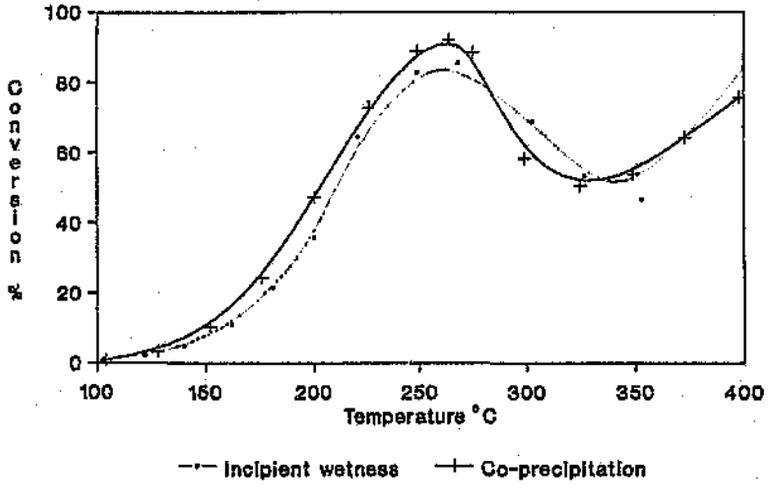

Figure 4.10 Comparison of the catalytic activities of 2% Pd/TiO_2 catalyst prepared from incipient wetness and co-precipitation methods (Catalyst: reduced at 400°C for 16 h with hydrogen)

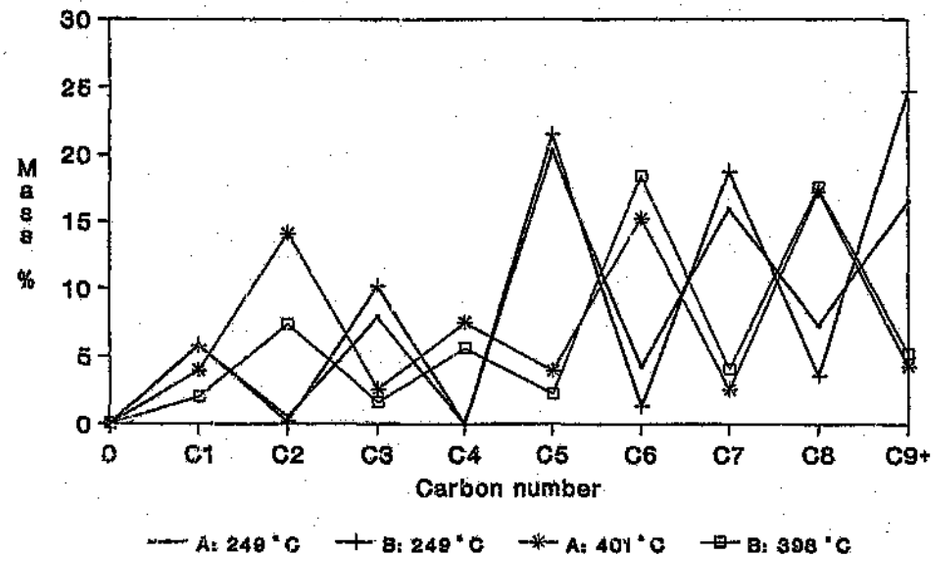

Figure 4.11 Comparison of the catalytic selectivities of 2% Pd/TiO_2 catalyst prepared from incipient wetness and co-precipitation methods; (A) incipient wetness, (B) co-precipitation (Catalyst: reduced at 400°C for 16 h with hydrogen)

4.3.5 Comparison of the conversion of ethanol to hydrocarbons over 2% Pd/TiO_2 in the presence of hydrogen and nitrogen

The 2% Pd/TiO_2 catalyst was prepared by the incipient wetness technique, calcined at 400°C for 16 h in air and reduced <u>in situ</u> at 400°C for 16 h with hydrogen. Hydrogen or nitrogen were utilized as carrier gases in the reaction. The results are shown in Table 4.7, 4.8 and Figure 4.12 to 4.14.

The ethanol conversion for both carrier gases (hydrogen and nitrogen) increases with increasing reaction temperature to maximum conversion (H_2, T = 301°C, total conversion = 92.96%; N_2, T = 268°C, total conversion = 85.59%), before the conversion decreases. For instance at 350°C the total conversion = 66.13% for H_2 and = 46.43% for N_2. After 350°C the conversions change for both carrier gases (see Table 4.7 and 4.8). Significantly in the low temperature range (100°C to 270°C), it can be seen that the use of a hydrogen carrier gas results in a change in the product spectrum in the ethanol conversion reaction compared to the use of a nitrogen carrier gas (Figure 4.12).

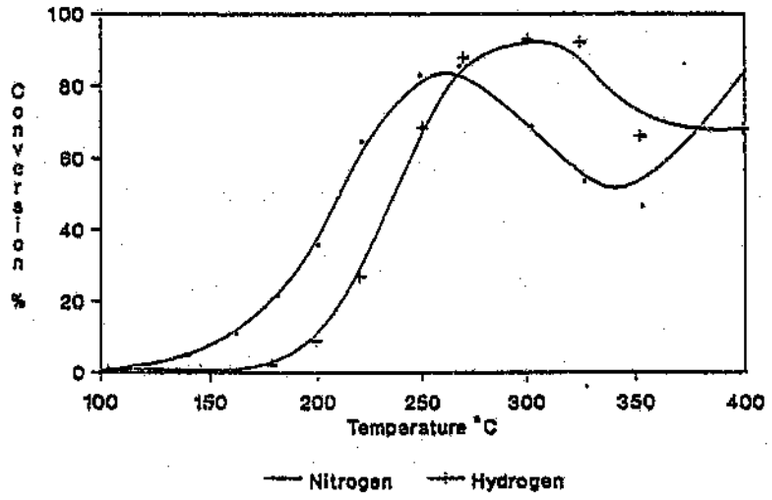

Figure 4.12 Comparison of carrier gas H_2 and N_2 for ethanol conversion over 2% Pd/TiO_2 catalyst

The use of hydrogen as the carrier gas also favours the production of light hydrocarbons, mainly methane, propane and C_5, and yields only small quantities of acetaldehyde, ethane and higher olefins and aromatics. On the other hand, using nitrogen as a carrier gas, the major products are higher hydrocarbons C_6, C_7, C_8, and C_{9+}.

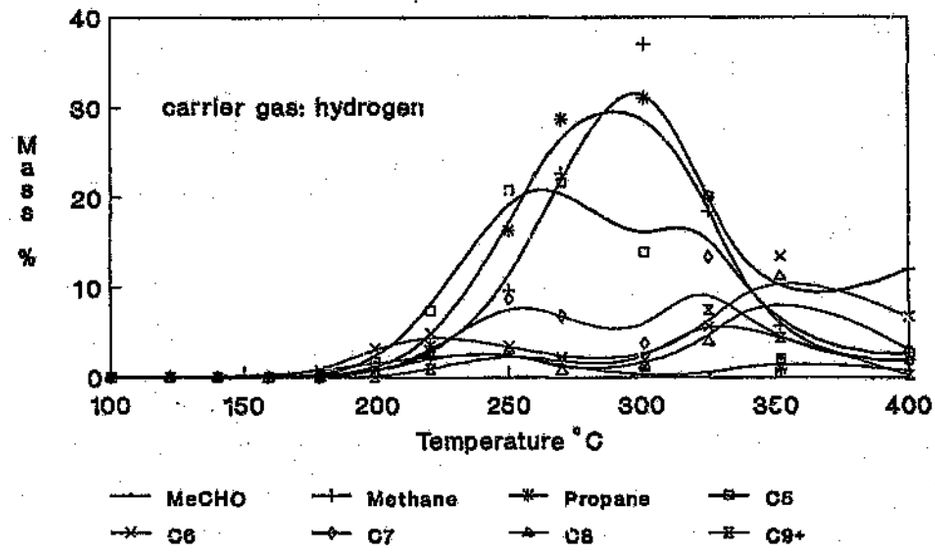

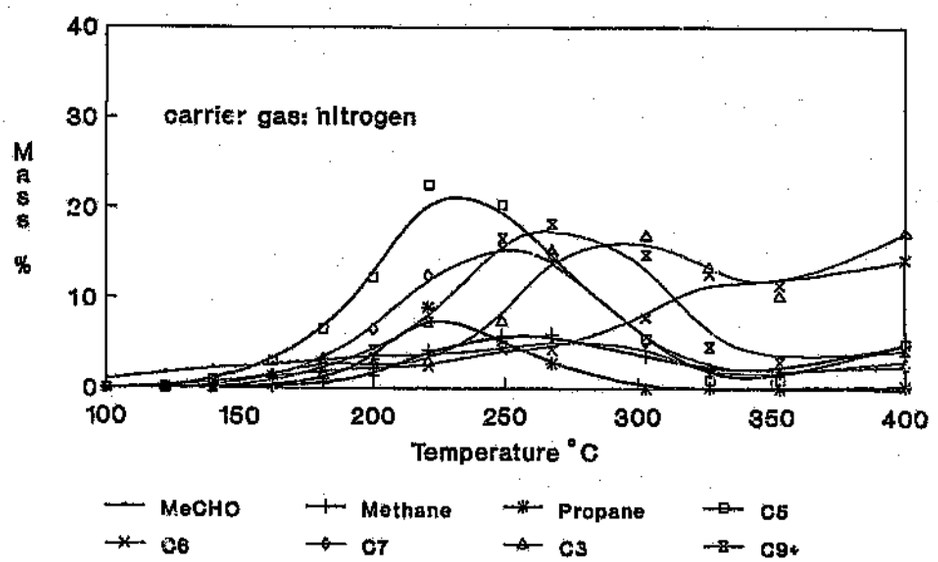

Figure 4.13 Product selectivity versus reaction temperature for a 2% Pd/TiO_2 catalyst in the ethanol conversion reaction

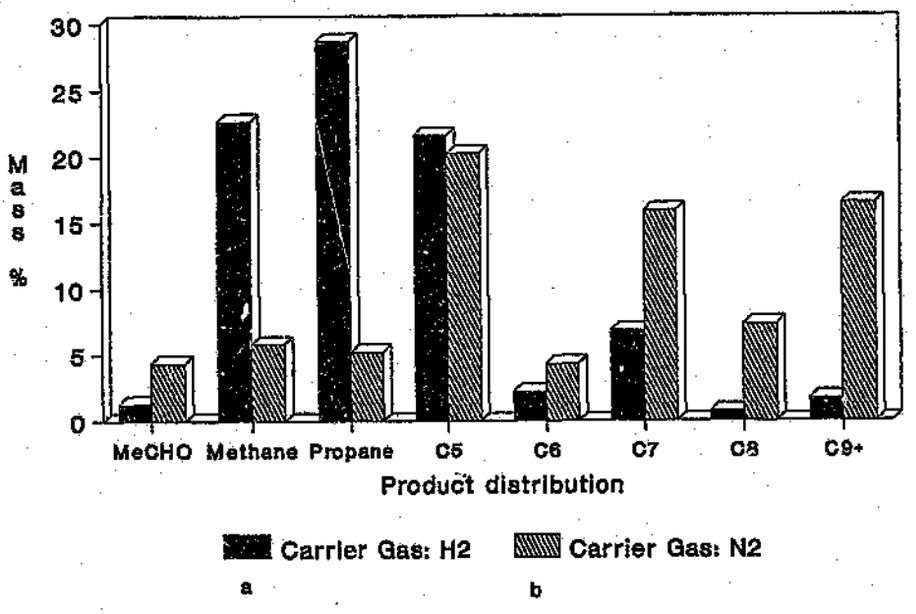

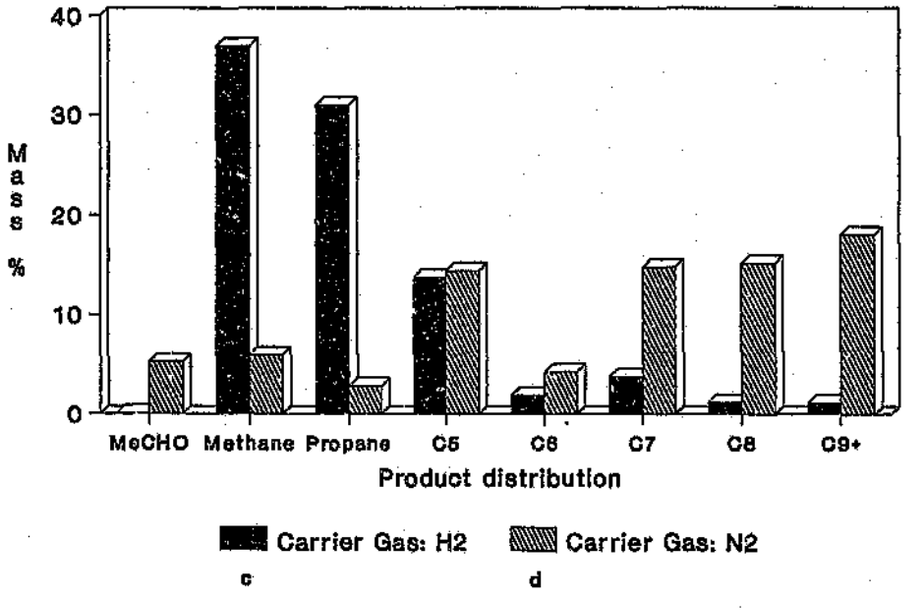

Figure 4.14 Comparison of product sprecta for ethanol conversion using H_2 and N_2 carrier gases

a: T= 270°C, total conversion= 87.95%

b: T=249°C, total conversion= 82.85%

c: T= 301°C, total conversion= 92.96%

d: T= 268°C, total conversion=85.59%

A similar experiment was carried out using the metal free TiO_2 support and the ethanol conversion was investigated in the presence of both the nitrogen and hydrogen carrier gases. The reaction was carried out in the temperature range 200°C - 400°C, and an ethanol feed rate of 0.5 ml h^{-1}. From the results, Table 4.9, it appears that the product spectrum is typical of an acid catalyst. The main products were diethyl-ether with maximum ± 24% (% by mass) yield at 350°C while other products increased linearly with increasing temperature. At the maximum temperature used (400°C), however, the main products were C_2 (ethene and ethane) hydrocarbons. This result appears not to be affected by the nature of carrier gas.

Table 4.7 Catalytic performance of the 2% Pd/TiO_2 for ethanol conversion in the presence of hydrogen as carrier gas[a]

Temp. (°C)	Conv. %	Product distribution (% by mass)												
		Et_2O	MeCHO	C1	C2	C2=	C3	C3=	C4	C5	C6	C7	C8	C9+
103	0.67	0.66	0	0.01	0	0	0	0	0	0	0	0	0	0
122	1.01	0.97	0.03	0.01	0	0	0	0	0	0	0	0	0	0
140	0.66	0.52	0.12	0.02	0	0	0	0	0	0	0	0	0	0
159	0.57	0.05	0.33	0.07	0.02	0	0	0	0	0.05	0.05	0	0	0
178	2.09	0.11	0.73	0.24	0.08	0	0.08	0	0	0.17	0.68	0	0	0
199	8.83	0	1.55	0.73	0.18	0	0.80	0	0	1.63	3.13	0.38	0.43	0
220	26.64	0	2.35	1.99	0.40	0	3.55	0	0	7.37	4.94	2.79	2.33	0.92
250	68.39	0	2.67	9.66	1.27	0	16.32	0	0	20.74	3.42	8.70	2.95	2.66
270	87.95	0	1.29	22.65	2.21	0	28.74	0	0	21.63	2.20	6.84	0.71	1.68
301	92.96	0	0.10	37.02	2.95	0	31.04	0	0	13.80	1.92	3.75	1.20	1.18
325	92.11	0	0.30	18.42	3.09	0	19.92	0	0	20.11	5.62	13.28	3.92	7.45
352	66.13	4.57	2.03	5.75	9.90	0.50	0.90	1.86	7.78	1.99	13.38	1.89	11.14	4.44
399	67.92	1.95	0.77	12.01	30.03	1.00	1.98	1.86	3.99	2.63	6.69	1.68	3.10	0.23

[a] Catalyst, prepared using incipient wetness technique; H_2 flow rate, 21 ml min^{-1}; EtOH flow rate, 1.0 ml h^{-1}

Table 4.8 Ethanol conversion over 2% Pd/TiO_2 (nitrogen as carrier gas)[a]

Temp. (°C)	Conv. %	Product distribution (% by mass)												
		Et_2O	MeCHO	C1	C2	C2=	C3	C3=	C4	C5	C6	C7	C8	C9+
103	0.98	0	0.97	0.01	0	0	0	0	0	0	0	0	0	0
122	2.09	0	1.69	0.04	0	0	0.03	0	0	0.13	0.17	0	0.03	0
140	4.78	0	2.24	0.07	0	0	0.08	0.03	0	0.83	0.64	0.22	0.67	0
162	11.01	0	2.63	0.19	0.01	0	0.32	0.09	0	2.98	1.30	1.27	1.43	0.79
181	21.53	0	3.08	0.52	0.02	0	1.01	0.19	0	6.48	1.86	3.23	2.93	2.21
200	35.67	0	3.57	1.38	0.05	0	3.15	0	0	12.12	2.32	6.48	2.44	4.16
221	64.49	0	3.67	4.23	0.15	0	8.91	0	0	22.44	2.42	12.49	2.84	7.34
249	82.85	0	4.34	5.80	0.52	0.01	5.18	2.73	0	20.24	4.29	15.91	7.[illegible]	16.51
268	85.59	0	5.22	5.91	0.64	0.05	2.77	4.25	0	14.44	4.24	14.78	15.21	18.08
303	68.68	3.98	4.85	3.54	0.99	0.35	0	5.16	0	5.44	7.81	5.04	16.77	14.75
327	53.21	10.76	1.30	2.19	3.20	1.44	0.08	0.77	0	0.92	12.59	2.18	13.26	4.52
353	46.43	10.92	1.57	1.76	2.63	1.67	0.07	0.59	0	0.96	11.40	1.75	10.16	2.95
401	84.09	9.70	3.08	4.92	8.83	5.26	0.33	2.23	6.49	4.93	14.24	2.56	17.23	4.29

[a] Catalyst, prepared using incipient wetness technique; N_2 flow rate, 21 ml min^{-1}; EtOH flow rate, 1.0 ml h^{-1}

Table 4.9 Comparison of carrier gas (N_2 and H_2) for ethanol conversion over metal free TiO_2 catalyst (carrier gas flow rate: 21 ml min^{-1}, ethanol flow rate: 0.5 ml h^{-1})

Temp. (°C)	Conv. %	Product distribution (% by mass)										
		Et_2O	MeCHO	C1	C2	C2=	C3=	C4	C5	C6	C7	C8+
						N_2 carrier gas						
251	1.29	1.29	0	0	0	0	0	0	0	0	0	0
270	5.19	5.03	0	0	0	0.16	0	0	0	0	0	0
303	31.19	19.21	0.51	0	1.00	2.04	0	0	0	0	8.43	0
349	47.84	24.08	0.77	0	7.17	9.28	0.40	1.25	0	3.51	0.86	0.52
395	60.11	1.80	0.39	0.23	17.01	17.94	2.25	7.46	1.83	7.34	1.91	1.95
						H_2 carrier gas						
200	0.75	0	0	0.01	0	0	0	0	0	0	0	0
251	0.94	0.84	0.06	0.01	0	0.03	0	0	0	0	0	0
301	11.12	8.78	0.41	0.07	0	1.16	0	0	0.03	0.63	0.04	0
349	41.28	18.13	0.84	0	5.10	7.92	0.37	0	0.30	6.08	0.80	1.74
395	63.94	1.61	0.38	0.22	14.76	16.70	2.48	9.59	2.75	9.51	1.33	4.61

The reductive dehydroxylation reaction can proceed via a number of mechanism [16 - 19]:

(1) Dehydration followed by hydrogenation of an olefin.

$$RCH_2CH_2OH \xrightarrow{-H_2O} RCH{=}CH_2 \xrightarrow{+H_2} RCH_2CH_3$$

It is also possible that dehydration to an ether could yield the saturated hydrocarbons.

(2) Direct hydrogenolysis of the hydroxyl group.

$RCH_2OH \longrightarrow RCH_3$ and $R'CH_3 + 2\ H_2O$

where $R'CH_3$ is the product of skeletal isomerization accompanying the reductive dehydroxylation of alcohols.

(3) Dehydrogenation of the alcohol followed by decarbonylation of the intermediate aldehydes (termed reductive dehydroxymethylation).

$$RCH_2OH \xrightarrow{-H_2} RCHO \begin{cases} \longrightarrow RH \\ \longrightarrow CO \xrightarrow{H_2} CH_4 + H_2O \end{cases}$$

The hydrogenolysis of primary alcohols to paraffins, having one carbon atom less than the parent alcohol has been observed for nickel-kieselguhr and other catalysts [17, 18].

The reductive dehydroxylation and the dehydration reaction (to give olefins and ethers) are related to the intrinsic acidic properties of the catalysts [17]. These reactions can be blocked by removing the acidity of the catalyst. For instance, Pines and Kobylinski [16, 17, 19] reported that when the acidic sites on a Ni supported acid catalyst were neutralized by sodium ions the nickel lost its ether formation abilities and became a dehydrogenation and dehydroxymethylating catalyst.

The presence of hydrogen as carrier gas can be essential for the maintenance of the activity of the catalyst and can also greatly influence the reactivity and selectivity of the catalyst [20]. Licht et al. [21 - 23] have reported on the effect of hydrogen carrier gas on the alcohol conversion to ethers.

The product spectrum permits the determination of the dominant mechanism in the reaction at low temperature as follows:

(1) The predominance of odd numbered over even numbered carbon atom products is consistent with a reductive dehydroxymethylation mechanism (N_2 or H_2 carrier gas).

(2) The presence of large quantities of methane is suggestive of a chain growth termination reaction (H_2 as carrier gas). Under an N_2 atmosphere, H_2 gas is generated in the reaction, which subsequently yields hydrogenated products. However, chain growth competes with hydrogenation under N_2 and the limited quantities of H_2 results in products with chain length > C_6.

(3) Of interest is the lack of any C_4 product but large quantities of C_5 and C_3 products. The variable C_3 product composition produced in N_2 and H_2 carrier gases (e.g. 250°C N_2: 7.91%, H_2: 16.3%) for similar C_5 product yields highlights the competitive nature of the chain growth versus hydrogenation reaction routes.

4.3.6 The effect of reaction temperature cycles

It is well known that catalyst deactivation can occur via several processes such as posioning, fouling, reduction of active area by sintering, loss of active species etc. [4, 5, 24], Marcilly and France [25] also indicated that palladium containing catalysts deactivate in the hydrocracking reaction via coke formation on the active surface, aging of the hydrogenation function and inhibition of the acidic function. A catalyst will frequently undergo reconstruction during reaction, causing a change in the total area and nature of the surface. A change in the number and nature of the active sites can cause "aging" of the catalyst [26].

The ethanol conversion reaction was studied using varying reaction temperature cycles. Low temperature (*ca.* 250°C) and high temperature (*ca.* 360°C) alternating temperatures were used. In experiment 1 (Table 4.10) an initial reaction temperature (251°C) gave 90.18% ethanol conversion and when the temperature was increased (359°C) a conversion of 71.41% was obtained. Analysis of the products showed that, similar to the earlier studies, the ratio of odd to even numbered hydrocarbons changed with temperature. When the temperature was dropped back to 251°C the conversion of ethanol also instantly dropped to a very low value (± 7%; 60 min). On increasing the reaction temperatures to 359°C the conversion of ethanol again increased (61,08%). Lowering the temperature (251°C) again resulted in a drop in the conversion of ethanol (± 6% products).

A similar experiment, to experiment 1 (exp. 2), was carried out but in this case the temperature was raised to 357°C

immediately (60 min) and then decreased to 250°C. The results obtained were similar to those from experiment 1. These results were compared with those in Figure 4.1 and Table 4.3. Results at the high temperature (selectivity, yield) were found to be independent of the experimental procedure, see Table 4.10 and Figure 4.15.

These results suggest that the deactivation of Pd occurs at high temperatures but that the activity of the TiO_2 is little affected by high temperatures. The reaction temperature cycle studies indicate inhibition of the metallic function which could be caused by coke deposited on the Pd atoms (see previous disscusion, section 4.3.2). A strong metal support interaction is also possible.

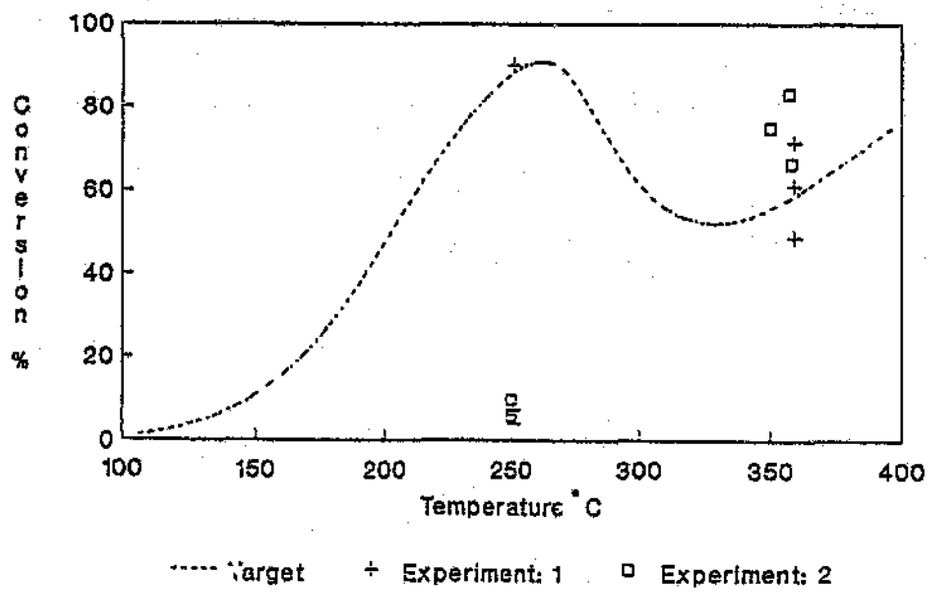

Figure 4.15 Effect of reaction temperature on ethanol conversion over 2% Pd/TiO_2 catalyst (Catalyst: uncalcined, reduced at 400°C/16 h in H_2)

Table 4.10 Effect of reaction temperature on catalytic activity and selectivity of 2% Pd/TiO_2 catalyst for ethanol conversion reaction[a]

Temp. (°C)	Run No.	Conv. %	Product distribution (% by mass)											
			Et_2O	MeCHO	C1	C2	C2=	C3[b]	C4	C5	C6	C7	C8	C9+
						Experiment: 1								
251	1	90.18	0	2.83	5.87	0.20	0	7.86	0	18.97	2.74	17.97	4.81	28.93
359	2	71.41	7.76	1.84	5.09	4.98	1.18	2.66	5.53	1.03	13.87	1.88	18.04	7.55
251	3	7.30	0.22	1.16	0.14	0.04	0.02	0.11	0	0.34	1.47	0.08	2.62	1.10
359	4	61.08	9.81	1.95	3.66	4.36	1.54	1.60	4.30	1.13	12.18	1.52	12.16	6.87
251	5	4.03	0.22	0.61	0.10	0.03	0.02	0.06	0	0.23	0.90	0.05	1.15	0.66
359	6	48.67	11.28	1.91	2.79	3.92	1.74	1.10	0	1.04	10.77	1.52	8.75	3.85
						Experiment: 2								
357	1	83.02	5.10	1.93	5.9[b]	4.16	1.08	2.97	5.46	4.38	14.33	3.23	17.11	17.29
250	2	9.62	0.21	1.92	0.18	0.06	0.03	0.15	0	0.52	2.03	0.09	3.10	1.33
350	3	74.80	5.32	1.92	3.04	2.47	0.93	1.41	4.08	1.08	24.83	1.14	17.09	11.49
250	4	7.32	0.17	1.25	0.13	0.04	0.03	0.08	0	0.39	1.53	0.07	2.36	1.27
358	5	66.32	8.15	2.18	3.33	3.49	1.47	1.36	4.22	1.30	13.95	1.57	16.29	9.01
250	6	5.76	0.15	0.75	0.08	0.02	0.02	0.04	0	0.30	1.23	0.07	1.96	1.14

[a] Catalyst: uncalcined, reduced at 400°C/16 h; [b] Propane

4.3.7 Investigation of the effect of calcination temperature on the catalytic activity and selectivity of a 2% Pd/TiO_2 catalyst

Calcination is a process used in general catalyst preparations, and may have several proposes [5]. These include: (a) loss of chemically bound water or CO_2, (b) changes in pore size distribution, (c) active phase generation, (d) surface conditioning, and (e) stabilization of mechanical properties.

In the above experiments (4.3.1 to 4.3.6) ethanol conversion experiments were performed over an uncalcined Pd/TiO_2 catalyst. The effect of calcination temperature on the catalytic performance of the 2% Pd/TiO_2 catalyst (calcined in air, 200°C, 400°C and 600°C, 16 h; reduced <u>in situ</u> at 400°C for 16 h) was ascertained. The results are summarized in Figures 4.16 to 4.18 and Table 4.11. From the results it can be seen that the uncalcined catalyst and the 200°C calcined catalyst give similar activity for the ethanol conversion reaction. However, increasing the calcination temperature (400°C, 600°C) results in a <u>decrease</u> in catalytic activity with the temperature increase (see Figure 4.16).

Similar product selectivities were obtained for all the catalysts (uncalcined; calcined at 200°C, 400°C and 600°C). However, the amount of each product (odd carbon numbered hydrocarbons) decreased with increasing calcination temperature in the low reaction temperature regime (< 280°C; see Figure 4.17). Above 280°C a similar decrease in product yield was observed but this time for even carbon numbered hydrocarbon products (see Figure 4.18).

Generally, all cat lysts showed an increase in the conversion of ethanol with an increasing reaction temperature with maximum coversions being achieved in the reaction temperature range 250°C - 275°C: 92.10% at 264°C (uncalcined); 89.73% at 275°C (calcination, 200°C); 79.34% at 249°C (calcination, 400°C) and 45.04% at 249°C (calcination, 600°C).

Calcination at the high temperatures was considered to affect the catalyst in several ways: (1) destruction of catalytic framework (the decrease in the surface area of the catalyst after calcination is indicative of such a structural change), and (2) dehydroxylation of some of the Brönsted acid sites, leading to the generation of Lewis acid sites. Detreköy et al. [27] have reported that the concentration of hydroxyl groups reaches a maximum at 400°C and thereafter decreases linearly; at the same time Lewis acid sites start appearing, with their concentration reaching a maximum at about 550°C followed by a decrease at higher temperatures. The sum of the Brönsted and Lewis acid site concentration reached a maximumat about 420°C.

In the case of the 2% Pd/TiO_2 the decreased activity could also be due to sintering associated with high temperature calcination which reduced the catalyst surface area.

This series of experiments reveals that the optimum calcination temperatures should be below 400°C.

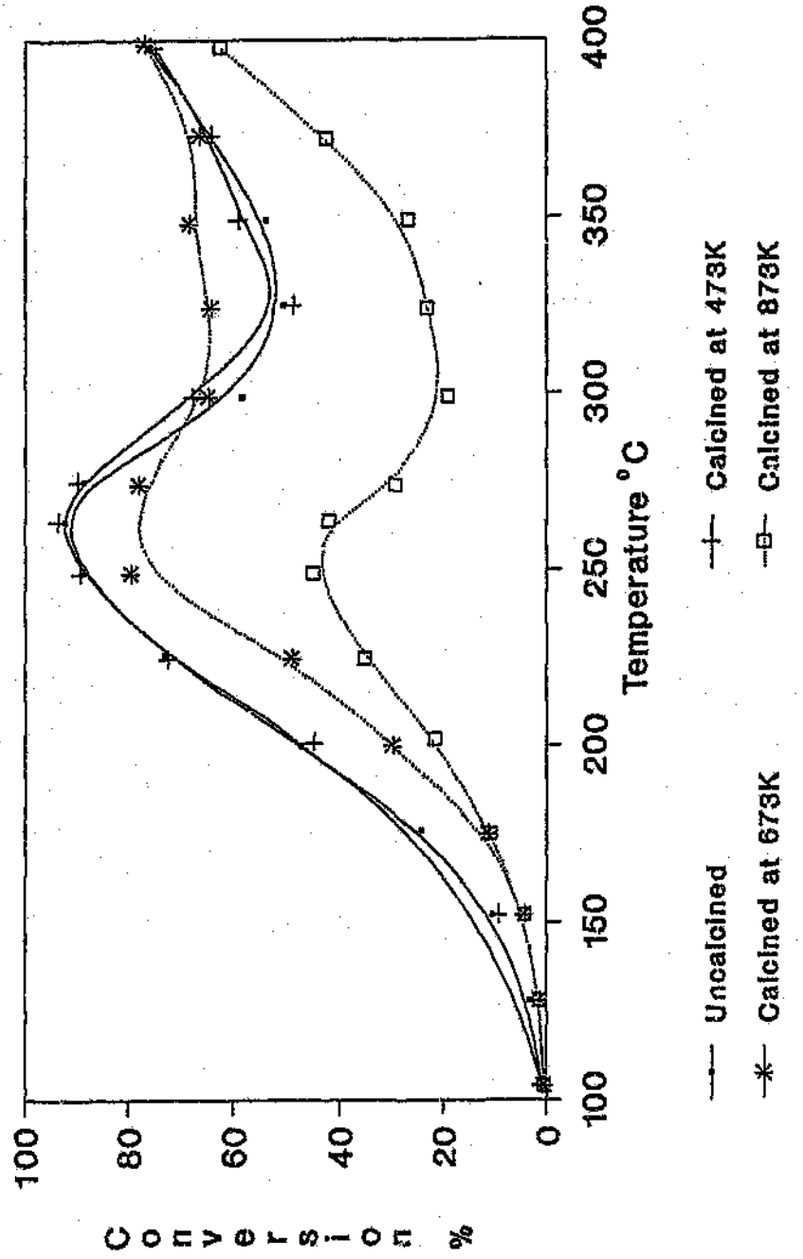

Figure 4.15 A comparison of different calcination temperature on the catalytic activity of 2% Pd/TiO_2 catalyst in the ethanol conversion reaction

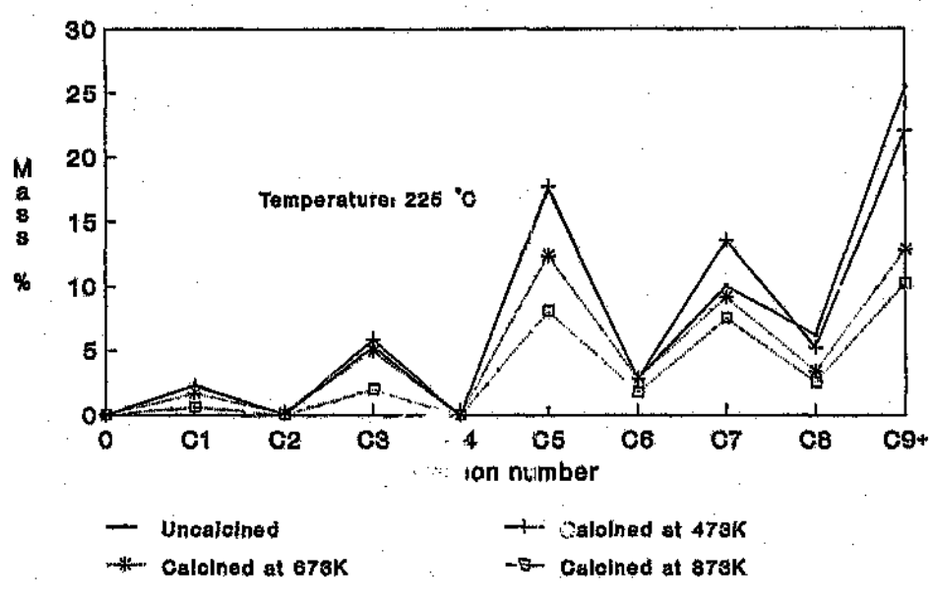

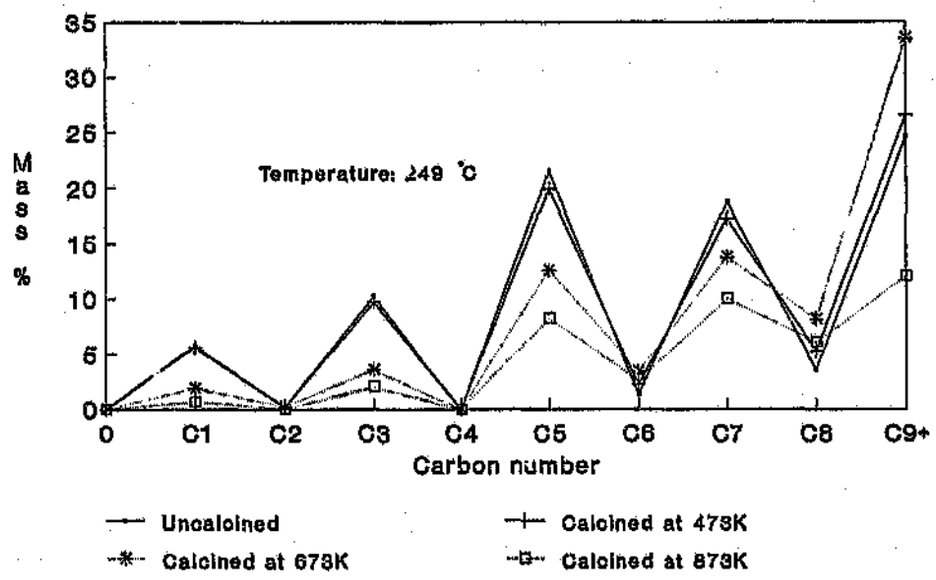

Figure 4.17 The effect of calcination temperature on the catalytic selectivity of 2% Pd/TiO_2 catalyst for the ethanol conversion reaction in the low temperature range (225°C - 249°C)

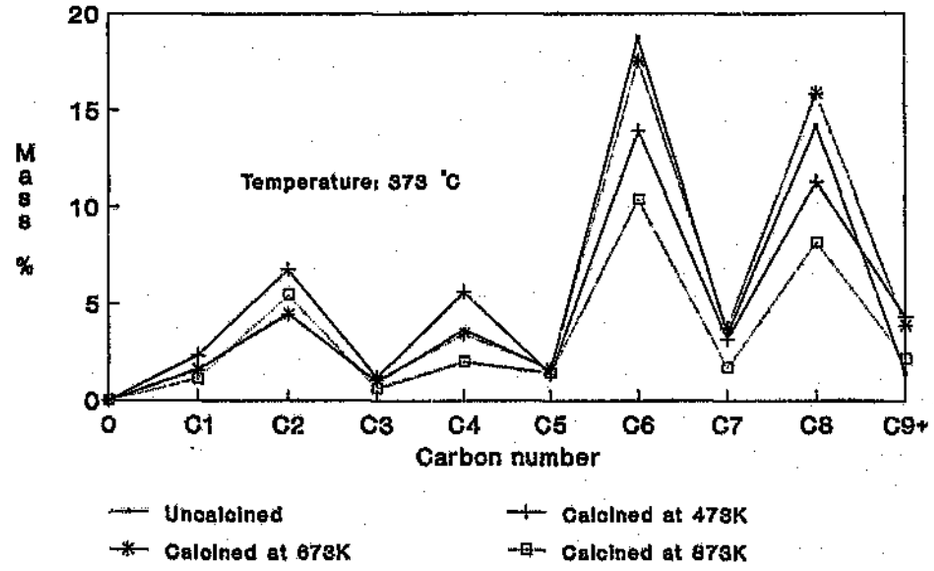

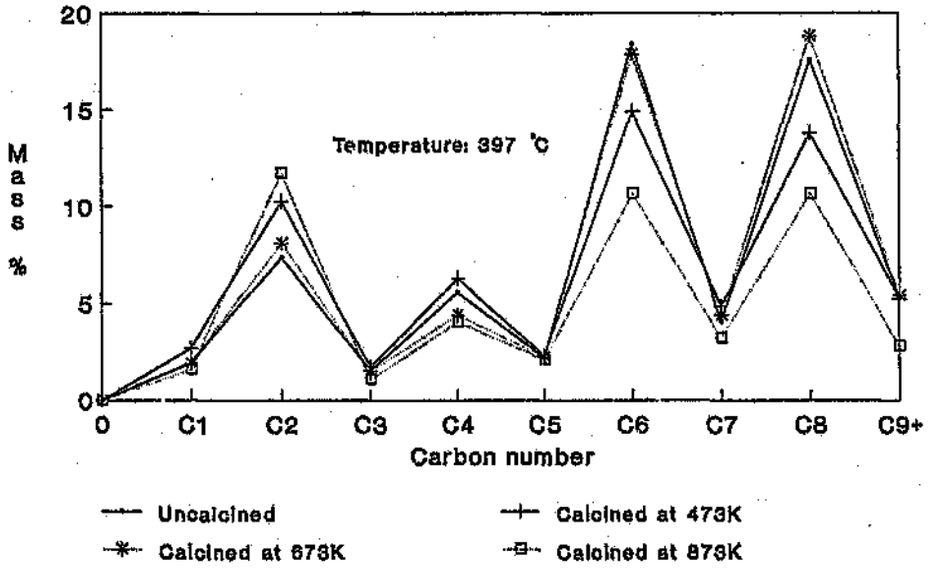

Figure 4.18 The effect of calcination temperature on the catalytic selectivity of 2% Pd/TiO_2 catalyst for ethanol conversion in the high temperature range (373°C - 397°C)

Table 4.11 Comparison of different calcination temperature on 2% Pd/TiO_2 catalyst for ethanol conversion at various reaction temperatures

Temp. (°C)	Conversion (%)	Temp. (°C)	Conversion (%)	Temp. (°C)	Conversion (%)	Temp. (°C)	Conversion (%)
Uncalcined		Calcined at 200°C		Calcined at 400°C		Calcined at 600°C	
104	0.88	104	0.81	104	0.40	104	0.15
152	10.25	152	9.21	152	4.07	152	4.18
200	47.27	201	44.88	200	29.71	202	21.63
226	73.01	225	72.35	225	49.06	225	35.25
249	88.87	249	89.22	249	79.34	249	45.04
264	92.10	275	89.73	274	78.01	274	29.50
299	58.28	299	67.67	299	64.64	299	19.13
325	50.49	325	48.80	324	63.98	324	23.23
349	53.82	349	59.01	348	68.28	349	26.72
373	64.13	373	64.17	373	66.30	372	42.49
398	75.85	397	74.84	398	76.68	397	62.47

All catalyst reduced at 400°C for 16 hours with H_2 before the ethanol conversion reaction

4.3.8 Investigation of the effect of hydrogen reduction temperature on the activity of a 2% Pd/TiO_2 catalyst in the ethanol conversion reaction

Generally metal is formed by reduction of a metal oxide at an elevated temperature after contact with flowing hydrogen or hydrogen diluted with nitrogen [4, 5]. This reaction is highly exothermic. If the initial temperature is too high, or the hydrogen purity is too high, it is possible that "hot spots" may develop on the catalyst which will promote sintering [28 - 30]. A considerable excess of hydrogen may be required to sweep away the product water. If present in too high a concentration, water vapor may accelerate the sintering of an oxide, and it can also retard the rate of the reduction reaction by forming a hydroxylated surface [31, 32]. The mechanism of sintering may be described by two alternative theories [33 - 35]. The first is that of the interparticle model, which postulates that atoms escape from the crystallite to the support surface. These atoms rapidly migrate over the support, and are then recaptured by the crystallite upon collision. The energy needed for this to take place is supplied by the reduction of the metal. This is a diffusion model. The second theory states that at elevated temperature the particles begin to vibrate. If sufficient energy can be provided, the vibration is such that particles touch and coalesce. In both these models, large particles grow at the expense of smaller ones. This results in an attendant lowering of the exposed surface area.

Numerous studies have been reported on the reduction of palladium supported on TiO_2 [36 - 42]. Tauster, Stevenson et al. [38, 43] have reported data for a 2% Pd/TiO_2 catalysts

(Table 4.12). After reduction at 458 K, the catalyst exhibited H/M and CO/M chemisorption ratios between one-half and unity (where M is the total number of metal atoms), indicative of highly dispersed palladium. After reduction at 773 K, however, the hydrogen and carbon monoxide uptake decreased to near zero. Furthermore, oxidation of a reduced Pd/TiO_2 catalyst followed by re-reduction in hydrogen at 453 K almost completely restored the normal chemisorptive properties of the sample. Subsequent treatment in hydrogen at 773 K again led to suppression of hydrogen adsorption. Therefore, the effect is interpreted to be due to an electron transfer from the partially reduced oxide surface to the metal particles, or a localized strong bond between the reduced cation in the support and the metal, or the contamination of metal catalyst surface by reduced support [38, 44 - 46].

Table 4.12 Effect of pretreament on H_2 and CO chemisorption on 2% Pd/TiO_2 [38, 43]

Treatment	H/Pd	CO/Pd
H_2, 453 K	0.93	0.53
H_2, 773 K	0.05	0.02
H_2, 453 K	0.05	0
O_2, 673 K; H_2, 453 K	0.89	0
O_2, 773 K	0.03	0

Burch [47], Vishwanathan and Narayanan [48] also proposed a metal/TiO_2 interaction after various reduction and oxidation treatments. This effect in now known as the strong metal supoport interaction (SMSI) effect. The model proposed to account for these different effects is illustrated in Figure 4.19.

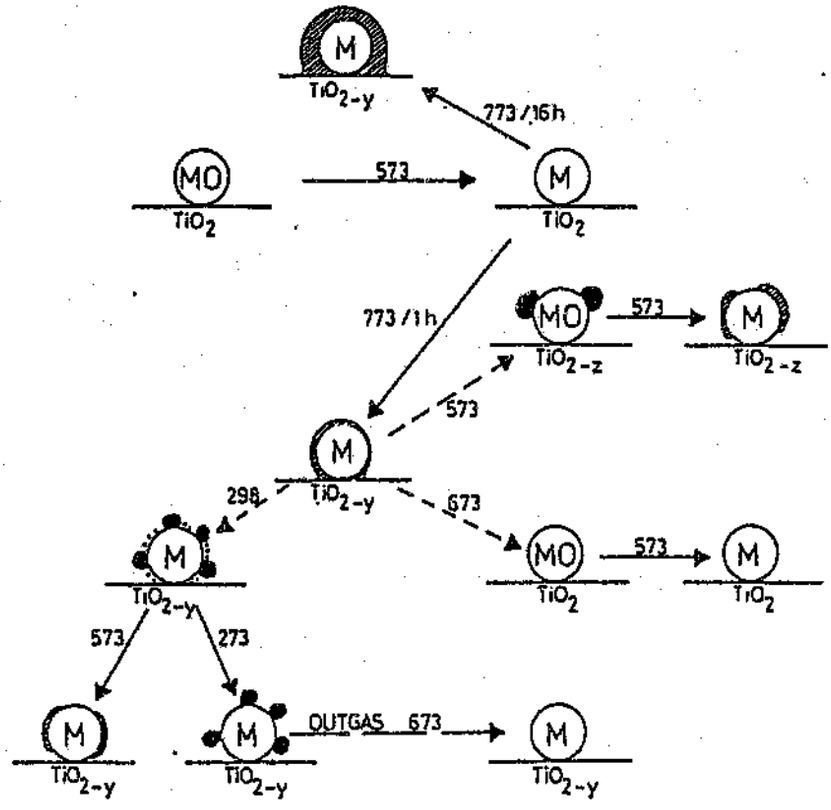

Figure 4.19 Changes in the physical state of titania-supported catalysts after various reduction and oxidation treatments (M, metal particles; MO, metal oxide particles; ▒, surface TiO_x phase; ●, surface TiO_2 phase; ·, adsorbed oxygen atoms; solid arrows indicate reduction, dashed arrows indicate oxidation, numbers indicate temperatures in K) [47]

Experiments performed by Vannice et al., [49, 50] with Pd/TiO_2 samples indicated that high temperature reduction decreased the heats of adsorption of CO and H_2. However reduction at 473 K, gave strong adsorption of CO and H_2. This work suggest that 2% Pd/TiO_2 may only require an *ca.* 473 K reduction temperature for the development of SMSI.

In situ Differential Scanning Calorimetry (DSC) was used to study the effect of hydrogen reduction on the 2% Pd/TiO_2 catalyst and metal free TiO_2 support (for experimental details, see Chapter two, section 2.4). Samples were reduced in situ in the DSC instrument with flowing hydrogen (flow rate: 21ml min^{-1}) in the temperature range 30°C - 400°C (ramp 5°C min^{-1}). The results are shown in Figure 4.20. The metal free TiO_2, as expected, showed no heat loss / absorbtion in the 30°C - 400°C range. On the other hand, the 2% Pd/TiO_2 catalyst indicated a significant absorbtion in the temperature range 100°C - 200°C.

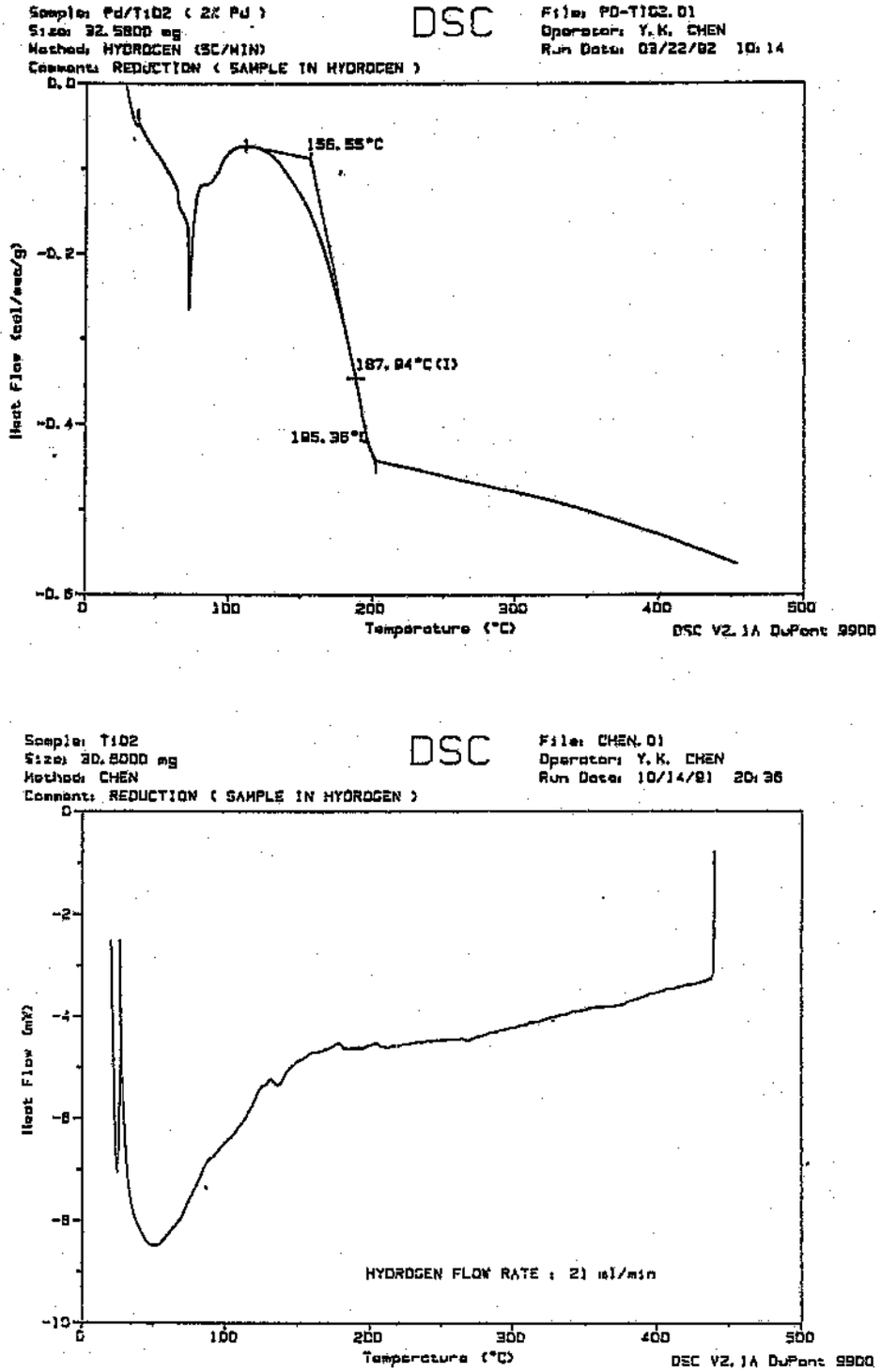

Figure 4.20 DSC spectrum of (I) fresh 2% Pd/TiO_2 and (II) metal free TiO_2 samples under flowing hydrogen gas (H_2 flow rate: 21 ml min^{-1})

The metal free TiO_2 support was reduced <u>in situ</u> at 200°C and 400°C in the reactor and then examined in the ethanol transformation reaction between 100°C - 400°C. The unreduced TiO_2 sample was also tested under similar conditions. The results are summarized in Table 4.13 and Figure 4.21. From the data it is clear that under similar reaction conditions, hydrogen reduction treatments do not affect the TiO_2 support with respect to catalytic activity and selectivity.

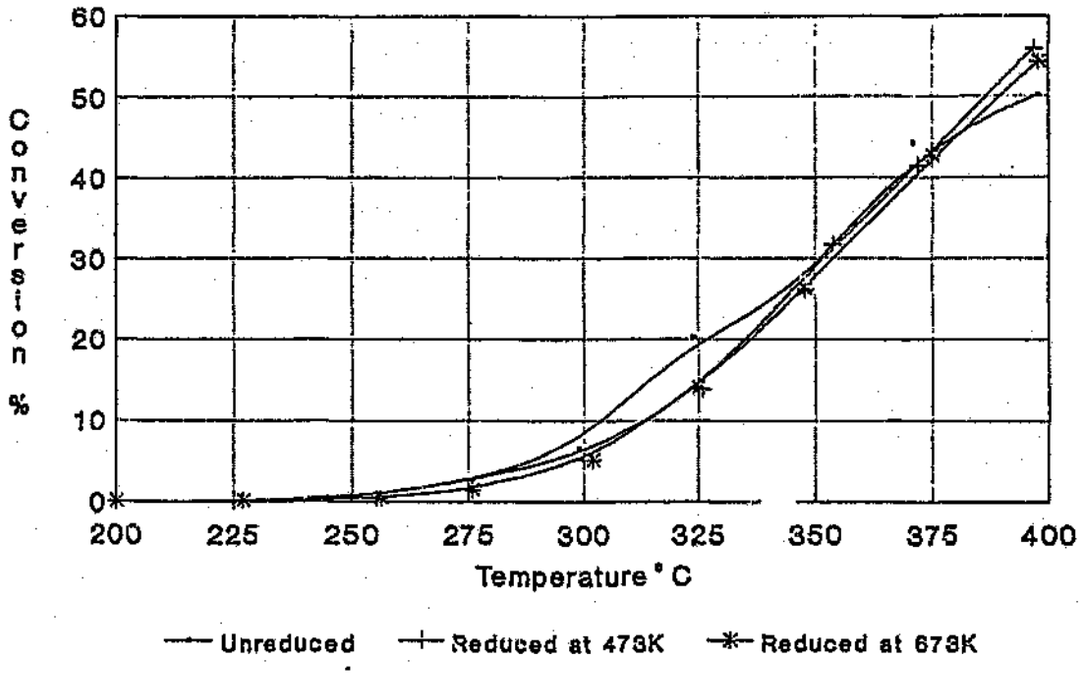

Figure 4.21 Effect of reduction temperature on the catalytic activity of metal free TiO_2 support in the ethanol conversion reaction

Table 4.13 Effect of reduction temperature on catalytic activity and selectivity of metal free TiO_2 for the ethanol conversion reaction

Temp. (°C)	Conv. %	Product distribution (% by mass) EtOEt	C2=	MeCHO	HC's[a]
Unreduced					
225	0	0	0	0	0
251	0.56	0.56	0	0	0
299	6.60	5.85	0.51	0	0.24
324	20.29	16.66	2.20	0.34	1.09
349	25.86	17.15	4.00	0.66	4.05
371	44.28	15.66	8.92	2.24	17.46
398	50.17	8.05	14.14	2.73	25.25
Reduced at 200°C					
225	0.06	0.06	0	0	0
255	0.42	0.40	0.01	0	0.01
300	5.12	4.39	0.34	0.14	0.25
326	13.83	10.80	1.40	0.29	1.35
354	31.70	19.81	5.51	0.57	5.81
372	41.43	13.91	9.16	0.82	17.54
397	55.90	6.62	17.17	1.44	30.67
Reduced at 400°C					
227	0.07	0.07	0	0	0
256	0.47	0.45	0.02	0	0
302	5.16	4.49	0.35	0.12	0.20
325	13.95	11.20	1.43	0.27	1.05
348	26.13	17.70	3.95	0.52	3.96
375	42.58	11.61	10.10	0.87	20.00
398	54.28	5.53	16.62	1.13	31.00

[a] Other hydrocarbons

Experiments were carried out to determine the effect of the hydrogen reduction temperature on the catalytic activity of Pd. The uncalcined 2% Pd/TiO_2 catalyst was loaded into the reactor and *in situ* reduction of the catalyst at various temperature (200°C, 400°C and 500°C) in a flowing stream of hydrogen gas (flow rate: 21 ml min^{-1}) for 16 hours was performed. The results are shown in Table 4.14 and Figure 4.22. Data for the unreduced 2% Pd/TiO_2 catalyst are also included for comparison. The unreduced catalyst (2% Pd/TiO_2) showed little activity towards ethanol conversion to hydrocarbon products (2.09% - 5.22% by mass) in the reaction temperature range 200°C - 275°C. As expected, reaction temperatures > 300°C gave increased conversion of ethanol (see Figure 4.22). Reduction of the Pd catalyst at 200°C leads to higher catalytic activity in the ethanol conversion reaction between 100°C - 350°C, but only a slight increase in activity is observed for the reaction temperatures > 350°C. The further increase in reduction temperature (400°C; 500°C) leads to a decline in the overall activity and selectivity of the catalyst. (see Table 4.14 and Figure 4.22).

A comparison of the catalytic activity of the 2% Pd/TiO_2 catalyst towards converting ethanol to hydrocarbons and oxygenate products with diffent reduction temperatures indicates an order of reactivity as follows: reduced at 200°C > reduced at 400°C > reduced at 500°C > unreduced.

Table 4.14 Comparison of the catalytic activity and product selectivities of 2% Pd/TiO_2 catalyst at different reaction temperatures

Temp. (°C)	Conv. %	Product distribution (% by mass)												
		Et_2O	MeCHO	C1	C2	C2=	C3	C3=	C4	C5	C6	C7	C8	C9+
2% Pd/TiO_2: uncalcined, unreduced														
200	2.36	0	0.59	0.04	0.03	0.02	0	0.42	0	0.43	0.22	0.25	0.36	0
250	5.22	0.55	0.89	0.11	0.15	0.15	0	0.32	0	0.20	0.78	0.18	1.51	0.38
275	2.09	1.19	0.25	0.01	0.01	0.06	0	0	0	0.06	0.17	0.11	0.23	0
347	34.68	17.45	0.78	0.02	1.41	3.02	0	0.13	0	0.31	5.88	1.11	3.16	1.41
372	56.20	9.98	2.15	0.07	2.38	4.74	0	0.55	0	2.28	14.05	1.98	12.23	5.79
397	64.69	7.40	3.89	0.17	3.02	7.04	0	1.06	0	3.86	14.11	2.38	15.26	6.50
2% Pd/TiO_2: uncalcined, reduced at 473 K/16 h in H_2														
200	46.38	0	1.48	0.51	0.02	0	1.47	0	0	8.47	2.79	8.92	6.75	15.97
249	90.36	0	1.51	2.50	0.11	0	5.54	0	0	17.32	3.17	16.53	7.66	36.02
264	91.34	0	2.01	1.68	0.20	0.01	1.54	1.50	0.06	11.24	4.06	18.90	17.63	32.51
349	45.88	11.77	0.77	0.45	1.24	1.14	0	0.24	0	0.64	11.88	2.20	10.97	4.58
372	66.45	12.04	2.06	0.93	2.26	2.25	0	0.65	5.12	1.68	19.47	3.05	15.02	1.92
398	80.20	9.68	3.32	1.05	3.16	3.89	0	0.99	6.57	2.74	19.43	3.90	19.68	5.79

Cont'd.....

Table 4.14-2

Temp. (°C)	Conv. %	Product distribution (% by mass) Et_2O	MeCHO	C1	C2	C2=	C3	C3=	C4	C5	C6	C7	C8	C9+
					2% Pd/TiO_2: uncalcined, reduced at 673 K/16 h in H_2									
200	42.03	0	1.25	0.33	0.02	0	0.93	0.18	0	7.49	2.47	7.42	6.99	14.95
249	83.08	0	1.76	1.01	0.09	0.01	1.33	0.99	0	10.24	3.43	24.93	12.04	27.25
264	74.40	1.17	2.56	0.72	0.14	0.04	0	1.76	0	7.59	6.14	10.62	20.11	23.55
348	45.52	12.26	0.77	0.27	0.88	1.00	0	0.16	0	0.67	12.91	2.33	11.00	3.27
372	70.76	10.79	1.95	0.60	1.79	2.06	0	0.50	4.68	1.76	20.51	3.75	17.97	4.40
398	81.13	9.82	3.29	0.75	2.89	3.79	0	0.87	7.15	3.14	21.22	4.06	18.64	5.51
					2% Pd/TiO_2: uncalcined, reduced at 773 K/16 h in H_2									
201	35.27	0	1.65	0.24	0.01	0	0.70	0.25	0	6.27	1.86	5.75	5.07	13.47
248	34.81	0.94	3.98	0.36	0.16	0.08	0	1.26	0	3.48	3.42	2.51	11.09	7.53
263	22.39	0.81	3.51	0.28	0.13	0.14	0	0.79	0	1.57	2.75	0.85	7.83	3.73
349	39.03	12.54	1.05	0.22	1.40	1.93	0	0.19	0	0.57	9.45	1.29	7.15	3.24
372	71.78	9.22	2.35	0.41	2.14	3.31	0	0.57	6.76	1.59	17.28	2.74	18.82	6.59
398	89.87	8.63	3.88	0.66	3.45	5.75	0	1.06	10.56	4.50	17.50	3.51	22.15	8.22

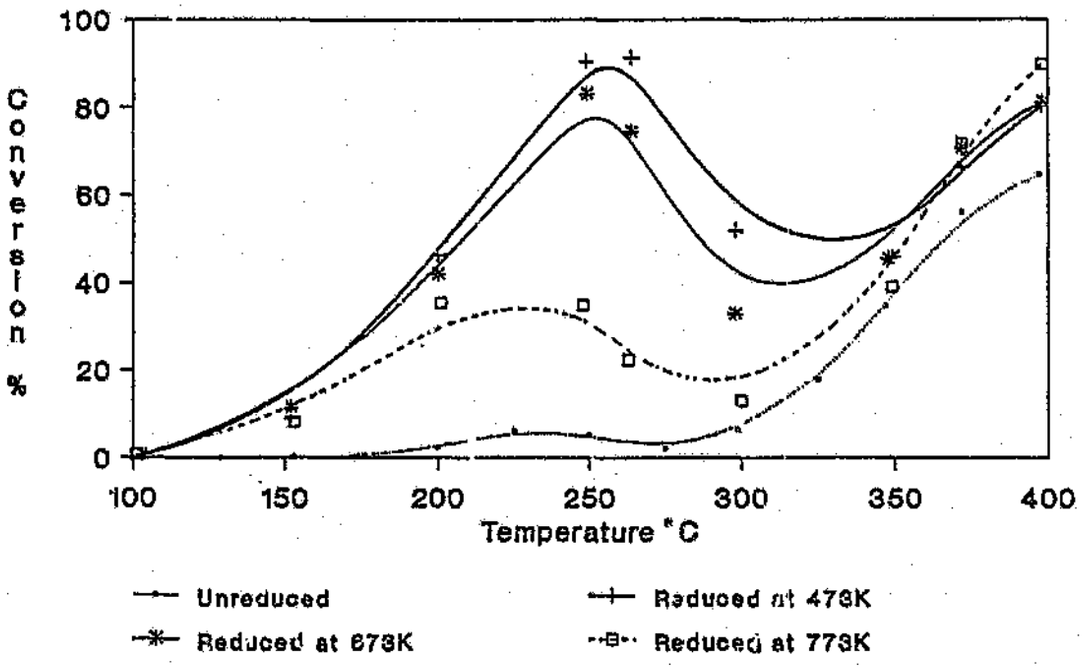

Figure 4.22 Comparison of the effect of the H_2 reduction temperature on the activity of a 2% Pd/TiO_2 catalyst in the ethanol conversion reaction

The results reveal the following:

1. The 2% Pd/TiO_2 catalyst is best reduced at T < 200°C.

2. Reaction over the TiO_2 support shows no changes in activity and selectivity due to hydrogen reduction.

3. For reaction temperatures > 300°C, reduction of 2% Pd/TiO_2 has little effect on the product spectrum.

4.3.9 Catalytic performance of a 2% Pd/TiO_2 catalyst using absolute ethanol

Ethanol is produced by the fermentation of carbohydrates found in grain or sugar crops to mixtures containing water and ethanol. Ethanol is usually separated from water by distillation to yield a 95% ethanol-water mixture. Further purification by distillation is not possible due to the azeotrope formed by the two components. Further purification requiring special techniques is particularly energy-consuming [51, 52].

The effect of absolute ethanol (99.8% - 100%, Labchem Ltd.) as feed, over 2% Pd/TiO_2 catalyst (uncalined, reduced at 200°C for 16 h in H_2) was investigated. The results are shown in Figures 4.23, 4.24 and Table 4.15. The results are also compared with studies using aqueous ethanol (96.0% v/v, alcohol/water) under the same experimental conditions. Figure 4.22 and Table 4.14.

In the 100°C - 280°C reaction temperature range ethanol conversion increased with increasing temperature for both absolute and aqueous ethanol and selectivities were similar (see Figure 4.23 and 4.24). Absolute ethanol favoured the higher conversions to C_1 and $C_3^=$ (methane and propene) when compared with conversion over aqueous ethanol.

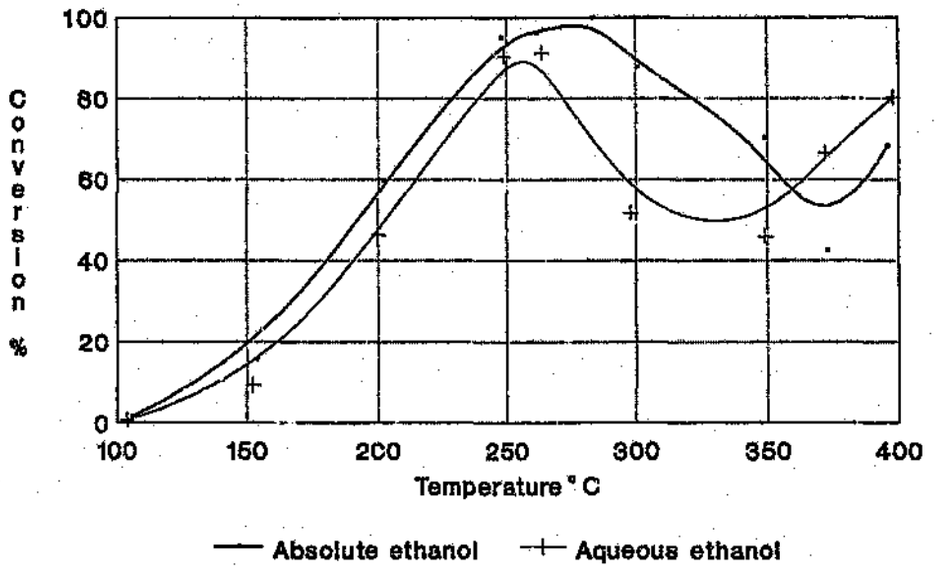

Figure 4.23 Comparison of ethanol conversion using absolute and aqueous ethanol over a 2% Pd/TiO_2 catalyst

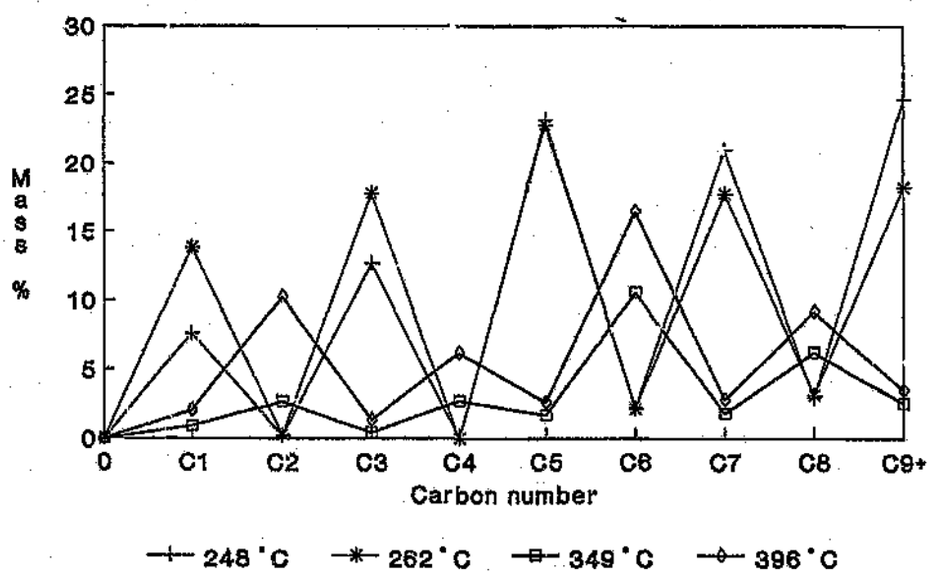

Figure 4.24 Product distribution of absolute ethanol conversion over 2% Pd/TiO_2 catalyst at various reaction temperature

Table 4.15 The conversion of absolute ethanol over a 2% Pd/TiO_2 catalyst

Temp. (°C)	Conv. %	Product distribution (% by mass)												
		Et_2O	MeCHO	C1	C2	C2=	C3	C3=	C4	C5	C6	C7	C8	C9+
106	1.48	0	0.50	0	0	0	0	0	0	0.09	0.30	0.27	0.21	0.11
154	15.70	0	1.36	0.07	0	0	0.16	0.04	0	2.77	2.00	2.04	4.00	3.26
202	59.74	0	1.81	0.99	0.03	0	0	2.66	0	14.04	3.95	12.83	7.20	16.23
248	95.11	0	0.72	7.62	0.15	0	0	12.69	0	23.15	2.24	20.96	2.95	24.63
262	96.36	0	0.50	13.8	0.27	0	0	17.80	0	22.78	2.13	17.72	3.13	18.23
284	100.0	26.52	0	6.68	0	0.29	0.43	7.99	1.24	0.37	3.21	19.08	6.76	27.43
289	84.28	1.46	6.13	2.91	0.25	0.04	1.21	2.89	0.10	12.72	3.28	13.64	13.91	25.74
301	87.73	3.90	2.37	2.66	0.47	0.09	0	5.19	0.53	8.60	7.48	16.47	21.00	18.97
349	70.24	40.11	0.62	0.91	1.87	0.81	0	0.44	2.70	1.67	10.54	1.82	6.22	2.53
373	42.50	11.03	2.57	0.01	2.32	2.04	0	0.60	0	1.71	9.24	2.22	9.26	1.50
396	68.20	10.79	3.01	2.03	5.89	4.38	0	1.34	6.20	2.61	16.46	2.81	9.17	3.51

Oudejans et al. [53] have observed that the yield of aromatics is increased by water in the ethanol transformation reaction over H-ZSM-5. On the contrary, Choudhary and Sansare [54] concluded that the presence of water in alcohol causes only a small decrease in the extent of aromatization but no significant change in the product distribution.

This study attempted to compare the effect of absolute and aqueous ethanol effect on the 2% Pd/TiO_2 catalysed reaction. However, no significant differences were observed on using absolute or 96% ethanol.

4.3.10 Acetaldehyde transformation over a 2% Pd/TiO_2 catalyst: The influence of nitrogen or hydrogen carrier gas

Acetaldehyde conversion was studied in the presence of nitrogen or hydrogen as carrier gas and an acetaldehyde WHSV of *ca.* 1.27 h^{-1}. The extrudate form of the 2% Pd/TiO_2 catalyst was used, and the results are listed in Tables 4.16, 4.17 and Figures 4.25, 4.26. With nitrogen as carrier gas the acetaldehyde conversion was 65% at 265°C after one hour. The products obtained (% by mass) were: crotonaldehyde (35.41%), Et_2O (0.33%), C_8 (14.04%), C_9 (7.33%) and C_1 to C_7 hydrocarbons (7.88%). From the product distribution it is clear that the major product produced from acetaldehyde, via a dehydration reaction, was crotonaldehyde (C_4H_6O). Very little catalyst deactivation ($\sim$ 8%) was observed over a period of 12 hours (Figure 4.25). The product selectivity details as a function of time on line are shown in Table 4.16.

On the other hand, when hydrogen was used as a carrier gas no crotonaldehyde, diethyl-ether or $C_2^=$, $C_3^=$, C_4 hydrocarbons were produced between 120°C - 300°C. At reaction temperatures > 220°C the total conversion of acetaldehyde was however > 99%. Acetaldehyde transformation in the 220°C - 280°C range gave the same products, as observed for the ethanol conversion reaction over a Pd/TiO_2 catalyst (low temperature range, nitrogen carrier gas) which favoured odd carbon numbered hydrocarbon formation (Figure 4.26).

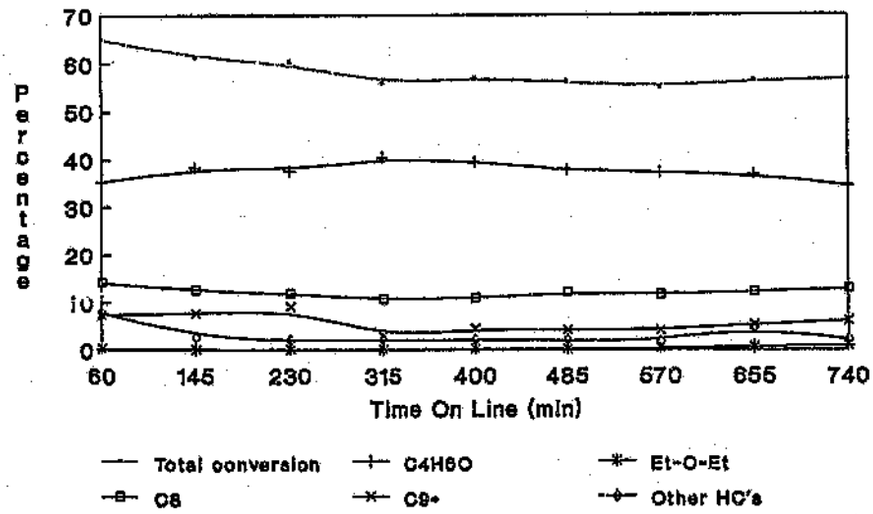

Figure 4.25 Acetaldehyde transformation over 2% Pd/TiO_2 with time on line; nitrogen as carrier gas (Catalyst: uncalcined, reduced at 200°C/16 h; T = 265°C; MeCHO WHSV = 1.27 h^{-1})

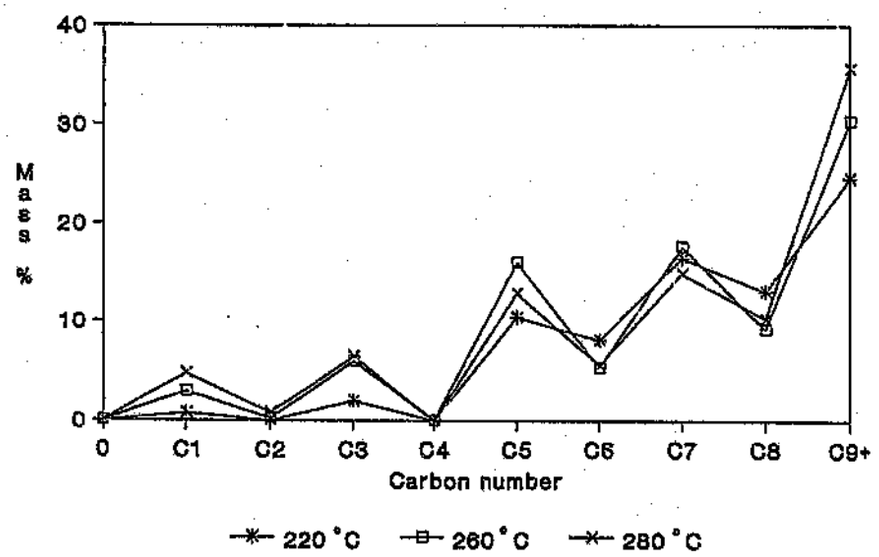

Figure 4.26 Product distribution of acetaldehyde transformation over 2% Pd/TiO_2 in the presence of hydrogen carrier gas (Catalyst: uncalcined, reduced at 200°C/16 h; T = 265°C; MeCHO WHSV = 1.27 h^{-1})

Acetaldehyde transformation over Pd/TiO_2 catalyst using hydrogen as carrier gas at low temperature (< 300°C) yields products resulting from rapid chain growth by a series of coupling reactions (see Figure 4.26). From the data, it can be concluded that, the initial step in ethanol conversion is dehydrogenation of ethanol to acetaldehyde.

$$C_2H_5OH \rightleftharpoons CH_3CHO + H_2$$

and

$$CH_3CHO \rightarrow CH_4 + CO$$

$$\text{aldehyde} \longrightarrow C_{2n+1} \text{ hydrocarbons} + CO$$

An interesting observation relates to the large amounts of EtOH formed from acetaldehyde at low temperature. This suggest an equilibrium reaction $CH_3CHO + H_2 \rightleftharpoons CH_3CH_2OH$ under the reaction conditions. At higher temperatures only small amounts of EtOH are detected as the equilibrium is influenced by the $CH_3CHO \rightarrow CH_4 + CO$ reaction and the coupling reactions, which are then followed by decarboxylation reactions.

It seems likely that the subsequent products are formed by coupling of aldehydes. For instance when N_2 is used as carrier gas the crotonaldehyde (ca. 37%) and C_8 (ca. 13%) products dominate. These products would rapidly be decarboxylated under H_2. Also of note is the lack of C_4 products when H_2 is the carrier gas - as found for the ethanol reaction.

Table 4.16 Acetaldehyde transformation over a 2% Pd/TiO_2 catalyst with time on line; The influence of nitrogen carrier gas

Time on line (min)	60	145	230	315	400	485	570	655	740
Conversion (%)	64.99	61.18	60.17	55.69	56.83	56.06	54.83	56.25	56.50
Product distribution (% by mass)									
EtOH	0.62	0.20	0.14	0.14	0.12	0.10	0.12	0.12	0.11
EtOEt	0.33	0.11	0.09	0.12	0.14	0.18	0.36	0.54	0.91
Methane	1.19	0.78	0.71	0.85	0.82	0.81	0.82	0.77	0.61
Ethene	0.01	0	0	0	0	0	0.01	0.01	0.01
Ethane	0.04	0.03	0.03	0.04	0.04	0.04	0.04	0.04	0.02
Propene	1.36	0.37	0.23	0.23	0.20	0.18	0.17	0.18	0.23
Propane	0.14	0.09	0.09	0.10	0.12	0.15	0.18	0.25	0.43
C4H6O	35.41	38.27	37.50	40.21	39.48	37.76	37.19	36.71	34.45
C5	2.18	0.57	0.39	0.42	0.44	0.40	0.07	0.06	0.52
C6	0.81	0.31	0.21	0.24	0.21	0.19	0.19	0.05	0.06
C7	1.53	0.32	0.11	0.10	0.10	0.13	0.11	0.18	0.22
C8	14.04	12.51	11.73	10.54	10.84	11.96	11.51	12.12	12.80
C9+	7.33	7.62	8.94	2.70	4.32	4.16	4.06	5.22	6.13

Catalyst: uncalcined, reduced at 200°C/16 h; MeCHO WHSV = 1.27 h^{-1}; T = 265°C

Table 4.17 Catalytic performance of 2% Pd/TiO_2 in acetaldehyde transformation at various reaction temperatures; The influence of hydrogen carrier gas

Temp. (°C)	Conv. %	Product distr' (% by mass)											
		EtOH	Et_2O	C1	C2	C2=	C3	C4	C4=	C5	C6	C7	C8	C9+
122	73.08	32.98	0	0.03	0	0	0.03	0	0	4.69	5.42	16.56	4.99	8.38
178	96.86	29.27	0	0.18	0	0	0.37	0	0	4.19	8.76	16.54	13.52	24.03
220	99.12	22.91	0	0.73	0.02	0	1.98	0	0	10.39	9.08	16.39	13.03	24.59
260	99.08	11.58	0	2.93	0.21	0	5.96	0	0	15.93	5.35	17.54	9.21	30.37
280	99.28	8.21	0	4.71	0.79	0	6.38	0	0	12.83	5.56	14.83	10.29	35.68
300	99.76	7.26	0	6.13	1.76	0	5.84	0	0	8.88	8.12	12.97	11.74	37.06

Catalyst: uncalcined, reduced at 200°C/16 h; MeCHO WHSV = 1.27 h^{-1}

4.3.11 Diethyl-ether transformation over a 2% Pd/TiO_2 catalyst

In this study the conversion of diethyl-ether over 2% Pd/TiO_2 catalyst was examined in the temperature range 100°C - 400°C. Nitrogen gas was utilized as a carrier gas. The results are summarized in Table 4.18 and Figure 4.27.

Conversion of diethyl-ether (Table 4.18) increased with increasing reaction temperature between 300°C - 400°C (6.63% in to 52.17%). In the temperature range 100°C - 250°C very low conversion (< 1%) was detected. It is thus apparent that diethyl-ether transformation to hydrocarbons only occurs in the higher temperature range (> 300°C). As can be seen from Figure 4.27 the hydrocarbon selectivity in the temperature range 350°C - 396°C shows higher selectivity towards even numbered hydrocarbons and increasing temperature increased the even numbered hydrocarbons formation. These results are very different to the results noted for the ethanol conversion over the same catalyst (2% Pd/TiO_2) under similar reaction conditions and are summarized below:

$$2\ C_2H_5OH \xrightarrow{H^+} C_2H_5OC_2H_5 + H_2O$$

$$C_2H_5OC_2H_5 \xrightarrow{C_2H_4} C_{2n+2}\ \text{hydrocarbons}$$

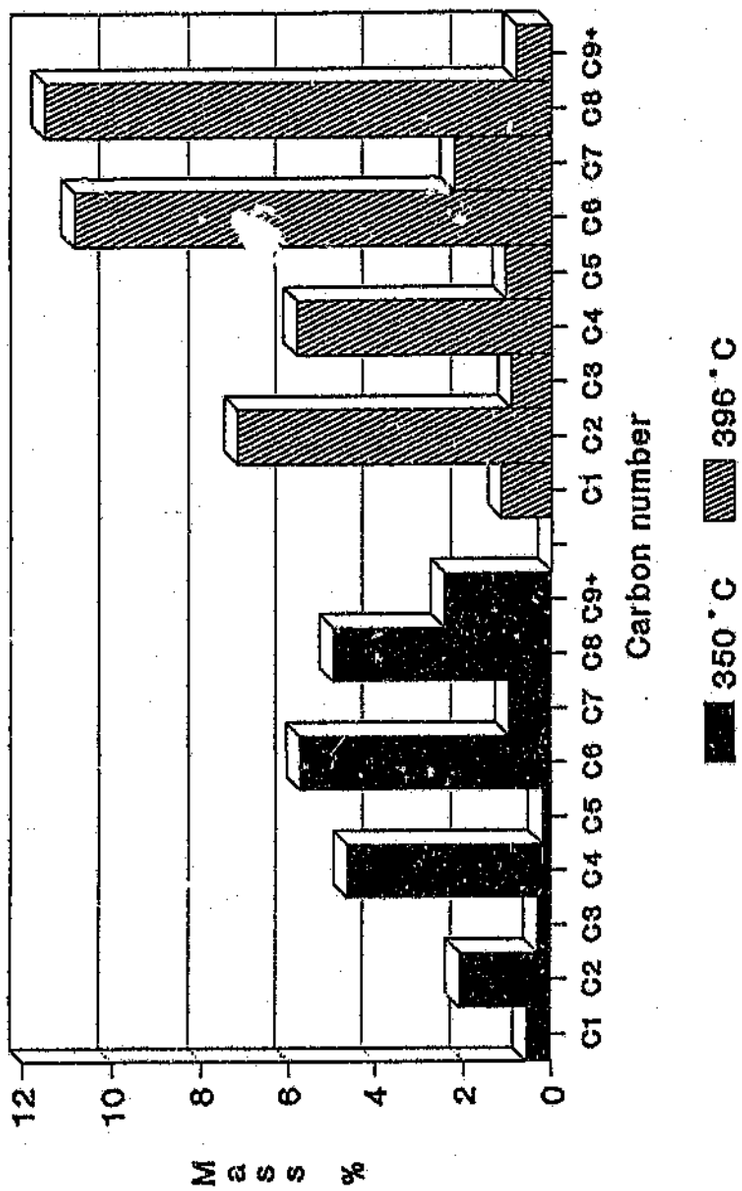

Figure 4.27 Hydrocarbon selectivity as a function of diethyl-ether conversion over 2% Pd/TiO_2 using N_2 as carrier gas (Catalyst: uncalcined, reduced at 200°C/16 h; Et_2O WHSV = 0.71 h^{-1})

Table 4.18 Diethyl-ether transformation over a 2% Pd/TiO_2 catalyst

Temp. (°C)	Conv. %	Product distribution (% by mass)												
		EtOH	MeCHO	C1	C2	C2=	C3	C3=	C4	C5	C6	C7	C8	C9+
106	0.15	0	0	0	0	0	0	0	0	0	0.15	0	0	0
154	0.22	0	0	0.01	0	0	0	0	0	0	0.15	0.06	0	0
204	0.94	0	0	0.01	0.01	0.01	0	0.03	0.04	0	0.15	0.07	0.62	0
251	1.07	0.06	0.04	0.04	0.01	0.02	0	0.08	0.23	0	0.26	0	0.14	0.19
300	6.33	1.00	0.09	0.10	0.07	0.09	0	0.06	1.09	0.02	1.21	0.12	1.63	1.15
350	27.37	4.99	0.35	0.56	1.13	0.97	0	0.33	4.66	0.23	5.75	0.98	4.98	2.44
396	52.17	9.11	1.63	1.14	3.45	3.74	0	0.90	5.82	1.03	10.84	2.22	11.51	0.78

Catalyst: uncalcined, reduced at 200°C/16 h; Et_2O WHSV = 0.71 h^{-1}

4.3.12 Regeneration studies over Pd/TiO_2 catalysts

All alcohol reactions (such as alcohol conversion to hydrocarbons) are acompanied by the formation of undesirable high-molecular weight products ("coke") which can be strongly bonded to the catalyst's external and internal surfaces, causing deactivation [55 - 57]. The deactivation rate depends on the relative rate of formation of these by-products, a rate which can be different from one catalytic system to another. Deactivation of catalysts can occur in two ways [58, 59], viz., site coverage (active sites poisoned by coke adsorption) or pore blockage (active sites inaccessible to reactants)

The deposition of coke within the catalyst results in loss of surface area, a decrease in diffusivity, changes in selectivity of the catalyst, and a resultant overall decrease in catalytic activity [60, 61]. To restore catalyst activity, the coke must be removed, without altering the catalyst structure. Generally, this is done by burning off the carbonaceous deposits with oxygen/nitrogen mixtures at high temperature, giving CO, CO_2 and H_2O as products [62].

In view of the deactivation of the Pd/TiO_2 catalyst (section 4.3.2, where for example coke deposition is thought to be a major factor associated with deactivation), the effect of repeated catalyst regeneration on catalytic activity was studied. After initial deactivation of the 2% Pd/TiO_2 catalyst, the reactor temperature was increased to 500°C under a stream of air for 4 hours. After purging with nitrogen gas, ethanol was then passed over the catalyst at

a reaction temperature between 100°C - 400°C, (EtOH WHSV = 0.806 h^{-1}; aqueous ethanol N_2 flow rate = 21 ml min^{-1}, catalyst reduced at 200°C/16 h) and the results were compared with those of the fresh catalyst. The results are summarized in Figure 4.28 and Table 4.19. From this table it can be seen that the catalytic activity and product selectivity decreased after catalyst regenerations. (see Table 4.19). The regeneration step was carried out a second time and the catalytic reaction repeated under identical reaction conditions. Again a decrease in catalytic activity and selectivity were observed.

In a separate experiment the regeneration was carried out under milder reaction conditions. In this instance N_2 was added to the carrier gas to dilute the O_2 stream (500°C) to avoid any unwanted hydrothermal effects. Under these conditions the catalyst showed little decrease in activity and little change in catalytic selectivity. Furthermore, the repeated regeneration of this catalyst again gave little loss in catalytic activity. This indicates that the loss of activity during ethanol conversion is not due to the destruction or loss of active centres but rather due to the deposition of carbonaceous deposits on the active centres of the catalyst. Analysis of the coke deposits, using TGA confirmed that a carbonaceous deposit was a contributing factor towards catalyst deactivation. Thus 4.35% (mass) "coke" was deposited on the catalyst in 10 hours when a typical catalytic reaction was performed in the temperature range 100°C to 400°C.

In summary the catalytic activity of 2% Pd/TiO_2 for ethanol conversion to hydrocarbons after regeneration (500°C, 4 h) showed that air or oxygen diluted with nitrogen were successful in restoring catalytic activity, although not to the extent of the original activity. The repeated

regeneration studies, each time, gave little loss in catalytic activity. The catalyst after regeneration was not restored to its original white colour, rather its colour after re-activation was a light grey colour.

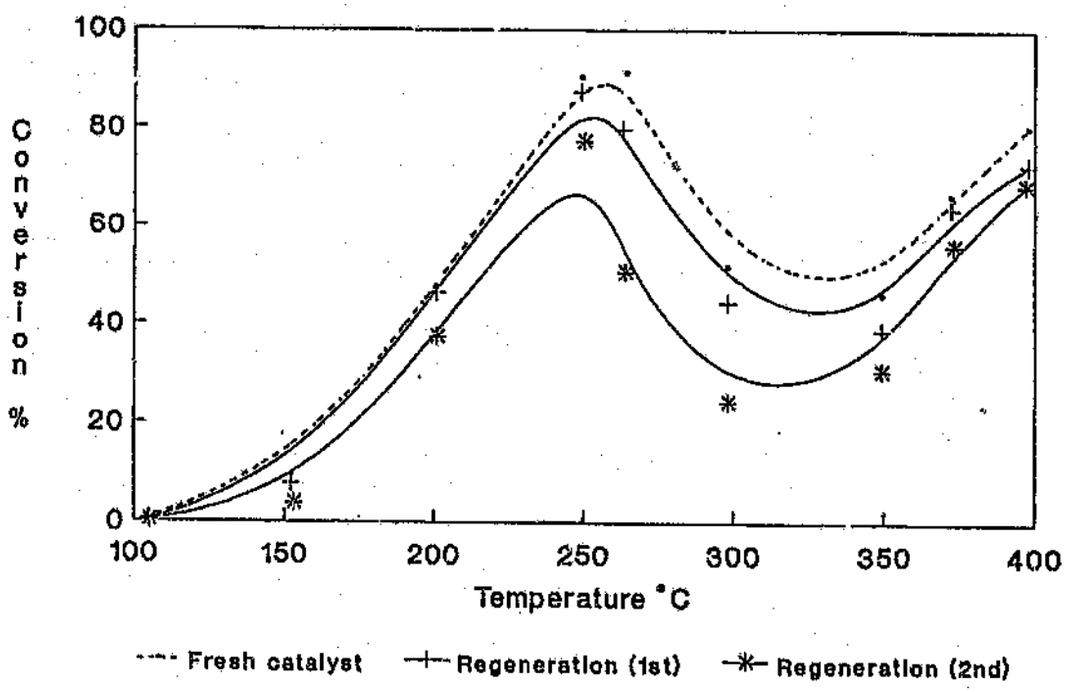

Figure 4.28 Effect of successive air regeneration cycles on catalytic activity for the ethanol conversion reaction over 2% Pd/TiO_2 catalyst

Table 4.19 Effect of air regeneration on product selectivity for ethanol transformation over a 2% Pd/TiO_2 catalyst

Temp. (°C)	Conv. %	Product distribution (% by mass)												
		Et_2O	MeCHO	C1	C2	C2=	C3	C3=	C4	C5	C6	C7	C8	C9+
Fresh catalyst														
200	46.38	0	1.48	0.51	0.02	0	1.47	0	0	8.47	2.79	8.92	6.75	15.97
249	90.36	0	1.51	2.50	0.11	0	5.54	0	0	17.32	3.17	16.53	7.66	36.02
264	91.34	0	2.01	1.68	0.20	0.01	1.5	50	0.06	11.2	4.06	18.90	17.63	32.51
349	45.88	11.77	0.77	0.45	1.24	1.14	0	24	0	0.6	11.88	2.20	10.97	4.58
372	66.45	12.04	2.06	0.93	2.26	2.25	0	0.65	5.12	1.68	19 /	3.05	15.02	1.92
398	80.20	9.68	3.32	1.05	3.16	3.89	0	0.99	6.57	2.74	19.43	3.90	19.68	5.79
1st regeneration														
201	46.54	0	1.56	0.26	0.01	0	0.73	0.18	0	7.64	2.62	7.68	7.43	18.43
249	87.33	0	2.07	1.23	0.07	0	2.62	0.89	0	14.81	3.66	20.73	8.27	32.98
263	79.76	0	2.77	0.77	0.13	0.02	0.50	1.73	0	9.13	4.63	15.12	20.22	24.74
349	38.63	9.04	0.82	0.44	1.11	1.04	0	0.24	0	0.62	9.79	1.38	10.99	3.16
372	63.78	9.98	1.84	0.78	1.89	2.22	0	0.58	4.54	1.36	17.15	2.68	16.49	4.27
398	72.60	9.01	3.95	1.21	3.30	4.67	0	1.05	5.48	2.60	17.67	2.73	16.51	4.42
2nd regeneration														
201	37.36	0	1.52	0.20	0.01	0	0.58	0.20	0	6.58	2.03	7.12	5.52	13.60
250	77.26	0	3.21	0.43	0.03	0.01	0.40	0.85	0.03	7.92	3.45	16.32	12.22	32.39
264	50.76	1.14	3.95	0.24	0.04	0.03	0	0.88	0	4.69	4.86	6.93	16.78	11.22
349	30.51	7.67	0.93	0.34	0.96	1.19	0	0.22	0	0.61	9.39	1.09	5.80	2.31
373	56.15	9.88	2.27	0.57	1.72	2.81	0	0.48	3.95	1.45	16.65	3.26	11.57	1.54
397	68.61	9.16	4.63	0.86	2.78	5.98	0	0.78	4.63	2.63	15.99	4.17	14.36	2.64

4.3.13 Investigation of the influence of supports (γ-Al_2O_3, Al-PILM) on the Pd catalysed reaction

Sodium exchanged montmorillonite pillared with NH_4^+ ions was synthesized. Palladium nitrate was then co-precipitated with the montmorillonite to obtained the 2% Pd/Al-PILM (see Appendix 4). The 2% Pd/γ-Al_2O_3 (Merck γ-Al_2O_3) was prepared by using the incipient wetness technique. These catalysts were tested in the ethanol conversion reaction and the results are listed in Tables 4.20, 4.21, and shown in Figures 4.29 and 4.30.

The catalytic activity of 2% Pd/Al-PILM was similar to the 2% Pd/γ-Al_2O_3 catalyst. From these results it seems that both supports have little effect on the catalyst activity. The 2% Pd/Al-PILM catalyst, gave a maximum yield of 31.38 wt.% diethyl-ether and 4.12 wt.% acetaldehyde at 245°C. The total conversion of ethanol occured at 345°C and yielded two major products; methane (54.02 wt.%) and ethane (45.02 wt.%). At higher temperatures ($\sim$400°C) the catalyst showed high selectivity (> 90 wt.%) toward ethene (Figure 4.29 and Table 4.20). The 2% Pd/γ-Al_2O_3 gave maximum yields of 12.52 wt.% diethyl-ether (293°C) and 7.57 wt.% acetaldehyde (258°C). Total conversion of ethanol occured between 317°C - 367°C to give mainly methane ($\pm$ 90 wt.%). At higher reaction temperature (> 400°C) ethane formation was favoured (see Figure 4.30 and Table 4.21).

The γ-Al_2O_3 used as support exhibited only alcohol dehydration activity at temperatures of 300°C [63] (Chapter three). In chapter three, it was shown that both γ-Al_2O_3 and Al-PILM catalysts showed that the major product was

diethyl-ether (low temperature) and ethene (high temperature). Addition of palladium to both supports, resulted in the detection of a dehydrogenating capability with activity depending on the reaction temperature. Pepe et al. [64] showed that decomposition of isopropanol over $Cu/\gamma\text{-}Al_2O_3$ catalyst exhibited dehydrogenation activity below 170°C and dehydrogenating and dehydrating reaction activity above this temperature. They also proposed that surface Cu^0 species were responsible for the dehydrogenation pathway. Sivaraj and Rao [65] also demonstrated that reaction of ethanol with $\gamma\text{-}Al_2O_3$ containing $\leq$ 9 wt.% copper content exhibited both dehydration and dehydrogenation activity, while $\gamma\text{-}Al_2O_3$ loaded with copper ($\geq$ 21.65 wt.%) showed only dehydrogenation activity.

Results observed in this study are consistent with the above report. Thus the low loading of Pd and the low reaction temperature are consistent with a dual pathway mechanism, viz.

$$2\ C_2H_5OH \xrightarrow{-\ H_2O} C_2H_5OC_2H_5$$

and

$$C_2H_5OH \xrightarrow{-H_2} CH_3CHO \xrightarrow{-CO} CH_4$$

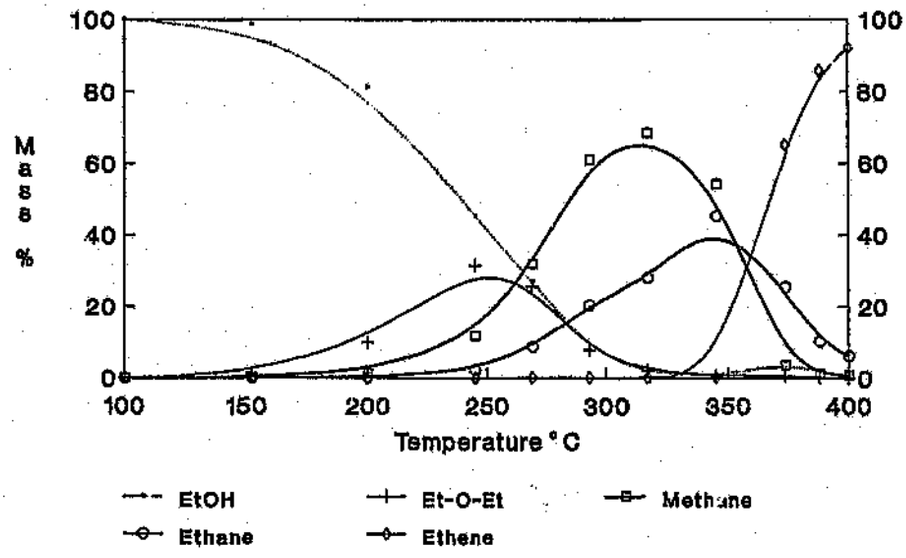

Figure 4.29 Ethanol conversion over 2% Pd/Al-PILM catalyst

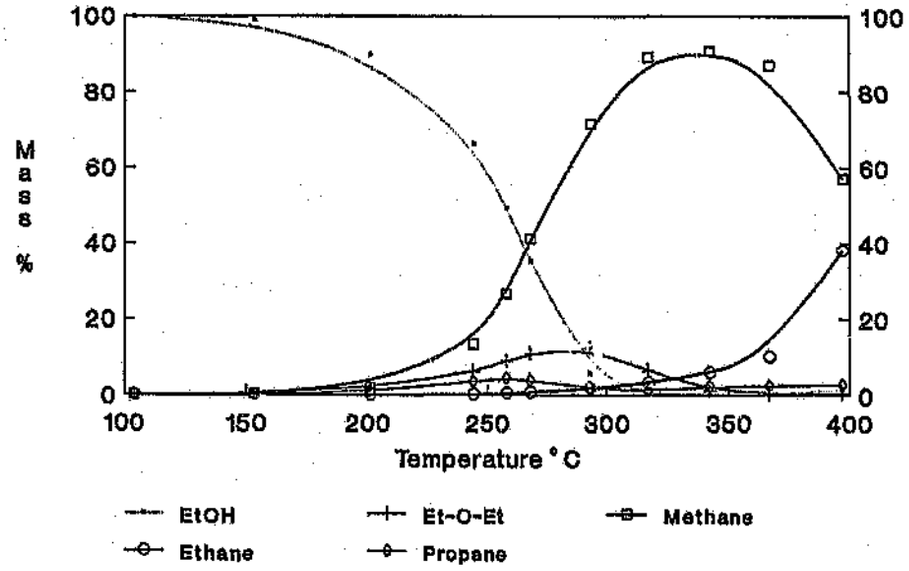

Figure 4.30 Ethanol conversion over 2% Pd/Al_2O_3 catalyst

Table 4.20 Ethanol transformation over 2% Pd/Al-PILM catalyst*

Temp. (°C)	Conv. %	Product distribution (% by mass)										
		EtOH	Et_2O	MeCHO	C1	C2	C2=	C3	C3=	C4	C5	C6
104	0.04	99.96	0	0.04	0	0	0	0	0	0	0	0
152	1.28	98.72	0.76	0.29	0.11	0	0	0.03	0.01	0	0.01	0.07
200	18.86	81.14	10.04	1.57	1.10	0.09	0	1.07	0	0	0.39	4.60
245	54.92	45.08	31.38	4.12	11.69	2.15	0.01	3.14	0	0	0.99	1.44
269	73.15	26.85	25.34	3.41	31.71	8.75	0.03	2.40	0	0	1.18	0.33
293	92.14	7.86	7.88	1.21	60.87	20.22	0.04	1.28	0	0	0.64	0
317	98.65	1.35	1.88	0.22	68.23	27.67	0.02	0.63	0	0	0	0
345	100.0	0	0.64	0	54.02	45.02	0.03	0.29	0	0	0	0
374	95.37	4.63	0.68	0.34	3.60	25.26	65.13	0	0.31	0.05	0	0
388	98.07	1.93	0.15	0.56	1.10	10.18	85.75	0	0.25	0.08	0	0
414	99.35	0.65	0	0.44	0.64	6.01	91.99	0	0.18	0.09	0	0
438	99.64	0.36	0	0.16	0.60	5.98	92.63	0	0.21	0.06	0	0

* Catalyst: reduced at 200°C/16 h

Table 4.21 Ethanol transformation over 2% $Pd/\gamma-Al_2O_3$ catalyst[a]

Temp. (°C)	Conv. %	Product distribution (% by mass)								
		EtOH	Et_2O	MeCHO	C1	C2b	C3	C3=	C5	C6+
104	0.07	99.93	0	0.06	0.01	0	0	0	0	0
153	1.06	98.94	0.07	0.66	0.16	0	0.04	0.01	0	0.12
201	10.22	89.78	1.81	2.83	1.89	0.02	0.86	0	0.38	2.43
244	33.85	66.15	6.13	7.42	13.45	0.20	3.62	0	1.68	1.35
258	50.72	49.28	8.95	7.57	26.69	0.45	4.42	0	1.72	0.92
268	64.72	35.28	10.92	6.19	41.00	0.76	3.80	0	1.57	0.48
293	94.26	5.74	12.52	1.00	71.42	1.76	1.88	0	0.58	5.10
317	100.0	0	6.54	0	89.07	3.25	1.14	0	0	0
342	100.0	0	1.19	0	90.64	5.80	2.19	0	0.18	0
367	100.0	0	0.43	0	86.92	10.18	2.47	0	0	0
397	98.42	1.58	0.55	0	57.02	38.08	2.77	0	0	0

[a] Catalyst: reduced at 400°C/16 h; [b] Ethane

4.3.14 A comparison of the effect of Pt, Rh and Ru TiO_2 supported catalysts on the ethanol conversion reaction

The Pt, Rh and Ru TiO_2 supported metals (2% by mass), were tested as catalysts and the results are shown in Table 4.22 to 4 24. The activities and selectivities were compared with those of 2% Pd/TiO_2 and a metal free TiO_2 catalyst. From Figure 4.31 it is clear that under similar conditions, Ru-containing catalysts do not significantly affect the activity of the TiO_2 support. However a comparison of the selectivities of Ru/TiO_2 and metal free TiO_2 (Table 4.24) reveals that the Ru-containing catalyst favours longer chain liquid products (C_5^+) and lower ethene and ethane concentrations than the metal free TiO_2. Thus, Ru on TiO_2 causes a shift from light hydrocarbons to higher hydrocarbon products.

The Pt- and Rh-containing catalysts appear to be similar to the Pd/TiO_2 catalyst. The product selectivity of Pt/TiO_2 and Rh/TiO_2 at low temperature was different while a similar product distribution was observed at higher temperature. Both metal containing catalysts promoted the ethanol conversion to a wide range of hydrocarbon and oxygenated products, and also favoured the formation of heavier products.

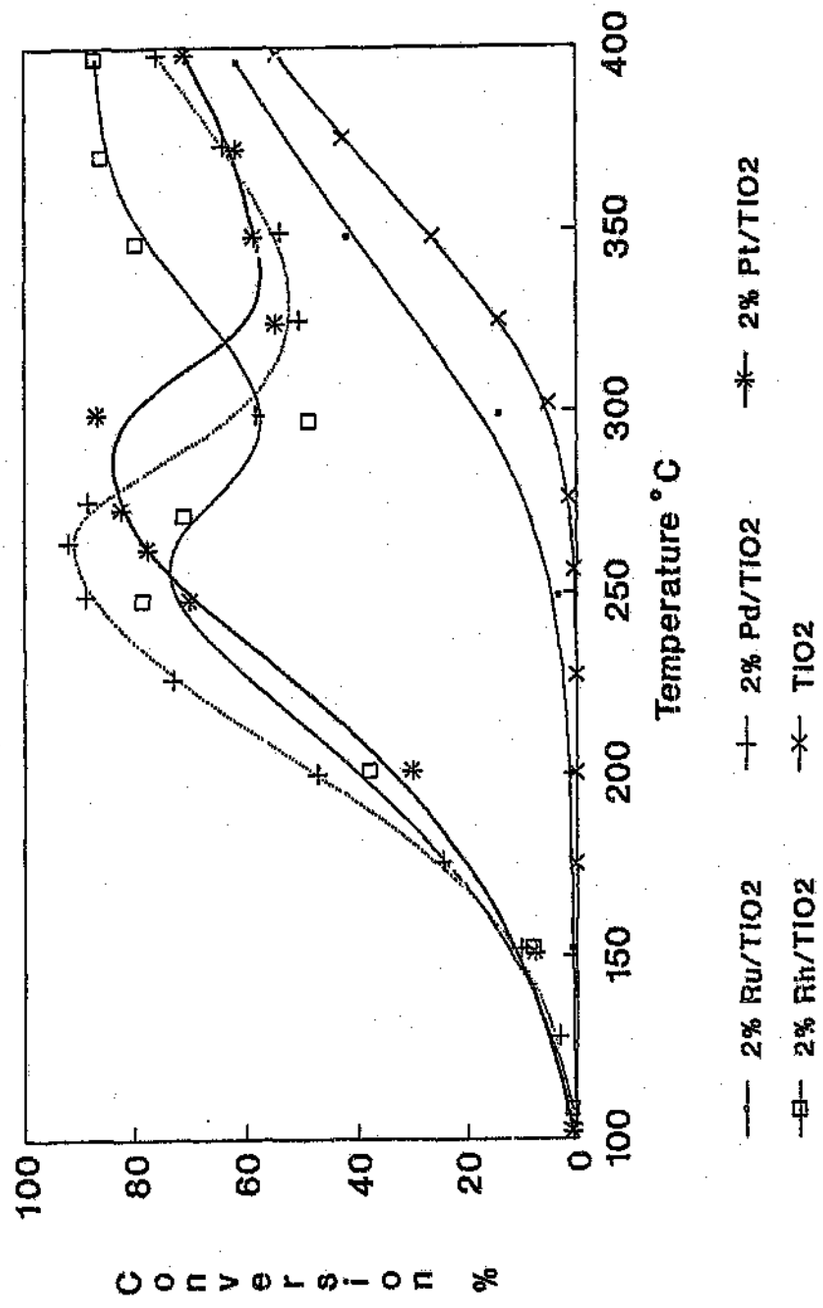

Figure 4.31 Comparison of the catalytic activity of the Ru, Pd, Pt, Rh loaded TiO_2 (2% metal by mass) and metal free TiO_2 catalysts.

Table 4.22 Catalytic performance of 2% Pt/TiO_2 catalyst in the ethanol conversion reaction (catalyst: reduced at 400°C/16 h)

Temp. (°C)	Conv. %	Product distribution (% by mass)												
		Et_2O	MeCHO	C1	C2	C2=	C3	C3=	C4	C5	C6	C7	C8	C9+
102	0.87	0	0.81	0	0	0	0	0	0	0.06	0	0	0	0
151	7.72	0.04	2.40	0.01	0.02	0.01	0	0.09	0	0.80	1.53	0.20	2.44	0.18
201	29.91	0.28	5.75	0.14	0.26	0.05	0.18	0.58	0	3.31	5.20	1.60	9.55	3.01
248	69.96	1.24	6.48	1.26	1.67	0.15	1.57	2.63	0	10.42	7.52	6.69	20.49	9.84
262	77.53	1.59	6.27	2.11	2.36	0.19	2.37	3.63	0.40	12.61	4.54	8.58	22.25	10.63
273	82.39	1.84	5.45	2.94	2.78	0.20	3.04	4.43	0.53	12.83	6.52	9.09	21.16	11.58
299	86.81	3.03	3.96	5.16	3.77	0.26	4.63	6.33	0.86	13.89	6.46	11.58	17.05	9.83
324	54.58	2.65	2.09	0.67	0.68	0.30	0	0.42	0	2.13	15.41	0.75	18.60	10.58
348	58.59	5.91	1.36	0.34	1.00	0.73	0	0.25	0	1.36	17.89	1.82	18.99	8.94
372	61.84	8.26	2.15	0.27	1.43	1.81	0	0.36	0	1.88	18.66	3.13	18.45	5.44
398	70.71	7.21	3.07	0.31	2.27	3.58	0	0.69	0	3.00	18.89	3.96	20.21	7.52

Table 4.23 Catalytic performance of 2% Rh/TiO_2 catalyst in the ethanol conversion reaction (catalyst: reduced at 400°C/16 h)

Temp. (°C)	Conv. %	Product distribution (% by mass)												
		Et_2O	MeCHO	C1	C2	C2=	C3	C3=	C4	C5	C6	C7	C8	C9+
108	0.78	0	0.69	0.02	0	0	0	0	0	0.07	0	0	0	0
152	8.12	0	2.07	0.16	0	0	0.03	0.09	0	1.05	0.97	0.16	3.38	0.21
201	37.83	0	2.89	1.40	0.06	0	0.69	0.09	0	5.46	3.25	4.75	11.94	7.30
248	78.38	0	2.14	7.11	0.72	0.03	4.05	3.53	0.23	12.50	4.57	14.60	12.64	16.26
271	71.00	1.87	3.24	5.36	0.78	0.26	0	7.20	0.45	10.20	5.95	8.89	13.77	13.03
297	48.63	2.06	3.99	1.96	0.27	0.38	0	1.82	0	4.09	8.99	1.68	14.13	9.26
346	79.76	4.54	1.72	2.49	1.37	0.68	0	1.27	5.35	1.48	17.86	5.50	23.34	14.16
370	86.01	7.26	1.48	3.51	2.65	1.19	0	1.71	5.66	3.19	19.03	7.65	23.15	9.53
397	87.12	9.10	0.96	7.92	7.26	1.78	0	2.89	4.80	3.63	18.52	8.31	17.05	4.90

Table 4.24 Comparison of the catalytic activity and product selectivities of 2% Ru/TiO_2 and metal free TiO_2 catalysts (catalysts: reduced at 400°C/16 h)

Temp. (°C)	Conv. %	Product distribution (% by mass) Et_2O	MeCHO	C1	C2	C2=	C3	C3=	C4	C5	C6	C7	C8	C9+
						TiO_2								
256	0.47	0.45	0	0	0	0.02	0	0	0	0	0	0	0	0
276	1.47	1.34	0.04	0	0.02	0.07	0	0	0	0	0	0	0	0
302	5.16	4.49	0.12	0	0.15	0.35	0	0	0	0	0.05	0	0	0
325	13.95	11.20	0.27	0	0.55	1.43	0	0.01	0	0	0.43	0.06	0	0
348	26.13	17.70	0.52	0.01	2.12	3.94	0	0.08	0	0	1.15	0.51	0.10	0
375	42.58	11.61	0.87	0.05	8.63	10.10	0	0.63	0	1.64	6.06	0.89	1.85	0.25
398	54.28	5.53	1.13	0.16	14.71	16.62	0.13	1.58	3.53	2.40	4.17	0.96	3.02	0.34
						2% Ru/TiO_2								
152	0.89	0	0.54	0	0	0	0	0.01	0	0.15	0.12	0	0.07	0
200	1.12	0	0.62	0	0	0	0	0	0	0.14	0.26	0	0.10	0
249	3.44	0.10	0.90	0.01	0	0.01	0	0	0	0.32	0.95	0.07	0.99	0.09
299	14.02	1.30	1.16	0.02	0.07	0.13	0	0.01	0	0.70	4.27	0.24	4.00	2.12
348	41.93	6.49	1.39	0.08	1.28	1.56	0	0.29	0	0.90	12.12	1.99	10.11	5.72
396	61.56	7.84	2.96	0.30	3.00	5.72	0	0.99	0	2.16	14.15	4.31	13.28	6.85
445	76.77	5.71	10.39	0.72	7.71	18.71	0.23	1.11	0	4.27	8.03	2.82	10.15	6.92

4.4 CONCLUSIONS

This study has revealed that addition of Pd to TiO_2 significantly influences the ethanol conversion reaction in the low temperature regime (200°C - 300°C). By careful variation of reaction parameters (reduction temperature, calcination temperature, etc.) the product yield in this region can be maximized. High temperatures (> 300°C) results in deactivation of thus low temperature effect. This is due possibly to coke formation, but also possibly due to a SMSI effect. Variation of the metal (Pt, Rh, Ru) also results in a change in the product spectrum from that measured over TiO_2. This study has thus indicated the way in which products from the ethanol reaction can be varied by judicious choice of variables.

REFERENCES

[1] A. Sabatier, Chem. Phys., 20 (8) (1910) 326.

[2] G.B. Paupp, S.A. Stevenson, J.A. Dumesic, S.J. Tauster and R.T.K. Baker, in "Metal-support Interaction in Catalysis Sintering, and Redispersion", S.A. Stevenson et al. (Eds.), Van Nostrand Reinhold Co., New York, (1987) Ch.7.

[3] M. Guisnet, in "Catalysis by Acids and Bases", B. Imelik et al. (Eds , Elsevier, Amsterdam, (1985) p.283.

[4] C.N. Satterfield, "Heterogeneous Catalysis in Practice", McGraw-Hill, New York, 1980.

[5] J.T. Richardson, "Principles of Catalyst Development", Plenum Press, New York, 1989.

[6] E.B. Maxted, in "The Poisoning of Metallic Catalysts, Advances in Catalysis", W.G. Frankenburg, E.K. Rieal and V.I. Komarewsky, (Eds.), Vol.3, Academic, New York, (1951) p.129.

[7] J. Brunelle, in "Preparation of Catalysts: Scientific Bases for the Preparation of Heterogeneous Catalysts", B. Delmon et al. (Eds.), Vol. II, Elsevier, Amsterdam, 1979.

[8] J.C. Summers and S.A. Ausen, J. Catal., 52 (1978) 455.

[9] E. Santacesaria, S. Carra and I. Adami, Ind. Eng. Chem. Prod. Res. & Dev., 16 (1977) 41.

[10] R. J. Fenoglio, W. Alvarez, G. M. Nunez and D. E. Resasco in "Preparation of Catalysts: Scientific Bases for the Preparation of Heterogeneous Catalysts", B. Delmon et al. (Eds.), Vol. V, Elsevier, Amsterdam, (1991) p.77.

[11] H. Matsumoto, Y. Saito and Y. Toneda, J. Catal., 19 (1970) 101.

[12] T.A. Dorling, B.W.J. Lynch and R.L. Moss, J. Catal., 20 (1971) 190.

[13] F.E. Shephard, J. Catal., 14 (1969) 148.

[14] M.A. Kohler, J.C. Lee, D.L. Trimm, N.W. Cant and M.S. Wainwright, Appl. Catal., 31 (1987) 309.

[15] B. Delmon et al (Eds.), "Preparation of Catalysts: Scientific Bases for the Preparation of Heterogeneous Catalysts"; Vol. I, II, III, and IV, Elsevier, Amsterdam, 1975, 1979, 1983, 1987.

[16] H. Pines and T.P. Kobylinski, J. Catal., 17 (1970) 391; paper 4.

[17] H. Pines and T.P. Kobylinski, J. Catal., 17 (1970) 375.

[18] H. Pines and P. Steingaszner, J. Catal., 10 (1968) 60.

[19] T.P. Kobylinski and H. Pines, J. Catal., 17 (1970) 384.

[20] J. Hensel and H. Pines, J. Catal., 24 (1972) 197.

[21] E. Licht, Y. Schächter and H. Pines, J. Catal., 31 (1973) 110.

[22] E. Licht, Y. Schächter and H. Pines, J. Catal., 34 (1974) 338.

[23] E. Licht, Y. Schächter and H. Pines, J. Catal., 55 (1978) 191.

[24] E.B. Maxted, in "The Poisoning of Metallic Catalysts, Advances in Catalysis", W.G. Frankenburg, E.K. Rieal and V.I. Komarewsky, (Eds.), Vol.3, Academic, New York, (1951) p.129.

[25] C. Marcilly and J.P. Franck, in "Catalysis by Zeolites", B. Imelik et al. (Eds.), Elsevier, Amsterdam, (1980) p.99.

[26] M.E. Dry, in "Catalysis: Science and Technolgy", J.R. Anderson and M. Boudart (Eds.), Vol.1 Springer-Verlag, (1981) Ch.4 p.195.

[27] E.J. Detreköy, P.A. Jocobs, D. Kalló and B. Uytterhoeven, J. Catal., 32 (1974) 442.

[28] E. Ruckenstein and I. Sushumna, in "Hydrogen Effects in Catalysis", Z. Paál and P.G. Menon (Eds.), Marcel Dekker Inc., New York, (1988) Ch.10.

[29] E. Ruckenstein, in "Metal-support Interactions in Catalysis, Sintering, and Redispersion", S.A. Stevenson et al. (Eds.), Van Nostrand Reinhold Co., New York, (1987) Ch.14.

[30] J.J. Chen and E. Ruckenstein, J. Catal., 69 (1981) 254.

[31] J.W. Geus, in "Materials Science Research, Vol. 10, Sintering and Catalysis, G.C. Kuczynski (Ed.), Plenum press, New York, (1975) p.29.

[32] R. Hughes, in "Deactivation of Catalysts", Academic press, London, 1984.

[33] E. Ruckenstein and B. Pulvermacher, J. Catal., 29 (1973a) 224.

[34] E. Ruckenstein and D.B. Dadyburjor, J. Catal., 48 (1977) 73.

[35] H.H. Lee, J. Catal., 62 (1980) 129.

[36] S.Y. Wang, S.H. Moon and M.A. Vannice, J. Catal., 71 (1981) 167.

[37] M.A. Vannice, S.Y. Wang and S.H. Moon, J. Catal., 71 (1981) 152.

[38] S.J. Tauster, S.C. Fung and R.L. Garten, J. Amer. Chem. Soc., 100 (1978) 170.

[39] S.J. Tauster, S.C. Fung, J. Catal., 55 (1978) 29.

[40] S.J. Tauster, S.C. Fung, R.T.K Baker and J.A. Horsley, Science, 211 (1981) 1121.

[41] M.A. Vannice and P. Chou, J. Chem. Soc. Chem. Commun., (1984) 1590.

[42] J.D. Bracey and R. Burch, J. Catal., 86 (1984) 384.

[43] S.A. Stevenson, G.B. Paupp, J.A. Dumesic, S.J. Tauster and R.T.K. Baker, in "Metal-support Interaction in Catalysis Sintering, and Redispersion", S.A. Stevenson et al. (Eds.), Van Nostrand Reinhold Co., New York, (1987) Ch.2.

[44] P. Meriaudeau, O.H. Ellestad, M. Dufaux and C. Naccache, J. Catal., 75 (1982) 243.

[45] B.A. Sexton, A.E. Hughes and K. Foger, J. Catal., 77 (1982) 85.

[46] B.H. Chen and J.M. White, J. Phys. Chem., 86 (1982) 3534.

[47] R. Burch, in "Hydrogen Effects in Catalysis", Z. Paál and P.G. Menon (Eds.), Marcel Dekker Inc., New York, (1988) Ch.13.

[48] V. Vishwanathan and S. Narayanan, J. Chem. Soc., Chem. Commun., (1988) 1233.

[49] M.A. Vannice and P. Chou, J. Chem. Soc., Chem. Commun., (1984) 1590.

[50] M.A. Vannice and C.C. Twu, J. Catal., 82 (1983) 213.

[51] R.M. Cursetji, A.N. Singh and A.V. Deo, Chem. age of India, 37 (6) (1986) 407.

[52] M.R. Ladisch and K. Dyck, Science, 205 (1979) 898.

[53] J.C. Oudejans, P.F. Vanden Oosterkamp and H. Van Bekkum, Appl. Catal., 3 (1982) 109.

[54] V.R. Choudhary and S.D. Sansare, Appl. Catal., 10 (1984) 147.

[55] M. Guisnet and P. Magnoux, Appl. Catal., 54 (1989) 1.

[56] D.E. Walsh and L.D. Rollmann, J. Catal., 49 (1979) 369.

[57] C.A. Fyfe, G.J. Kennedy, G.T. Kokotailo and C.T. De Schuter, J. Chem. Soc., Chem. Commun., (1984) 1093.

[58] P. Magnoux, P. Cartroud, S. Mignard and M. Guisnet, J. Catal., 106 (1987) 235.

[59] D.M. Bibby, N.B. Milestone, J.E. Patterson and L.P. Aldridge, J. Catal., 97 (1986) 493-502.

[60] M.R.S. Manton, CSIR Report CENG 184, Pretoria: CSIR, 1977.

[61] T. Themistocleous, Ph.D. Thesis, University of the Witwatersrand, Johannesburg, 1990.

[62] W.O. Haag, W.W. Kaeting, D.H. Olson and P.G. Rodewald, S.A. Patent Appl., 79/4816.

[63] C. Sivaraj, B. Prabhakara Reddy, B. Rama Rao and P. Kanta Rao, Appl. Catal., 24 (1986) 25.

[64] F. Pepe, C. Angeletti, S. De Rossi and M. Lo Jacono, J. Catal., 91 (1985) 69.

[65] C. Sivaraj and P. Kanta Rao, Appl. Catal., 45 (1988) 103.

CHAPTER FIVE

THERMODYNAMIC STUDY OF ETHANOL TRANSFORMATION OVER A 2% Pd/TiO_2 CATALYST

5.1 INTRODUCTION

The conversion of alcohol to chemical products has been performed over titania, alumina, and clay etc., under low pressures (1 bar) and *ca.* 300°C (see Chapter three). In general the reaction has been found to proceed via a dehydration reaction pathway which gives ethers and olefins [1 - 5]. On the other hand, for palladium supported catalysts on the same supports, but at lower temperatures, it has been found that a dehydrogenation reaction pathway competes with the dehydration pathway to give aldehydes (see Chapter four).

For the ether-alcohol dehydration reaction pathway, the following three main schemes have been proposed [1]: (I) a consecutive reaction, (II) a parallel reaction and (III) a combinations of consecutive and parallel reactions. These can be represented as follows:

(I) Consecutive reaction:

$$2\ CH_3CH_2OH \underset{K_3}{\overset{K_1}{\Longleftrightarrow}} C_2H_5OC_2H_5 + H_2O \xrightarrow{K_2} 2\ C_2H_4 + 2\ H_2O$$

(II) Parallel reaction:

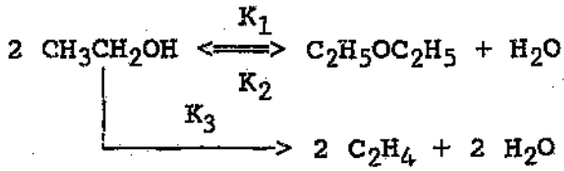

(III) Consecutive and parallel reaction:

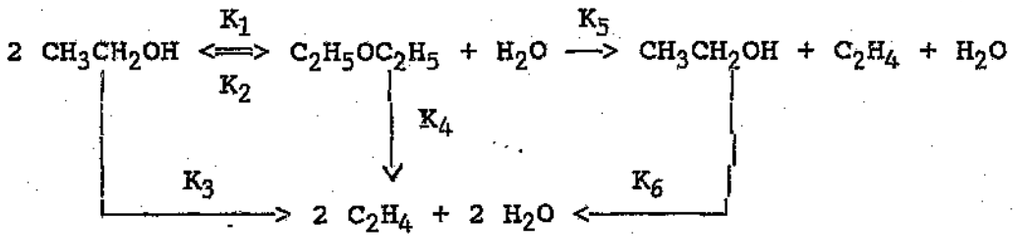

The detailed study of the ether-alcohol transformation to hydrocarbons over a Pd/TiO_2 catalyst was described in Chapter four. At $T > 300^{\circ}C$ it is assumed that the reaction occurs via the same schemes as listed above. However, in addition a dehydrogenation pathway to acetaldehyde was found for $T < 300^{\circ}C$, for which the following reaction scheme is proposed:

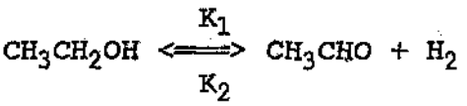

This study introduces the theory and experimental methods necessary to perform a thermodynamic study of the ethanol to hydrocarbons and oxygenates conversion reactions. Preliminary results from the thermodynamic study are presented with emphasis on acetaldehyde formation in the low temperature range ($100^{\circ}C$ to $300^{\circ}C$) and diethyl-ether, ethene formation in a second reaction pathway in the high temperature range ($300^{\circ}C$ to $400^{\circ}C$).

Equilibrium compositions of the products were determined by using the Process package (Simulation Sciences, Inc.) and

were compared with the experimentally determined results. The equilibrium constants (Ka) were used to determine whether specific reactions had reached equilibrium or not.

5.2 EQUILIBRIUM STUDY: THEORY

Chemical Equilibrium

A true heterogeneous catalyst accelerates the rate of approach to equilibrium but cannot alter that equilibrium. This is readily seen by considering a simple reversible reaction A ⇌ B. The standard free energy change is expressed as $\Delta G^\circ = - R T \ell nK = - R T \ell n(A_b/A_a)$, where A_b and A_a are the activities of product and reactant, respectively. The presence of the solid catalyst cannot change ΔG°, and hence does not change the ratio A_b/A_a [6].

Equilibrium Constants

The equilibrium constants in chemically reacting systems are calculated from readily available standard Gibbs free energies of formation (ΔG°_f). The equilibrium constant and Gibbs free energy of reaction are given by [7 - 10]:

$$(Ka)_{T^*} = \exp \frac{-\Delta G^\circ}{R T^*} \qquad (5\text{-}1)$$

T^* usually 298 K

or

$$\Delta G^\circ = - R T^* \ell n(Ka)_{T^*} \qquad (5\text{-}2)$$

T^* usually 298 K

From equations (5-1) and (5-2), it is clear that the equilibium constant (Ka) may be calculated provided that the Gibbs free energy of formation ($\Delta G°_f$) is known [7 - 10]. The method of calculation of $\Delta G°_f$ is discussed in Appendix 5.

The equilibrium constant is a function of temperature only and can be calculated from the equation (5-3):

$$\ell n \frac{(Ka)_{T2}}{(Ka)_{T1}} = \int_{T^*}^{T} \frac{\Delta H°_{T^*} + \int \Delta C_p \, dT}{RT^2} \, dT \qquad (5\text{-}3)$$

The derivation of equation (5-3) is given in Appendix 5.

5.3 EXPERIMENTAL APPARATUS AND PROCEDURE

The reactions were carried out in a glass fixed-bed continuous flow reactor system at atmospheric pressure. This reactor is essentially a miniature fixed-bed reactor, and is the simplest kind of reactor to use for the thermodynamic studies. The reactor heating unit, which fits around the outside of the reactor (see Figure 2.2 in Chapter two), is regul ted within the temperature range 100°C and 400°C.

Heating tape was wrapped over the entire reactor to compensate for heat loss. In addition accurate temperature control was required. (approx. 1°C variation was achieved). A detailed description and diagram of the experimental rig is given in Chapter two, section 2.2.

Aqueous ethanol (96% C_2H_5OH, 4% H_2O, v/v) and pure ethanol (Labchem Ltd., 99.8% - 100%) were fed by means of a syringe pump (feed rate 1.0 and 0.28 ml h^{-1}) over a 2% Pd/TiO_2 extruded catalyst. The vapourized ethanol was diluted with a stream of dry N_2 at various flow rates, over a large temperature range (100°C to 400°C). The total flow rate was varied and controlled at 21.0 cm^3 min^{-1}, 64.0 cm^3 min^{-1} and 96.0 cm^3 min^{-1}.

The extruded 2% Pd/TiO_2 catalyst was prepared using the co-precipitation technique described in Appendix 1. About 1.0 g of the wet catalyst was placed in the reactor and dried <u>in situ</u> with N_2 for 3 h at 100°C. The catalyst was then reduced in H_2 for 16 h at 200°C before beginning the reaction. (Note: the exact dry catalyst weight was determined by TGA techniques). The method of analysis and the data manipulation details were also described in Chapter two, section 2.3.

The analysis of the preliminary results using this equipment are presented below. In the thermodynamic study the theoretical product spectrum was determined and was checked to see if any of the reactions had reached equilibrium.

The equilibrium concentrations were calculated for the species in the reaction at a particular temperatures using the Simulation Sciences Inc., Process package (the calculation was limited to species present at that temperature of the reaction). A detailed listing of the input data for the Process Package appears in Appendix 7.

5.4 RESULTS

The experimental reactions were performed using 0.92 g of the Pd/TiO_2 catalyst (determined after water loss by a TGA; 1.94% Pd by mass using AA spectrophotometry) with different carrier gas feed rates. Tables 5.1 to 5.4 show the experimental results obtained for ethanol conversion at different temperatures. It may be noted from these studies that under the specified conditions a large product spectrum is observed in the temperatures range (150°C - 400°C) used. For ethanol conversion to hydrocarbons and oxygenates, the possible reaction pathways together with rate constant nomenclature used are illustrated in Figure 5.1.

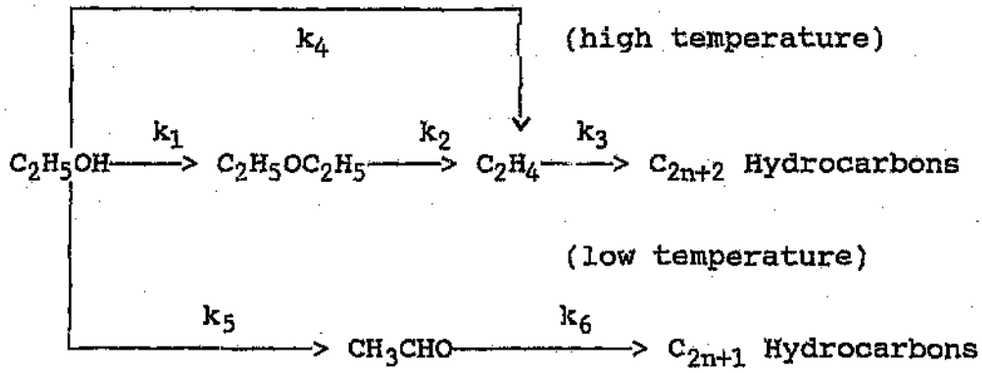

where k_i is the rate constant

$k_3 \gg k_1, k_2, k_4$

and $k_6 \gg k_5$

Figure 5.1 Ethanol transformation to hydrocarbons over Pd/TiO_2 catalytic reaction parthways

We propose that for the reaction at low temperature $k_3 \ll k_6$ and for the reaction at high temperature $k_6 \ll k_3$. It is further proposed that $k_3 \gg k_1$, k_2, k_4 and $k_6 \gg k_5$. This is supported by the data in Tables 5.1 to 5.4 since the product distributions of $C_2H_5OC_2H_5$, C_2H_4 as well as for CH_3CHO are low compared to the C_{2n+2} and C_{2n+1} Hydrocarbon yields. At low temperature ($T < 300^{\circ}C$) the dehydrogenation pathway giving acetaldehyde and odd number hydrocarbons occurs. At $T > 300^{\circ}C$ the second reaction pathway begins to operate producing diethyl-ether, ethene and even number hydrocarbons. These results are shown in Figure 5.2, and Tables 5.1 to 5.4.

In these studies an increase in the nitrogen flow rate results only in a decrease in ethanol conversion to products in the first reaction pathway (dehydrogenation, 100°C to 300°C; see Figure 5.3). From this figure it can be observed that the highest conversion, at about 260°C, occurs at low N_2 feed rates. Furthermore, the acetaldehyde and diethyl-ether concentrations obtained under the different experimental conditions exhibits no significant change under varying flow rates (see Tables 5.1 to 5.4).

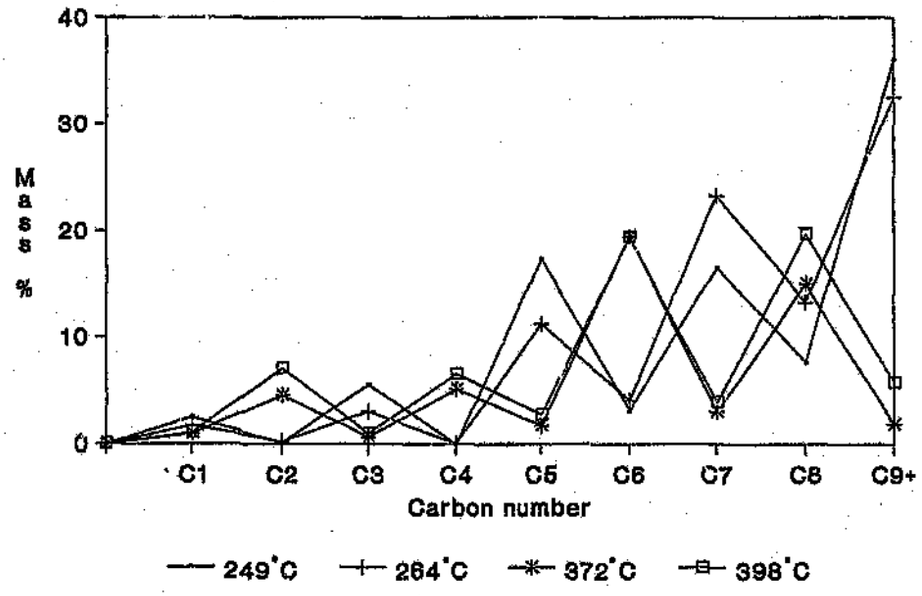

Figure 5.2 Product distribution of the ethanol transformation reaction at different reaction temperatures (N_2 flow rate = 21 ml min^{-1}, WHSV = 0.806 h^{-1})

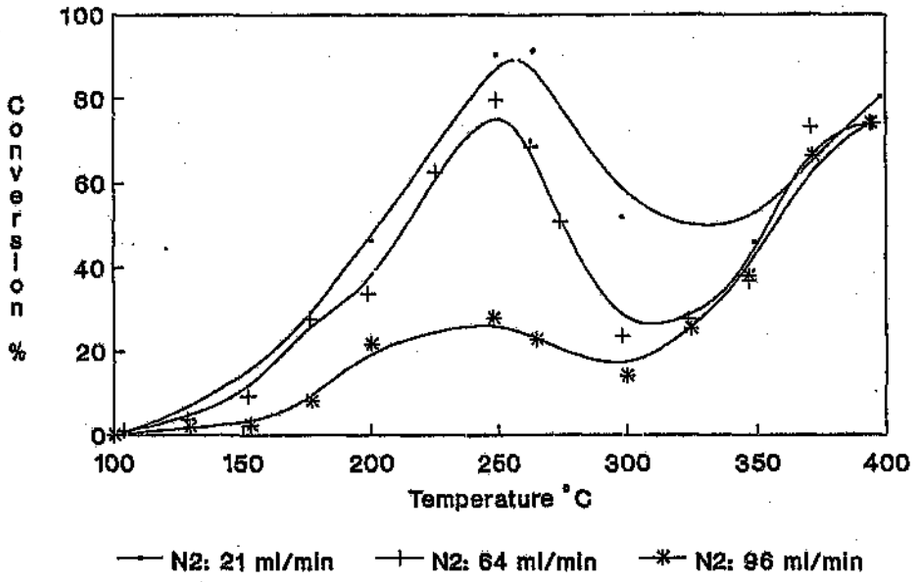

Figure 5.3 Comparison of ethanol conversion at the various nitrogen flow rates (WHSV = 0.806 h^{-1})

Table 5.1 Equilibrium study for the ethanol conversion reaction at N_2 flow rate: 21 ml min^{-1}
WHSV = 0.806 h^{-1} (a aqueous ethanol 96%)

Temp. (°C)	Conv. %	Product distribution (% by mass)												
		Et_2O	MeCHO	C1	C2	C2=	C3	C3=	C4	C5	C6	C7	C8	C9+
104	0.68	0	0.47	0	0	0	0	0	0	0	0	0.21	0	0
152	9.24	0	1.21	0.05	0	0	0.09	0.04	0	1.50	0.92	0.98	2.80	1.65
200	46.38	0	1.48	0.51	0.02	0	1.47	0	0	8.47	2.79	8.92	6.75	15.97
249	90.36	0	1.51	2.50	0.11	0	5.54	0	0	17.32	3.17	16.53	7.66	36.02
264	91.34	0	2.01	1.68	0.20	0.01	1.54	1.50	0.06	11.24	4.06	18.90	17.63	32.51
298	51.80	2.38	2.72	0.75	0.25	0.17	0	1.74	0	3.30	8.92	2.84	17.20	11.53
349	45.88	11.77	0.77	0.45	1.24	1.14	0	0.24	0	0.64	11.88	2.20	10.97	4.58
372	66.45	12.04	2.06	0.93	2.26	2.25	0	0.65	5.12	1.68	19.47	3.05	15.02	1.92
398	80.20	9.68	3.32	1.05	3.16	3.89	0	0.99	6.57	2.74	19.43	3.90	19.68	5.79

Table 5.2 Equilibrium study for the ethanol conversion reaction at N_2 flow rate: 21 ml min^{-1}
WHSV = 0.226 h^{-1} (a aqueous ethanol 96%)

Temp. (°C)	Conv. %	Product distribution (% by mass)												
		Et_2O	MeCHO	C1	C2	C2=	C3	C3=	C4	C5	C6	C7	C8	C9+
105	1.78	0	0.60	0.01	0	0	0	0	0	0.04	0	0.99	0.05	0.09
152	19.42	0	1.07	0.07	0	0	0.12	0.09	0	2.94	1.26	2.91	4.68	6.28
209	69.96	0	1.23	1.34	0.03	0	3.31	0	0	15.90	2.04	16.44	4.32	25.35
248	81.31	0	2.06	1.40	0.15	0.04	0	3.25	0.09	12.04	3.85	16.72	11.69	30.02
266	66.21	3.49	2.99	1.17	0 16	0.11	0	3.60	0.25	6.93	4.81	8.79	17.01	16.90
298	53.97	3.51	1.81	0.92	0.27	0.23	0	1.17	1.63	1.53	10.71	2.72	19.70	9.77
347	76.64	9.59	1.56	2.14	2.07	1.34	0	1.40	4.37	1.03	16.96	6.32	24.51	5.35
371	78.56	11.18	1.80	3.81	4.77	2.94	0	2.19	4.85	1.65	16.62	5.22	19.20	4.33
396	86.78	9.09	2.20	5.42	8.39	7.39	0	3.28	8.67	2.56	16.83	5.17	16.35	1.43

Table 5.3 Equilibrium study for the ethanol conversion reaction at N_2 flow rate: 64 ml min^{-1} WHSV = 0.806 h^{-1} (a aqueous ethanol 96%)

Temp. (°C)	Conv. %	Product distribution (% by mass)												
		Et_2O	MeCHO	C1	C2	C2=	C3	C3=	C4	C5	C6	C7	C8	C9+
104	0.92	0	0.76	0.01	0	0	0	0	0	0	0	0.15	0	0
129	3.65	0	1.25	0.03	0	0	0.03	0.04	0	0.62	0.23	0.28	0.93	0.24
152	9.32	0	1.47	0.07	0	0	0.10	0.06	0	1.59	0.87	0.91	2.88	1.37
176	27.60	0	1.71	0.24	0.01	0	0.51	0.20	0	5.59	1.69	4.82	5.12	7.71
199	33.70	0	2.89	0.63	0.02	0	1.35	0.31	0	7.62	2.22	5.64	4.72	8.30
225	62.55	0	2.93	1.36	0.06	0	2.78	0.64	0	13.33	2.84	12.16	7.79	18.66
249	79.61	0	3.16	1.69	0.16	0.03	0.94	2.39	0.09	11.18	4.02	14.95	15.43	25.57
263	68.39	2.83	3.42	1.05	0.15	0.12	0	3.11	0.20	6.19	5.16	8.65	20.36	17.15
274	50.89	2.54	4.53	0.93	0.14	0.13	0	2.40	0.21	4.89	5.23	4.46	15.68	9.75
298	23.70	0.03	1.76	0.37	0.10	0.14	0.98	0.40	0	0.97	6.58	0.20	8.11	4.06
324	27.73	4.58	1.01	0.45	0.46	0.56	0	0.18	0	0.56	8.54	0.80	8.52	2.07
347	36.86	8.89	1.56	0.66	0.89	1.30	0.25	0	0	0.65	9.78	1.61	7.94	3.33
371	73.13	11.93	2.92	1.55	2.36	3.35	0	0.78	5.98	1.63	16.30	4.53	15.55	6.25
395	74.02	11.29	7.07	1.57	2.56	5.42	0	0.83	3.99	3.30	15.58	2.40	16.70	3.31

Table 5.4 Equilibrium study for the ethanol conversion reaction at N_2 flow rate: 96 ml min^{-1}
WHSV = 0.806 h^{-1} (a aqueous ethanol 96%)

Temp. (°C)	Conv. %	Product distribution (% by mass)												
		Et_2O	MeCHO	C1	C2	C2=	C3	C3=	C4	C5	C6	C7	C8	C9+
95	0	0	0	0	0	0	0	0	0	0	0	0	0	0
130	1.81	0	0.31	0	0	0	0	0	1.49	0	0	0	0	0
153	2.41	0	1.07	0.02	0	0	0	0.08	0	0.39	0	0.30	0.55	0
177	8.16	0	1.76	0.07	0.01	0	0	0.33	0	1.73	0.41	1.25	1.33	1.27
200	21.66	0	2.88	0.20	0.03	0.01	0	0.87	0	3.76	1.12	3.40	4.55	4.84
248	28.00	1.24	5.34	0.47	0.07	0.10	0	1.56	0	2.71	2.60	1.90	7.76	4.25
265	22.68	1.19	4.70	0.46	0.07	0.12	0	1.30	0	1.89	2.79	0.77	6.54	2.85
300	14.12	1.58	1.39	0.19	0.09	0.15	0	0.11	0	0.46	4.19	0.14	4.29	1.53
325	25.41	6.20	1.25	0.33	0.48	0.72	0	0.13	0	0.43	7.11	0.40	5.96	2.40
347	37.86	11.14	2.36	0.55	0.94	1.70	0	0.26	0	0.82	9.55	1.07	7.13	2.34
372	66.27	[illegible].71	5.54	0.91	1.88	3.95	0	0.52	4.26	2.49	13.66	1.77	13.23	5.35
394	73.98	13.[illegible]	8.15	1.01	2.77	7.10	0	0.75	5.63	3.55	13.50	1.74	12.53	4.01

THERMODYNAMIC CALCULATIONS

The theoretical equilibrium constants have been calculated for the following reactions:

R X N #1 $2\ C_2H_5OH \rightleftharpoons C_2H_5OC_2H_5 + H_2O$

R X N #2 $C_2H_5OH \rightleftharpoons C_2H_4 + H_2O$

R X N #3 $C_2H_5OC_2H_5 \rightleftharpoons 2\ C_2H_4 + H_2O$

R X N #4 $C_2H_5OH \rightleftharpoons CH_3CHO + H_2$

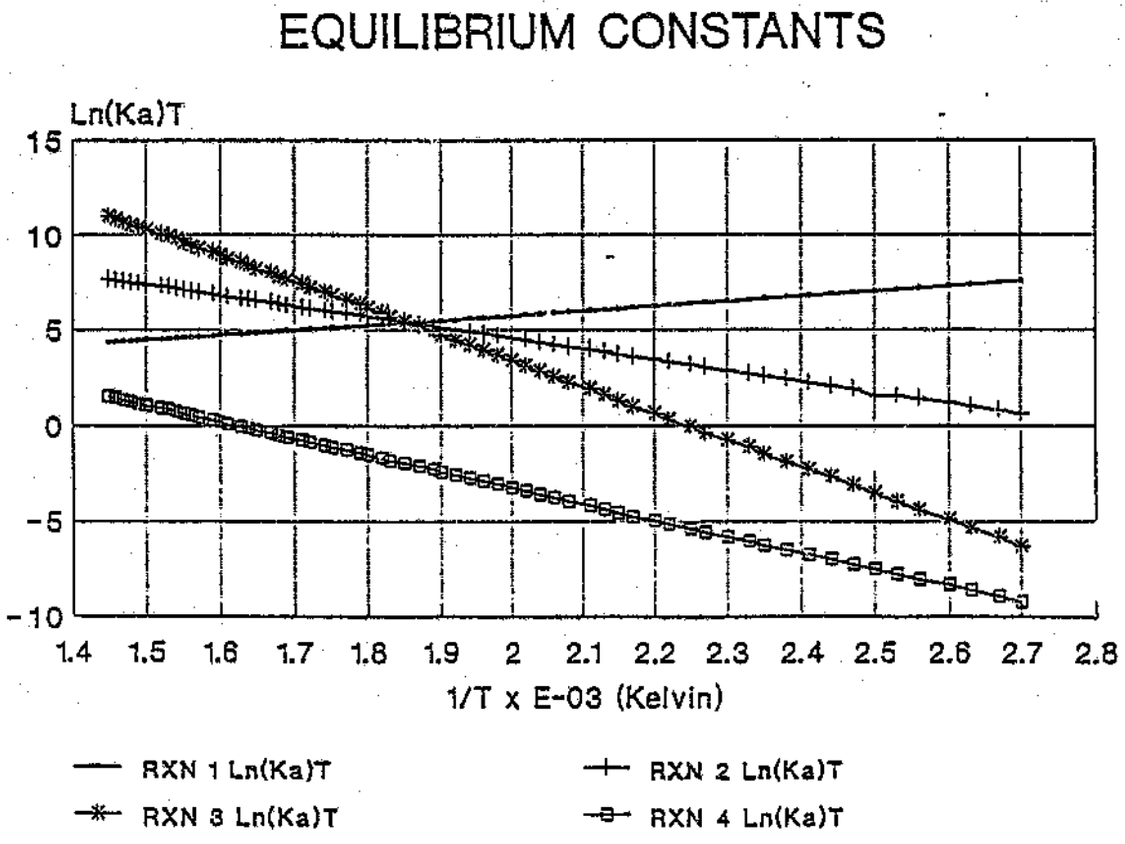

Figure 5.4 Theoretical equilibrium constants $\ln(Ka)_T$ vs temperature ($1/T\ K \times 10^{-03}$)

The theoretical equilibrium constants are plotted in Figure 5.4. The relationship was developed for the variation of the equilibrium constant with temperature ($\ln$ (Ka) vs 1/T). For detailed calculations see Appendix 6. This was done to compare individual reaction equilibria with actual experimental data. The equilibrium constants were evaluted at various temperatures ranging from 373 K to 673 K.

Reaction #1 is exothermic and the equilibrium constant ($\ln$(Ka)) increases with a decrease in temperature, but reaction #2, #3 and #4 are endothermic and the equilibrium constants decrease with an increase in temperature.

COMPARISON WITH THEORY

Experimental Ka's were calculated at different nitrogen feed rates, and various ethanol pumping rates. These Ka's were obtained by making the simplifying assumption that partial pressures are equal to fugacity (assuming ideal gas behaviour).

In the dehydration reaction pathway (reactions #1 to #3), the experimental values suggest that only reaction #1 asymptotes towards the actual calculated Ka curves as temperature increases (see Figure 5.5). Other reactions, in the high temperature range (280°C - 400°C), give experimental values that are parallel to the actual calculated Ka curves (see Figures 5.6 and 5.7).

Experimental conditions:

a: N_2: 21 ml min^{-1}
WHSV: 0.806 h^{-1}
(aqueous 96%)

b: N_2: 21 ml min^{-1}
WHSV: 0.798 h^{-1}
(absolute)

c: N_2: 21 ml min^{-1}
WHSV: 0.226 h^{-1}
(aqueous 96%)

d: N_2: 64 mlmin^{-1}
WHSV: 0.806
(aqueous 96%)

e: N_2: 96 ml min^{-1}
WHSV: 0.806 h^{-1}
(aqueous 96%)

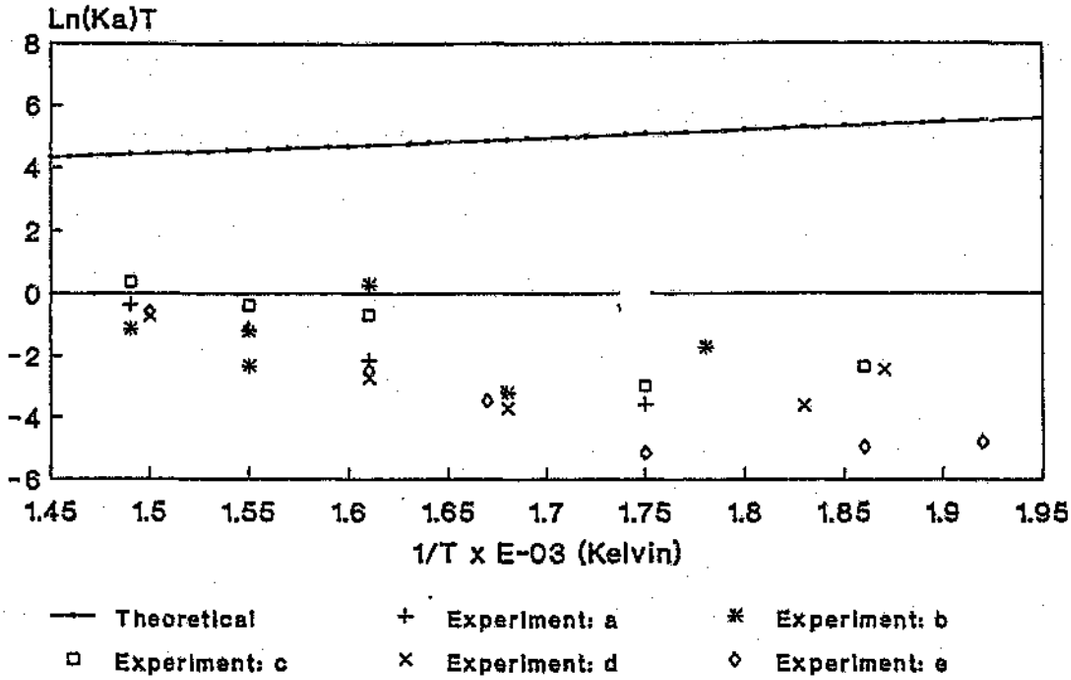

Figure 5.5 Comparison of equilibrium constants for reaction #1: 2 $C_2H_5OH \rightleftharpoons C_2H_5OC_2H_5 + H_2O$

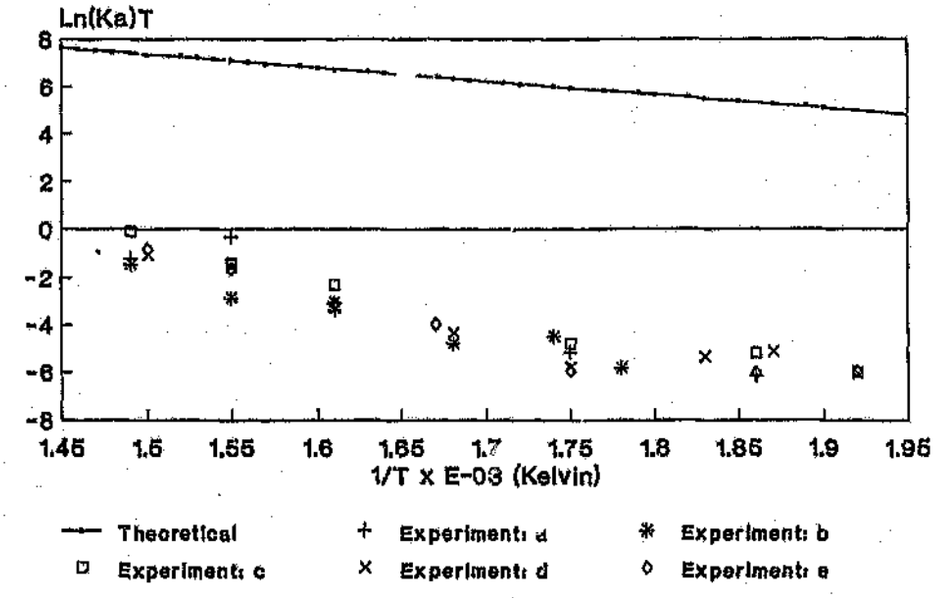

Figure 5.6 Comparison of equilibrium constants for reaction #2: $C_2H_5OH \rightleftharpoons C_2H_4 + H_2O$

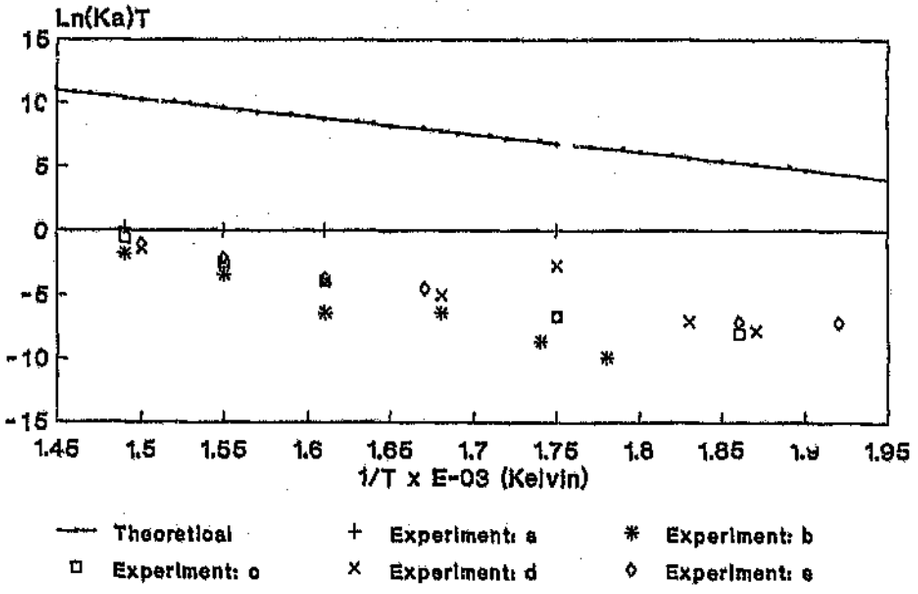

Figure 5.7 Comparison of equilibrium constants for reaction #3: $C_2H_5OC_2H_5 \rightleftharpoons 2\ C_2H_4 + H_2O$

The concentration of ethanol and contact time of ethanol with catalyst affect the asymptotic behavior; the lower the WHSV (low concentration of ethanol, longer contact time with catalyst) the more the "measured" equilibrium constant approaches that of the theoretical equilibrium (see Figure 5.5).

The first reaction pathway (dehydrogenation of ethanol to acetaldehyde reaction #4) is the only reaction that appears to actually reach equilibrium in the region of detectable compositions (at 538 K; see Figure 5.8).

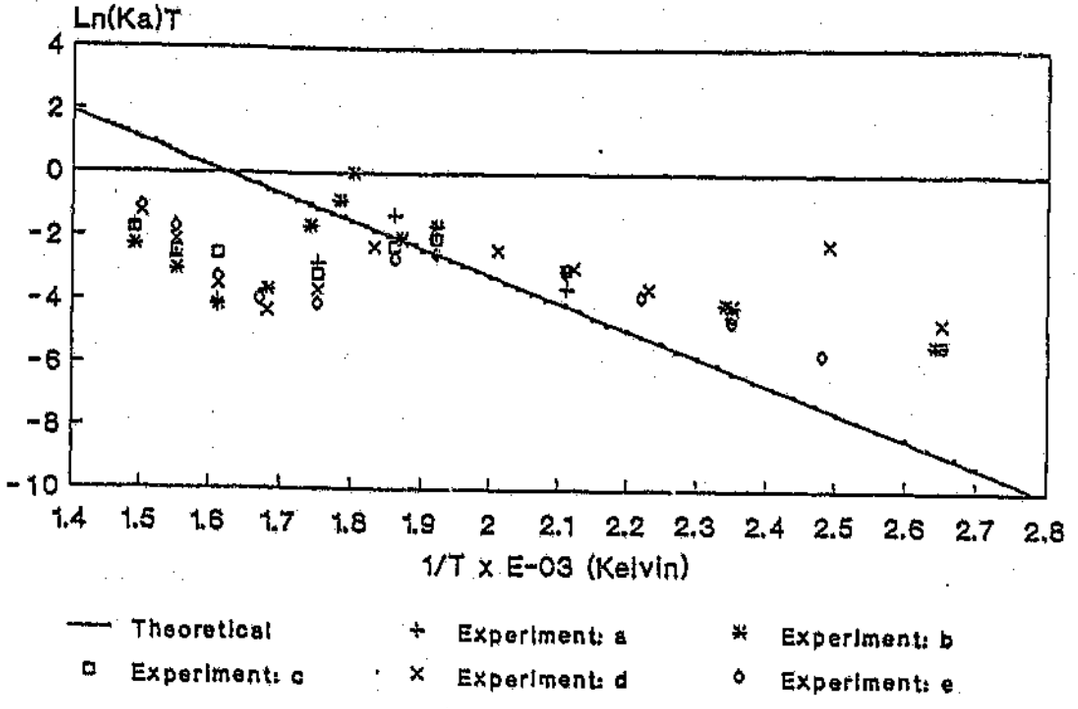

Figure 5.8 Comparison of equilibrium constants for reaction #4: $C_2H_5OH \rightleftharpoons CH_3CHO + H_2$

For comparison, the mass percentages of the theoretical and experimental equilibrium compositions are given in Table 5.5. The theoretical equilibrium compositions calculated at various nitrogen flow rate in various temperature ranges, suggest that methane and benzene should be dominant products. However the experimental results show that C_7, C_8 and C_9^+ equilibrium concentrations were higher than theoretical concentrations while benzene and methane concentrations are lower than the theoretical values. Actual theoretical values at T = 264°C yielded methane (> 37%), benzene (> 56%), toluene (± 6%), and xylene (± 0.2%), respectively.

It appears from the experimental results that the equilibrium concentration increases with an increase in temperature. However, the reaction equilibrium concentrations in the dehydration reaction pathways show virtually no change with temperature increase. The reaction reaches equilibrium at a slightly lower temperature (< 150°C) for lower nitrogen flow rates.

Table 5.5 Comparison of equilibrium compositions

Temp. (°C)	Hydrocarbon selectivity (% by mass)												Other HC's
	EtOH		CH_4		C_2H_6		C6		C7		C8		
	A	B	A	B	A	B	A	B	A	B	A	B	B
N_2 flow rate: 21 ml/min													
152[a]	0	90.76	37	0.05	0	0	45.35	0.92	16.	[illegible]	0.97	2.80	4.49
264[a]	0	8.66	37.59	1.68	0	0.20	54.47	4.06	7.74	18.90	0.2	17.63	48.87
349[b]	0	54.12	37.75	0.45	0.02	1.24	57.15	11.88	5.01	2.20	0.07	10.97	19.14
398[b]	0	19.80	37.79	1.05	0.02	3.16	58.00	19.13	4.09	3.90	0.1	19.68	32.98
N_2 flow rate: 64 ml/min													
152[a]	0	90.68	37.27	0.07	0	0	49.41	0.87	12.79	0.91	0.53	2.88	4.59
263[a]	0	31.61	37.72	1.05	0	0.15	56.53	5.16	5.65	8.65	0.1	20.36	33.02
347[b]	0	63.14	37.85	0.66	0.02	0.89	58.49	9.78	3.60	1.61	0.04	7.94	15.98
395[b]	0	25.98	37.87	1.57	0.02	2.56	59.13	15.58	2.94	2.40	0.04	16.70	35.21
N_2 flow rate: 96 ml/min													
153[a]	0	97.59	37.37	0.02	0	0	51.01	0	11.22	0.30	0.4	0.55	1.54
265[a]	0	77.32	37.77	0.46	0	0.07	57.31	2.79	4.84	0.77	0.08	6.54	12.05
347[b]	0	62.14	37.87	0.55	0.01	0.94	58.97	9.55	3.11	1.07	0.04	7.13	18.62
394[b]	0	26.02	37.89	1.01	0.01	2.77	59.51	13.50	2.56	1.74	0.03	12.53	42.43

A: Theoretical, B: Experiment, WHSV = 0.806 h^{-1} (a aqueous ethanol 96%), Catalyst: 2% Pd/TiO_2

[a] Temperature of ethanol dehydrogenation reaction; [b] Temperature of ethanol dehydration reaction

5.5 DISCUSSION

Stability of the catalysts:

Before any detailed thermodynamic and kinetic measurements can be made it is imperative to determine the stability of the catalysts over a range of temperatures and/or a long reaction time period (dehydration or dehydrogenation) [2, 5, 11]. It was found however that the 2% Pd/TiO_2 catalyst deactivates ($\sim$ 10% in 6 h) and hence was hence not an appropriate reaction for an indepth thermodynamic and/or kinetic study of the ethanol transformation reaction. The conversion of EtOH to Et_2O, C_2H_4 or CH_3CHO shows poor selectivity (see Tables 5.1 to 5.4) even though the conversion of EtOH to other products e.g. C_6 etc. is good.

The above results do give an idea as to what pathways can be proposed for the reaction mechanism. These results also suggest the temperature range in which to perform kinetic studies in order to either enhance or suppress various reaction pathways so as to eventually have a rate expression for each step. In the kinetic study, another method of ensuring that each individual reaction is at equilibrium is by feeding into the reactor the equilibrium component compositions for that specific reaction.

5.6 CONCLUSIONS

In our studies, the proposed ethanol dehydration reaction to ether or ethene was never achieved under equilibrium conditions. Only in the dehydrogenation reaction was some data measured which were consistent with theoretical equilibrium data (see Figure 5.7). We thus have shown that the three of the four reactions are kinetically limited under our conditions.

In reaction systems, thermodynamic studies can be of great value in predicting the possible extents of reaction and the most suitable reaction conditions. The ethanol dehydration and/or dehydrogenation is not one of these systems.

Acid catalysts such as γ-Al_2O_3, ZSM-5 dehydrate alcohols to yield as primary product the ethers. These are formed at low temperatures in agreement with thermodynamic predictions for the reaction. For the Pd/TiO_2 catalyst the ethanol dehydrogenation reaction occurs at lower temperature and only at higher temperatures does dehydration of ethanol to diethyl-ether occur.

REFERENCES

[1] P.L. Yue and O. Olaofe, Chem. Eng. Res. Des., 62 (1984) 81.

[2] J. Simonik and H. Pines, J. Catal., 24 (1972) 211.

[3] V.R. Padmanabhan and F.J. Eastburn, J. Catal.,24 (1972) 88.

[4] D.E. Brynat and W.L. Kranich, J. Catal., 8 (1967) 8.

[5] L. Kabel and L.N. Johanson, A.I.Ch.E. Journal, 8 (5) (1962) 621.

[6] C.N. Satterfield, "Heterogeneous Catalysis in Practice", McGraw-Hill book Co., New York, (1980) Ch.1 pp.14-15.

[7] R.E. Balzhiser, M.R. Samuels and J.D. Eliassen, "Chemical Engineering Thermodynamics, The Study of Energy, Entropy and Equilibrium", Prentice-Hall, Inc., Englewood Cliffs, New Jersey, 1972.

[8] S.I. Sandler, "Chemical and Engineering Thermodynamics", John Wiley & Sons, Inc., New York, 1977.

[9] J.M. Smith and H.C Van Ness, "Introduction to Chemical Engineering Thermodynamics", 3rd Edn., McGraw-Hill book Co., New York, 1975.

[10] K. Denbigh, "The Principles of Chemical Equilibrium", 4th Edn., Cambridge Univ. press, 1981.

[11] B. Diep and M. Wainwright J. Chem. Eng. Data 32 (1987) 330.

CHAPTER SIX

SUMMARY AND CONCLUSIONS

In this dissertation a number of metals supported on TiO_2 were investigated for use as ethanol conversion catalysts. The various metals have been found to influence catalytic activity and/or selectivity in the transformation of ethanol to hydrocarbon products. The metals investigated in this study were compared with the metal free TiO_2 support. Comparative studies using modified clay and γ-Al_2O_3 were also used and established the effect of the strong acid function on the above reaction.

In the temperature range 100°C - 400°C, the Co-, Cu- and Ni-containing catalysts revealed similar conversion and activities to the metal free TiO_2 for the reaction. Generally at reaction temperatures below 250°C the ethanol conversion was low. At reaction temperatures of 300°C, conversion of ethanol had increased to ± 6%. Maximum conversion was achieved at 400°C (about 55%). Only the Al-containing sample gave a slight increase in activity and appeared to enhance diethyl-ether formation at low temperature (< 350°C). However, addition of metal catalysts gave significant changes to the product selectivities. In particular higher long chain hydrocarbon (C_6^+) selectivities, and increased catalyst life times were noted. The overall similarty in product distributions for the ethanol reaction over these metal containing catalysts suggests a similar reaction mechanism. Further, the higher the metal content of the catalyst the higher the C_6^+ liquid product contend.

A stable alumina pillared interlayered montmorillonite (Al-PILM) catalyst with a microporous structure and high specific surface area, was synthesized. Ammonium treatment of the Al-PILM catalyst improved the catalytic stability and activity in the ethanol conversion reaction.

γ-Al_2O_3 was found to be a very effective and selective catalyst for conversion of ethanol to diethyl-ether at low temperature (*ca.* 350°C, ± 50 wt.%) and ethene at high temperature (*ca.* 400°C, > 98 wt.%).

Pd/TiO_2 has been found to show activity for both the dehydrogenation and dehydration of ethanol at 100°C - 400°C. Furthermore, addition of Pd to TiO_2 resulted in a dramatic change in the product spectrum for ethanol transformation to hydrocarbons at low reaction temperatures (< 300°C). The product selectivities varied with reaction temperatures for the two different reaction pathways. At low temperatures the Pd reacted with the ethanol to yield acetaldehyde and favoured production of odd numbered hydrocarbons. On the other hand, in the high temperature regime the second reaction pathway - a dehydration reaction - yielded diethyl-ether, ethene and even numbered hydrocarbons.

The catalytic performance of Pd/TiO_2 was found not to be affected by the metal salt counterion over a broad range of reaction conditions. A comparison of two preparation methods (incipient wetness and co-precipitation) to obtain 2% Pd/TiO_2, indicated that the preparation methods did not significantly affect the catalyst behaviour.

A comparison of the conversion of ethanol to hydrocarbons over 2% Pd/TiO_2 in the presence of hydrogen and nitrogen was investigated. The product spectrum permitted the

determination of the dominant mechanism in the reaction at low temperature:

(1) The predominance of odd numbered over even numbered carbon atom products is consistent with a reductive dehydroxymethylation mechanism (N_2 or H_2 carrier gas).
(2) The presence of large quantities of methane is suggestive of a chain growth ter. ination reaction (H_2 as carrier gas). Under an N_2 atmosphere, H_2 gas is generated in the reaction, which subsequently yields hydrogenated products. However, chain growth competes with hydrogenation under N_2 and the limited quantities of H_2 results in products with chain length > C_6.
(3) Of interest is the lack of any C_4 product but large quantities of C_5 and C_3 products. The variable C_3 product composition produced in N_2 and H_2 carrier gases for similar C_5 product yields highlights the competitive nature of the chain growth versus hydrogenation reaction routes.

Again, in this study, addition of Pd to TiO_2 significantly influenced the ethanol transformation reaction in the low temperature regime (200°C - 300°C). The reaction temperature cycle s s indicated a high temperature (> 300°C) deactivation o. this low temperature effect. This appeared to be caused by coke deposited on Pd, but also possibly due to a SMSI effect. However, this catalyst after deactivation can successfully be reactivated. Further, repeated regeneration gave little loss in catalytic activity.

A comparison of the catalytic activity of the 2% Pd/TiO_2 catalyst reduced at different temperatures indicated the

order of reactivity to be: reduced at 200°C > reduced at 400°C > reduced at 500°C > unreduced. On the other hand, the hydrogen reduction treatments do not affect the activity of the TiO_2. At higher calcination temperatures pretreated 2% Pd/TiO_2 also showed declined catalytic activity. It can therefore be concluded that the lower activity of the catalyst calcined at higher temperature is due to sintering associated with the reduced catalyst surface area. In this investigation of the effect of calcination and reduction temperature; the 2% Pd/TiO_2 catalyst (extrudate) has superior activity and selectivity when the calcination temperatures are below 400°C (16 h in air) and a reduction temperature of about 200°C (16 h in hydrogen) is used. These conditions yield a catalyst of suitable mechanical strengh.

From an economic viewpoint, an attempt was made to compare both absolute and 96% aqueous ethanol as a reagent for the 2% Pd/TiO_2 catalysed reaction. This investigation revealed no significant changes in catalytic activity and product selectivities for the two reactant feeds.

As mentioned above, both γ-Al_2O_3 and Al-PILM catalysts only showed ethanol dehydrogenation to diethyl-ether and/or ethene. Addition of 2% Pd metal to the above two catalysts modified the product selectivities. The Pd-containing γ-Al_2O_3 and Al-PILM catalysts gave both dehydration and dehydrogenation activity in the ethanol conversion reaction.

When Pt, Rh and Ru were loaded on TiO_2 a change in the product spectrum was also noted. The results for the Pt and Rh metals proved to be similar to that for the Pd metal, e.g. high selectivity toward (C_6 - C_9^+) heavy liquid products.

A thermodynamic study of the ethanol transformation over a 2% Pd/TiO_2 catalyst, at various total flow rates and ethanol feed rates were performed. An increase in the nitrogen flow rate resulted in a decrease in ethanol conversion to products in the low temperature region (< 300°C). Higher conversions occured at low N_2 feed rates (N_2 = 21 ml/min). Further, the lower concentration of ethanol and longer contact time with the catalyst revealed that the measured equilibrium constant (K_a) approached that of the theoretical equilibrium.

APPENDIX 1 Techniques used to prepare metal loaded TiO_2 catalysts

I. Incipient wetness method

A sample (5.0 g) of oxide support (TiO_2, Degussa, Titandioxid P 25), was placed in a 10 cm^3 evaporating basin and wetted with 7.5 ml distilled water. A glass rod was used to thoroughly mix the sample. The sample was then placed in an oven, dried at 110°C for 16 h, and ground to a fine powder using a pestle and mortar. The catalyst powder was then wetted with $Ni(NO_3)_2 \cdot 6H_2O$ (5.0 ml; 0.35 M) solution, dried at 110°C for 16 h and then calcined at 400°C for 16 h to give the 2% Ni/TiO_2 catalyst (2% Ni by mass). The preparation of other metels on TiO_2, was achieved using the same method.

II. Co-precipitation method for preparation of 2% Pd/TiO_2 catalyst

10.0 g of TiO_2 (Degussa, Titandioxid P 25) and 150 ml of distilled water were placed into a 500 ml beaker. An overhead stirrer with a paddle was then used to stir the suspension until a "white smooth" homogeneous solution was obtained. NH_4OH (1.0 M) was then added to the slurry until the pH of between 8 and 9 was obtained.

$Pd(NO_3)_2 \cdot H_2O$ (0.52 g, Osmium Co. Ltd.) was dissolved in 1.0 M HNO_3 (10.0 ml) and then distilled water (30.0 ml) was used to further dilute the solution. This yielded 0.25 M palladium/nitric acid solution which was used in the catalyst synthesis.

The sample solution was heated to 75°C - 80°C with continuous (overhead) stirring and then titrated very slowly with the 0.25 M palladium/nitric acid solution (40 ml) and 1.0 M ammonia solution see Figure A1.1. Adjustment of titration rate to maintain, pH and solution temperature for controlled precipitation were made. The total addition of the solution took about 3 - 4 h.

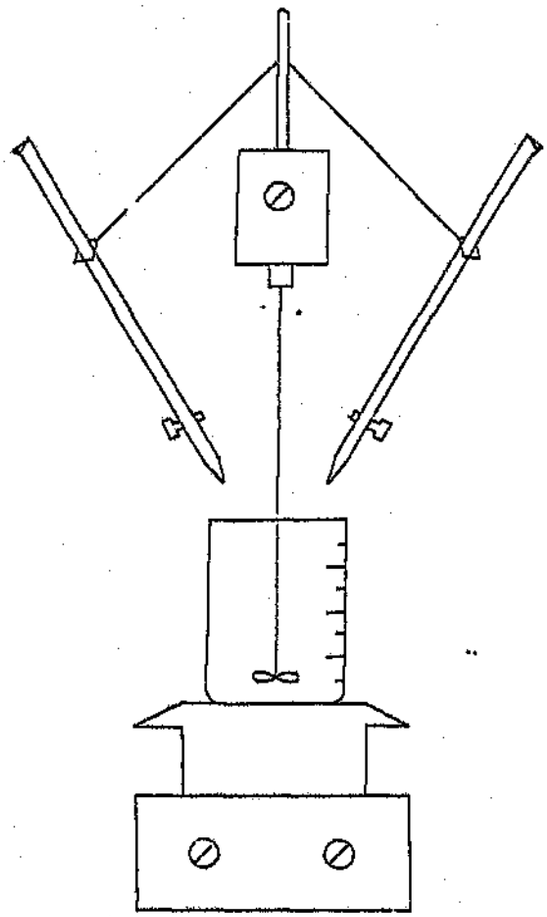

Figure A1.1 The catalyst prepartion of set-up

Stirring was then terminated and the suspension was allowed to stand undisturbed for 30 min at room temperature. The product was separated from the precipitate using a sintered glass filter frit under water pump vacuum. The product was scraped off the filter frit and extruded with a syringe pump (extrudate size 2 mm diam). The extrudate products were dried at 110°C for 16 h in air. The preparation steps are shown schematically in Figure A1.2.

The above preparative technique was used to prepare the 1% and 5% palladium or platinum supported catalysts.

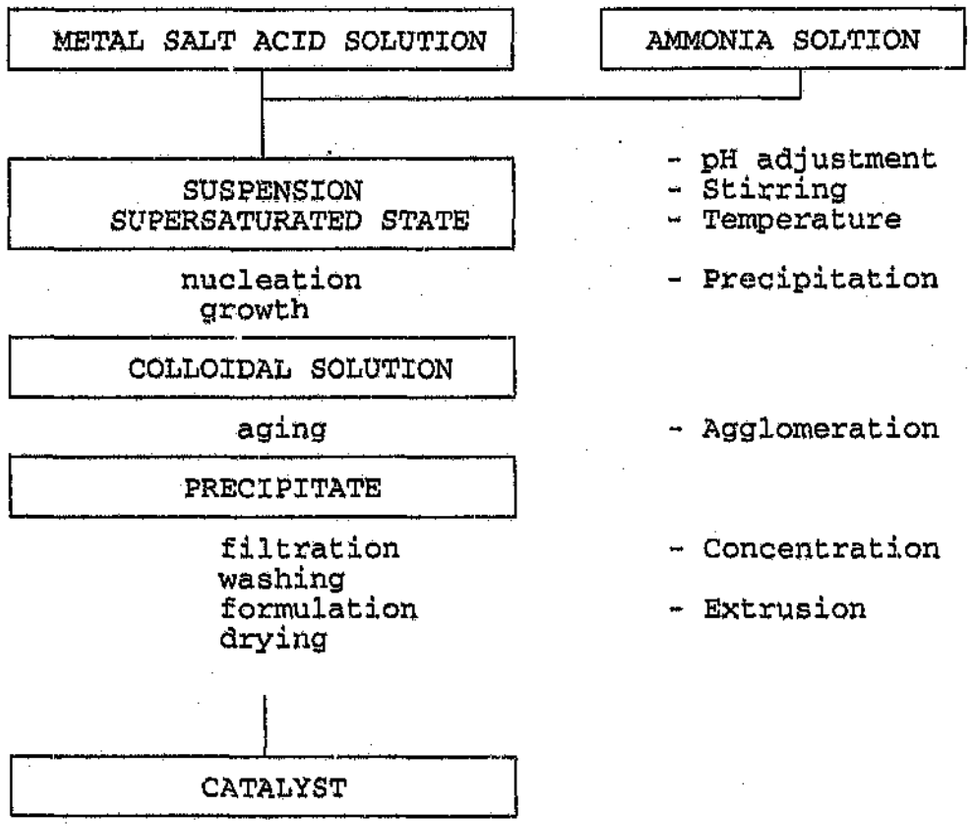

Figure A1.2 Co-precipitation mothod of preparation steps for dispersed meta. loading on oxide support

APPENDIX 2.1 Gas Chromatographic program details

Standard samples of all the expected reactants and products were recorded on the GC to obtain the retention times using a particular temperature program and carrier gas flow-rate (N_2). The retention times changed slightly when the temperature program and carrier gas flow-rate (N_2) were changed.

The GC settings for temperature programmed analysis of the oven, detector and injection port were as follows:

Detector	: F I D
Column	: 2 m x 1/8" Porapak Q
Carrier gas flow-rate	: 20 ml/min

Oven limit	: 250°C	Detector	: 250°C
Injection port	: 120°C	Initial temperature	: 135°C
Final temperature	: 240°C	Rise rate	: 5°C/min
Mode switch	: Prog	Function switch	: Single

Times settings:

Initial time	: 7 min	Final time	: 32 min
Function swich	: Run	Subambient switch	: Off

Electrometer settings:

Suppression current knob	: 1
Polarity switch	: +
Input range switch	: 100
Attenuation knob	: S

APPENDIX 2.2 The calibrated retention-times of different hydrocarbons and oxygenated compounds

Carbon number[a]	Compound	(RT)[b]/min
1	Methane	0.95
2	Ethene	1.40
	Ethane	1.57
3	Propene	2.67
4	Iso Butane	5.52
	Iso Butylene	5.99
	1-Butene	6.37
	2-Butene (cis & trans)	6.75
	n-Butane	6.92
	Cis-2-Butene	7.22
5	2,2-Dimethyl Propane	9.76
	Pentane	13.57
	2-Pentene (cis & trans)	13.86
	Cyclo-Pentene	14.84
6	1-Hexene	19.45
	Hexane	19.82
	Benzene	20.96
	Cyclohexene	22.07
7	1-Heptene	24.39
	Heptane	24.49
	Toluene	26.18
8	Iso-Octane	27.12

Carbon number[a]	Compound	(RT)[b]/min
8	1-Octene	28.76
	Octane	29.14
	Xylene	30.75
9	1-Nonene	34.39
	Nonane	35.35
10	n-Decane	43.42
	1-Decene	45.66

Oxygenated compounds	RT[b]/min
Ethanol (C_2H_5OH)	6.9
Diethyl ether ($C_4H_{10}O$)	13.22
Formaldehyde (HCHO)	3.56
Acetaldehyde (CH_3CHO)	4.26
Propionaldehyde (C_3H_6O)	11.04
Iso-butyraldehyde (C_4H_8O)	11.33
Crotonaldehyde (C_4H_6O)	19.93

[a] Number of carbon atoms in the molecule.

[b] RT = room temperature, 25°C.

APPENDIX 3 Correction of Gas Chromatographic data

Figure A3 showns a sample product chromatogram for ethanol conversion to hydrocarbons over Pd/TiO_2 (2% Pd by mass, reduced at 200°C, extrudate) catalyst. Porapak Q column, FID detector, and Packard model 428 GC were used to obtain the data shown in Figure A3.

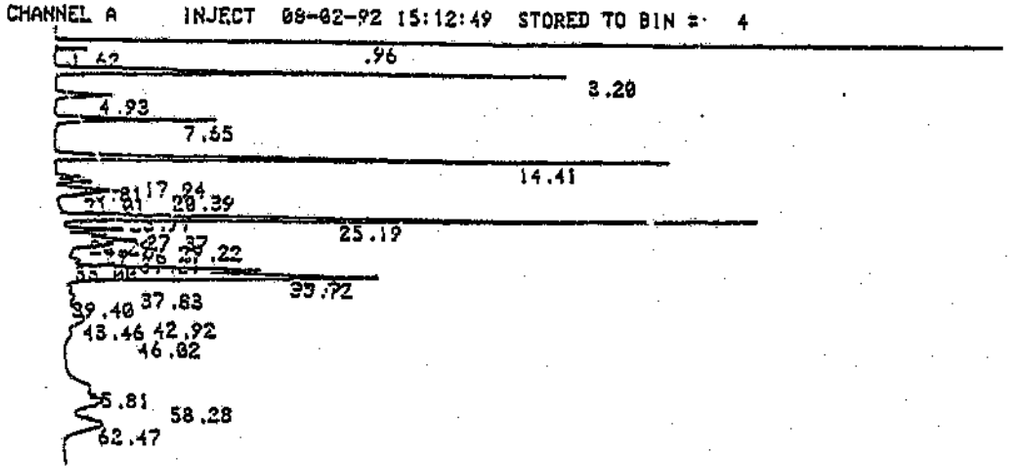

Y.K. CHEN 08-02-92 15:12:49 CH= "A" PS= 1.

FILE 1. METHOD 0. RUN 4 INDEX 4 BIN 4

PEAK#	AREAX	RT	AREA BC
1	2.668	0.96	388769 01
2	0.12	1.62	17598 01
3	5.907	3.2	860775 01
4	0.881	4.93	128371 01
5	4.372	7.65	637050 01
6	16.995	14.41	2476312 01
7	0.621	17.94	90475 02
8	0.849	18.81	123726 02
9	2.287	20.39	333255 02
10	0.956	21.01	139247 03
11	0.134	23.97	19571 02
12	17.627	25.19	2568500 08
13	1.506	27.37	219373 06
14	1.304	28.29	189990 06
15	2.716	29.22	395708 06
16	2.198	29.96	320162 06
17	0.44	31.21	64172 06
18	0.875	33.	127486 06
19	9.743	34.57	1419690 06
20	16.696	35.72	2432724 06
21	0.423	37.83	61663 06
22	0.804	39.4	117191 06
23	1.769	42.92	257691 06
24	1.441	43.46	209933 06
25	0.522	46.02	76069 07
26	0.556	55.81	81068 02
27	1.989	58.28	289760 02
28	3.601	62.47	524859 03
TOTAL	100.		14571010

Figure A3 Sample product chromatograph (T = 250°C; EtOH WHSV = 0.806 h^{-1})

To obtain quantitative data from the integrated response of the GC, each component area count was multiplied by a correction factor. This factor took into account the varying responses of the detector to each component. Each component concentration was expressed in terms of mass percentage.

The mass percentage of ethanol conversion and the selectivity were determined as follows:

$$\% \text{ conv. EtOH} = 100\% - \frac{AC_{(EtOH)} \times RF_{(EtOH)}}{\sum_{i=1}^{n} AC_i \times RF_i} \times 100\%$$

$$\% \text{ Selectivity } (S_i) = \frac{AC_i \times RF_i}{\sum_{i=1}^{n} AC_i \times RF_i} \times 100\%$$

Where $AC_{(EtOH)}$ = Area count of ethanol.

$RF_{(EtOH)}$ = Response factor of ethanol.

i = Component in the chromatogram.

$\% S_i$ = % selectivity of component i.

AC_i = Area count for component i.

RF_i = Response factor for component i.

$\sum_{i=1}^{n} AC_i \times RF_i$ = The summation of all the detector response corrected areas in the chromatogram

APPENDIX 4 Preparation of 2% Pd/Al-PILM catalyst of steps and method

I. Clay fractionation and Na^+ ion-exchange

Commercial montmorillonite K-10 (36.0 g), NaCl (85.0 g) and 800 ml of distilled water were placed into a large beaker. An overhead stirrer was used to agitate the suspension vigorously until it had obtained a "smooth" and homogeneous consistency. The suspension was left undisturbed for 8 h. The top volume of the suspension was then carefully syphoned-off into a receiving beaker. The volume syphoned-off was replaced by distilled water, and the suspension stirred again to obtain a homogeneous consistency which was again allowed to stand undisturbed for 8 h. This was repeated until the top volume of the suspension was clear of clay particles after standing. Clay particles remaining in the bottom volume of the water were discarded due to the fact that their particle size was > 2 micrometers.

The < 2 micrometer sodium exchanged clay particle fraction (Na^+-montmorillonite) which was collected in the receiving beaker was separated and washed free of chloride ions ($AgNO_3$ test) using centrifugation techniques. The wet clay was scraped out and then dried overnight at 110°C. The dry clumps of clay so obtained were ground to a fine powder.

II. Preparation of alumina pillared interlayered montmorillonite (Al-PILM)

Na^+-montmorillonite (25.0 g) was added in small portions to 1000 ml of a 0.1 M solution of aluminium chloride ($AlCl_3 \cdot 6H_2O$) and the suspension was then stirred vigorously.

The stirred suspension was then titrated very slowly (1 - 2 h) with 500 ml of 1.0 M sodium hydroxide solution. Stirring was then terminated and the suspension was allowed to stand undisturbed for one week at room temperature. The precipitate was separated from the water using a filter frit under water pump vacuum. The product was scraped off the filter, placed in approximately 500 ml distilled water, stirred and then filtered once again. This process was repeated two more times. Product was then scraped-off the filter frit and dried at 110°C for 16 h.

The dried product was ground to a fine powder and then calcined at 400°C for 4 h to obtain the alumina pillared interlayered montmorillonite (Al-PILM).

III. Ammonium ion exchanged activated Al-PILM

Al-PILM (10.0 g) was stirred at room temperature in 100 ml of 1.0 M NH_4NO_3 solution. After 30 min the suspension was filtered and washed with distilled water. This procedure was repeated four times. After the fourth filtration the material was washed with distilled water two more times. The NH_4^+-exchanged Al-PILM was then dried at 110°C for 4 h, and calcined at 500°C for 3 h.

IV. Preparation of palladium metal on Al-PILM

the co-precipitation method as described previously (Appendix 1) was used.

REFERENCES

[1] R.C. Mackenzie, Clay Miner. Bull., 3 (1956) 4.

[2] E. Kikuchi, T. Matsuda, J. Ueda and Y. Morita, Appl. Catal., 16 (1985) 401.

[3] J. Wollbrandt, Msc. Thesis, University of Pretoria, 1989.

[4] J. Sterte, in "Preparation of Catalysts: Scientific Bases for the Preparation of Heterogeneous Catalysts", B. Delmon et al. (Eds.), Vol.V, Elsevier, Amsterdam, (1991) p.301.

[5] E. Kikuchi, H. Seki and T. Matsuda, in "Preparation of Catalysts: Scientific Bases for the Preparation of Heterogeneous Catalysts", B. Delmon et al. (Eds.), Vol.V, Elsevier, Amsterdam, (1991) p.311.

[6] J.M. Adams, Applied Clay Science, 2 (1987) 309.

[7] W.Y. Lee, R.H. Raythatha and B.J. Tatarchuk, J. Catal., 115 (1989) 159.

[8] C. Pesquera, F. Gonzalez, I. Benito, S. Mendioroz and J.A. Pajares, Appl. Catal., 69 (1991) 97.

[9] D. Tichit, Z. Mountassir, F. Figueras and A. Auroux, in "Preparation of Catalysts: Scientific Bases for the Preparation of Heterogeneous Catalysts", B. Delmon et al. (Eds.), Vol.V, Elsevier, Amsterdam, (1991) p.345.

APPENDIX 5 The derivation of the equilibrium constant and relative temperature equation

ΔG° is evaluated from standard Gibbs free energies of formation ($\Delta \underline{G}^\circ_f$); the equation is given by [1 - 4]:

$$\Delta G^\circ = \sum_{i=1}^{c} \alpha_i \left(\Delta \underline{G}^\circ_f \right)_i \qquad \text{(A5-1)}$$

where α_i = componsition (i) of stoichiometric coefficient in the reaction.

$$\Delta G^\circ = - R\ T\ \ell n(Ka)_T \qquad \text{(A5-2)}$$

The equilibrium constant (Ka) changes with reaction temperatures. The effect of changes in temperature on the equilibrium constant is described by the Gibbs - Helmholtz equation:

$$\partial/\partial T \left(\frac{\Delta G^\circ}{T} \right)_{p^*} = - \sum_{i=1}^{c} \frac{\alpha_i (\Delta \underline{H}^\circ_f)_i}{T^2} = - \frac{\Delta H^\circ}{T^2} \qquad \text{(A5-3)}$$

$$\text{where } \Delta H^\circ = \sum_{i=1}^{c} \alpha_i (\Delta \underline{H}^\circ_f)_i \qquad \text{(A5-4)}$$

(standard - state heat of reaction)

From equation (A5-2) the ΔG° and Ka relationship is shown as follows:

$$R\ \ell nKa = - \frac{\Delta G^\circ}{T} \qquad \text{(A5-5)}$$

differentiating T in equation (A5-5) we obtain:

$$R \frac{d\ \ell nKa}{d\ T} = - \frac{d}{dT} \frac{\Delta G^\circ}{T} \qquad (A5\text{-}6)$$

Substituting the Gibbs-Helmholtz equation (A5-3) into equation (A5-6) we get:

$$R \frac{d}{dT} (\ell nKa) = \frac{\Delta H^\circ}{T^2} \qquad (A5\text{-}7)$$

or

$$\frac{d}{dT} \qquad \frac{\Delta H^\circ}{RT^2} \qquad (A5\text{-}8)$$

Equation (A5-8) is known as van't Hoff's equation. Ka is a function of temperature because the heat of reaction (ΔH°), is only a function of temperature. So, the heat of reaction is given by:

$$\frac{d\ \Delta H^\circ}{dT} dT = \Delta C_p \qquad (A5\text{-}9)$$

Integration of equation (A5-9) gives:

$$\int d\ \Delta H^\circ = \int \Delta C_p\ dT \qquad (A5\text{-}10)$$

or

$$\Delta H^\circ_T - \Delta H^\circ_{T^*} = \int \Delta C_p\ dT \qquad (A5\text{-}11)$$

$$\Delta H^\circ_T = \Delta H^\circ_{T^*} + \int \Delta C_p\ dT \qquad (A5\text{-}12)$$

The above equations give the standard enthalpy change of reaction, T* at 298 K so, $\Delta H^\circ_{T^*} = \Delta H^\circ_f$

$$\text{where } \Delta C_p = \sum_{i=1}^{C} \alpha_i \left(\Delta \underline{C}_p \right)_i \qquad \text{(A5-13)}$$

The heat capacity ($\underline{C}p_i$), of pure gas, i, is usually expressed in the literature as an empirical power series in temperature.

$$\underline{C}p_i = A_i + B_i * T + C_i * T^2 + D_i * T^3 \qquad \text{(A5-14)}$$

where A, B, C, D ($\underline{C}p_{vap.}$) = constants in the ideal gas heat capacity equation.

The integration of equation (A5-8), Van't Hoff's equation, gives:

$$\int d \ln Ka = \int \frac{\Delta H^\circ}{RT^2} dT \qquad \text{(A5-15)}$$

or

$$(\ln Ka)_{T2} - (\ln Ka)_{T1} = \int \frac{\Delta H^\circ}{RT^2} dT \qquad \text{(A5-16)}$$

$$\ln \frac{(Ka)_{T2}}{(Ka)_{T1}} = \int \frac{\Delta H^\circ}{RT^2} dT \qquad \text{(A5-17)}$$

Combining equations (A5-12) and (A5-17) gives:

$$\ln \frac{(Ka)_{T2}}{(Ka)_{T1}} = \int_{T^*}^{T} \frac{\Delta H^\circ_{T^*} + \int \Delta C_p \, dT}{RT^2} dT \qquad \text{(A5-18)}$$

Equation (A5-18) was used to develop a relationslip between the equilibrium constant and temperature.

A listing of $\underline{C}_p$'s, $\underline{H}^\circ_f$'s and $\underline{G}^\circ_f$'s, obtained from the literature [5, 6, 7], and a summary of the data obtained for the calculations are shown in Tables A6.1 and A6.2 in Appendix 6.

REFERENCES

[1] R.E. Balzhiser, M.R. Samuels and J.D. Eliassen, "Chemical Engineering Thermodynamics, The Study of Energy, Entropy and Equilibrium", Prentice-Hall, Inc., Englewood Cliffs, New Jersey, 1972.

[2] S.I. Sandler, "Chemical and Engineering Thermodynamics", John Wiley & Sons, Inc., New York, 1977.

[3] J.M. Smith and H.C Van Ness, "Introduction to Chemical Engineering Thermodynamics", 3rd Edn., McGraw-Hill book Co., New York, 1975.

[4] K. Denbigh, "The Principles of Chemical Equilibrium", 4th Edn., Cambridge univ. press, 1981.

[5] R.H. Perry and D.W. Green, "Perry's Chemical Engineers' Handbook", 6th Edn., McGraw-Hill book Co., 1984.

[6] "Handbook of Chemistry and Physics", CRC Press Inc., Boca Raton, Florida, 63rd Edn., 1982-1983.

[7] R.C. Reid, T.K. Sherwood and J.M. Prausnitz, "The Properties of Gases and Liquids", 3rd Edn., McGraw-Hill book Co., 1977.

APPENDIX 6 The calculation of equilibrium constants

The following equations were used for the calculation of the equilibrium constants for the ethanol system reaction from $\underline{C}_p$, $\underline{H}^\circ_f$ and $\underline{G}^\circ_f$ data. The calculations are restricted to reactions that are expected to occur in the system.

$$\ell n \frac{(Ka)_T}{(Ka)_{T^*}} = \int_{T^*}^{T} \frac{\Delta H^\circ_{T^*} + \int \Delta C_p \, dT}{RT^2} \, dT$$

or

$$\ell n(Ka)_T = \int_{T^*}^{T} \frac{\Delta H^\circ_{T^*} + \int \Delta C_p \, dT}{RT^2} \, dT + \ell n(Ka)_{T^*}$$

where

$$(Ka)_{T^*} = \exp \frac{-\Delta G^\circ}{R \, T^*}$$

and $$\Delta G^\circ_{T^*} = \sum_{\text{product}} \alpha_i * \underline{G}^\circ_f - \sum_{\text{reactant}} \alpha_i * \underline{G}^\circ_f$$

$$\Delta H^\circ_{T^*} = \sum_{\text{product}} \alpha_i * \underline{H}^\circ_f - \sum_{\text{reactant}} \alpha_i * \underline{H}^\circ_f$$

$$\Delta C_p = \sum_{\text{product}} \alpha_i * \underline{Cp}_i - \sum_{\text{reactant}} \alpha_i * \underline{Cp}_i$$

$$\underline{Cp}_i = A_i + B_i * T + C_i * T^2 + D_i * T^3$$

Table A6.1 Heat Capacity Data

$\underline{C_p} = A + B * T + C * T^2 + D * T^3$, (T = K)

Unit: J/mol K, Temperature range: 298 K - 1500 K

Component	Constant			
	A	B	C	D
H_2O	32.243	$1.923E^{-3}$	$1.055E^{-5}$	$-3.596E^{-9}$
C_2H_5OH	9.014	$2.140E^{-1}$	$-8.390E^{-5}$	$1.373E^{-9}$
$C_2H_5OC_2H_5$	21.424	$3.358E^{-1}$	$-1.035E^{-4}$	$-9.357E^{-9}$
C_2H_4	3.806	$1.565E^{-1}$	$-8.348E^{-5}$	$1.755E^{-8}$
CH_3CHO	7.716	$1.822E^{-1}$	$-1.006E^{-4}$	$2.380E^{-8}$
H_2	27.142	$9.273E^{-3}$	$-1.380E^{-5}$	$7.645E^{-9}$

Table A6.2 Standard Gibbs Energy and Standard Enthalpy of Formation Data

Unit: J/mol (1 atm, 298 K)

Component	$\underline{\Delta H°_f}$	$\underline{\Delta G°_f}$
H_2O	-241997	-228796
C_2H_5OH	-234814	-167950
$C_4H_{10}O$	-251274	-130396
C_2H_4	52405	68156
CH_3CHO	-166188.5	-131628.6
H_2	0	0

RXN # 1 = $2\ C_2H_5OH = C_2H_5OC_2H_5 + H_2O$

Ka_{298} = 12096.69097 or $\ell n(Ka)_{298}$ = 9.40069

$\Delta G°_{298}$ = - 23292

$\Delta H°_{298}$ = - 23643 (exothermic at 25°C)

ΔC_p = $35.639 - 0.090277\ T + 7.485E^{-05}\ T^2 - 1.5699E^{-8}\ T^3$

= $A - B * T + C * T^2 - D * T^2$

$\int_{298}^{T} \Delta C_p\ dT$ = $35.639\ T - 0.04514\ T^2 + 2.495E^{-05}\ T^3 - 3.92475E^{-09}\ T^4 - 7241.258$

= $a * T - b * T^2 + c * T^3 - d * T^4 - e$

$\ell n(Ka)_T$ = $3714.55043/T + 4.28642\ \ell nT - 5.42913E^{-03}\ T + 1.50041E^{-06}\ T^2 - 1.57347E^{-10}\ T^3 - 25.99562$

= $a'* 1/T + b'* \ell nT - c'* T + d'* T^2 - e'* T^3 - f$

RXN # 2 = $C_2H_5OH = C_2H_4 + H_2O$

Ka_{298} = 0.05232 or $\ell n(Ka)_{298}$ = - 2.95033

$\Delta G°_{298}$ = 7310

$\Delta H°_{298}$ = 45222 (endothermic at 25°C)

ΔC_p = $27.035 - 0.055577\ T + 1.097E^{-05}\ T^2 + 1.2581E^{-08}\ T^3$

= $A - B * T + C * T^2 + D * T^3$

$\int_{298}^{T} \Delta C_p\ dT$ = $27.035\ T - 0.02779\ T^2 + 3.65667E^{-06}\ T^3 + 3.14525E^{-09}\ T^4 - 5710.27249$

= $a * T - b * T + c * T^3 + d * T^4 - e$

$\ell n(Ka)_T$ = $- 4752.2043/T + 3.25159\ \ell nT - 3.34239E^{-02}\ T + 2.19899E^{-07}\ T^2 + 1.26097E^{-10}\ T^3 - 4.55482$

= $a'* 1/T + b'* \ell nT - C'* T + d'* T^2 + e'* T^3 - f$

RXN # 3 = $C_2H_5OC_2H_5$ = 2 C_2H_4 + H_2O

Ka_{298} = $2.26314E^{-07}$ or $\ell n(Ka)_{298}$ = - 15.30134

$\Delta G°_{298}$ = 37912

$\Delta H°_{298}$ = 114087 (endothermic at 25°C)

ΔC_p = $18.431 - 0.02088\ T - 5.291E^{-05}\ T^2 + 4.0861E^{-08}\ T^3$

= $A - B * T - C * T^2 + D * T^3$

$\int_{298}^{T} \Delta C_p$ = $18.43 \cdot T - 0.01044\ T^2 - 1.76367E^{-05}\ T^3 + 1.02152E^{-08}\ T^4 - 4179.15241$

= $a * T - b * T^2 - c * T^3 + d * T^4 - e$

$\ell n(Ka)_T$ = $- 13218.97507/T + 2.21676\ \ell nT - 1.25565E^{-03}\ T - 1.06061E^{-06}\ T^2 + 4.09540E^{-10}\ T^3 + 16.88610$

= $- a'* 1/T + b'* \ell nT - c'* T - d'* T^2 + e'* T^3 + f$

RXN # 4 = $C_2H_5C_{..}$ = CH_3CHO + H_2

Ka_{298} = $4.30046E^{-07}$ or $\ell n(Ka)_{298}$ = - 14.65937

$\Delta G°_{298}$ = 36321.4

$\Delta H°_{298}$ = 68625.5 (endothermic at 25°C)

ΔC_p = $25.845 - 0.02253\ T - 3.05E^{-05}\ T^2 + 3.0072E^{-09}\ T^3$

= $A - B * T - C * T^2 + D * T^3$

$\int_{298}^{T} \Delta C_p$ = $25.845\ T - 0.01127\ T_2 - 1.01667E^{-05}\ T^3 + 7.518E^{-09}\ T^4 - 6491.6745$

= $a * T - b * T^2 - c * T^3 + d * T^4 - e$

$\ell n(Ka)_T$ = $- 7473.0378/T + 3.10846\ \ell nT - 1.35547E^{-03}\ T - 6.11389E^{-07}\ T^2 + 3.01405E^{-10}\ T^3 - 6.84119$

= $- a'* 1/T + b'* \ell nT - c'* T - d'* T^2 + e'* T^3 - f$

APPENDIX 7 A workup of the input composition data for the Process package

A scheme of the input composition data for the Simulation Sciences Inc. Process package determination of the equilibrium concentrations. A aqueous ethanol (96% v/v, alcohol/water).

V.EtOH : $1.0\ ml\ h^{-1} \times 96\%$

$= 0.96\ cm^3\ h^{-1} \times 0.789\ g\ cm^{-3} \times 1/46\ g \cdot mol$

$= 0.0165\ mol\ h^{-1} = 1.65 \times 10^{-2}\ mol\ h^{-1}$

$V.H_2O$: $1.0\ ml\ h^{-1} \times 4\%$

$= 0.04\ cm^3\ h^{-1} \times 1\ g\ cm^{-3} \times 1/18\ g \cdot mol$

$= 2.22 \times 10^{-3}\ mol\ h^{-1}$

N_2 : $V/n = RT/P$

$= 0.082 \times 298/1$

$= 24.436\ m^3/K \cdot mol$

$= 24436\ cm^3/mol$

$V.N_2$ (ml/min)	$(\dot{N})N_2$ (mol/h)
21	5.16×10^{-2}
64	15.71×10^{-2}
96	23.57×10^{-2}

Nitrogen flow rates were used to dilut the ethanol concentration. The calculation of input composition at different flow rate is shown below.

N_2 ml/min	EtOH[a]	H_2O[a]	N_2[a]
21	22.95	3.18	73.87
64	9.13	1.26	89.61
96	6.29	0.87	92.84

[a] $mol\ h^{-1}$ (percentage)